THE UNIVERSITY OF MICHIGAN

COLLEGE OF ENGINEERING
DEPARTMENT OF AEROSPACE ENGINEERING
HIGH ALTITUDE ENGINEERING LABORATORY

Technical Report

The Calibration of and Interpretation of Data from the 0.55-0.85 Micron and 0.2-4.0 Micron Channels of the F-1 and F-4 MRIR Radiometers

F. L. BARTMAN

Under contract with:

National Aeronautics and Space Administration
Contract No. NASr-54(03)
Washington, D. C.

Administered through:

February 1966

OFFICE OF RESEARCH ADMINISTRATION · ANN ARBOR

THE UNIVERSITY OF MICHIGAN

COLLEGE OF ENGINEERING
Department of Aerospace Engineering
High Altitude Engineering Laboratory

Technical Report

THE CALIBRATION OF AND INTERPRETATION OF DATA FROM THE 0.55-0.85 MICRON AND 0.2-4.0 MICRON CHANNELS OF THE F-1 AND F-4 MRIR RADIOMETERS

F. L. Bartman

Approved by:

L. M. Jones, Director
High Altitude Engineering Laboratory

ORA Project 05863

under contract with:

NATIONAL AERONAUTICS AND SPACE ADMINISTRATION
CONTRACT NO. NASr-54(03)
WASHINGTON, D.C.

administered through:

OFFICE OF RESEARCH ADMINISTRATION ANN ARBOR

February, 1966

TABLE OF CONTENTS

TABLE OF CONTENTS (Concluded)

LIST OF TABLES

LIST OF FIGURES

LIST OF FIGURES (Continued)

LIST OF FIGURES (Concluded)

LIST OF MATHEMATICAL SYMBOLS

A_r = the effective area of the radiometer aperture, cm^2.

F = a correction factor for the atmospheric attenuation of the direct beam of the sun.

H_s = the solar constant = 0.1395 watts $\cdot$ cm^{-2}.

H_λ = spectral irradiance of MgO reflector by calibration lamp watts $\cdot$ cm^{-2}.

$H_{s\lambda}$ = solar spectral irradiance, watts cm^{-2}. $\Delta\lambda^{-1}$.

H_{si} = same as above (i used as a summation index).

k_n = constant, equal to ratio: spectral radiance of a source/relative spectral radiance of a source.

k_r = constant, equal to ratio: response of radiometer channel/relative response of radiometer channel.

m = optical path length, atmospheres.

N_c = radiance of calibrating source, watts $\cdot$ cm^{-2}. $steradian^{-1}$.

N'_c = effective radiance of a calibrating source, watts $\cdot$ cm^{-2}. $steradian^{-1}$.

$N_{c\lambda}$ = spectral radiance of calibrating source, watts $\cdot$ cm^{-2}. $steradian^{-1}$. $\Delta\lambda^{-1}$.

N_s = radiance of a surface reflecting solar radiation, watts $\cdot$ cm^{-2}. $steradian^{-1}$.

N'_s = effective radiance of a surface reflecting solar radiation, watts $\cdot$ cm^{-2}. $steradian^{-1}$.

$N'_s(100\%)$ = effective radiance of a surface reflecting solar radiation when surface has 100% diffuse reflectance.

$r(\theta_1,\phi_1)$ = directional reflectance of a surface.

R = distance between source and MgO reflectance plate.

R' = responsivity of a channel of the radiometer, averaged over the entire field of view.

T_λ^m = atmospheric transmission of wavelength λ over optical path m.

V_c = output voltage of radiometer when viewing calibrating source.

V_s = output voltage of radiometer when viewing a surface which is reflecting solar radiation.

V_{sc} = output voltage of radiometer when viewing sun directly through solar calibrate optics.

W_c = radiant emittance of calibrating source, watts $\cdot$ cm^{-2}.

W_c' = effective radiant emittance of calibrating source, watts $\cdot$ cm^{-2}.

$W_{c\lambda}$ = spectral radiant emittance of calibrating source, watts $\cdot$ $cm^{-2} \cdot \Delta\lambda^{-1}$.

z = solar zenith angle.

θ = angle in general sense.

θ_1 = zenith angle of incidence of a ray.

θ_2 = zenith angle of reflectance of a ray.

ϕ_1 = azimuth angle of incidence of a ray.

ϕ_2 = azimuth angle of a reflectance of a ray.

ϕ_λ = characteristic response of a channel of the radiometer.

ϕ_λ^{sc} = response of direct solar calibrate optics.

ϕ_λ' = relative characteristic response of a channel of the radiometer.

ϕ_i' = same as above (i used as a summation index).

λ = wavelength microns

$\Delta\lambda$ = wavelength interval, microns.

μ = microns.

π = 3.14159.

ρ_λ = spectral bi-directional reflectance of a surface.

$\overline{\rho}$ = average reflectance of a surface for solar radiation.

$\overline{\rho}'$ = effective average reflectance of a surface (as measured by radiometer).

$\rho(\theta_1,\phi_1,\theta_2,\phi_2)$ = bi-directional reflectance of a surface.

τ'_λ = extinction optical thickness.

$\psi_{c\lambda}$ = relative spectral radiance of calibrating source.

ψ_{ci} = same as above (i used as a summation index).

Ω = solid angle, steradians.

ABSTRACT

23806

A program of calibrations of the 0.55-0.85 micron and 0.2-4.0 micron channels of the F-1 and F-4 MRIR radiometers has been carried out and a hemisphere calibration source has been developed. The characteristics of the calibration source, the method of calibration and interpretation of data in terms of percent reflectance, and the system of direct solar calibrations for use on satellites are presented and discussed. Laboratory calibration data are presented and are shown to agree with Santa Barbara Research Center Data. The direct solar calibration data are presented and the limitation of this in-flight calibration system is discussed. An error analysis indicates a precision of ±2% and possible systematic errors of 5-8% in the calibrations. The possibility of large errors in the interpretation of reflectance data obtained with the MRIR is discussed and shown by example.

Author

1. INTRODUCTION

The NIMBUS 6 satellite which will be launched early in 1966 will carry a Medium Resolution Infrared Radiometer (MRIR) designed to measure the thermal radiation emitted, and the solar radiation reflected and scattered back out into space by the earth, clouds and the atmosphere.

Two flight models of the MRIR (models F-1 and F-4) have been tested and calibrated in the laboratory and on high altitude balloon flights by members of the High Altitude Engineering Laboratory of The University of Michigan, working under contract NASr-54(03) with NASA Goddard Space Flight Center.

The purpose of this report is to describe the method of calibration of the visible channels of the MRIR, to evaluate the accuracy of the calibration and to discuss the problem of interpretation of the data obtained with this type of instrument.

2. CHARACTERISTICS OF THE VISIBLE CHANNELS OF THE F-1 AND F-4 MRIR RADIOMETERS

The NIMBUS MRIR is a five-channel scanning radiometer designed to measure the flux of thermal radiation and the reflected and scattered solar radiation from the earth and its atmosphere.[1]

The optical design of the radiometer is illustrated schematically in Figure 1. Incoming radiation is reflected by the scanning mirror into the five Cassegranian telescopes and then passes through the chopper into the collecting optics, filter, and bolometer detector.

The associated electronics consists of preamplifiers, mixer circuits, power amplifiers, synchonous detectors, output filters, and power supply.

The relative characteristic response Φ'_λ of the two visible channels of the F-1 (flight model 1) radiometer are shown in Figures 2 and 3. The response of the one visible channel of the F-4 MRIR is also shown in Figure 3. This data was supplied with the radiometers by the Santa Barbara Research Center.

Other characteristics of the visible channels are illustrated by those of the F-4 MRIR visible channel, given in Table I.[2] The field of view contours of the 0.2-4.0 micron channel of the F-4 MRIR are shown in Figure 4.

TABLE I

NOMINAL CHARACTERISTICS OF F-4 MRIR

(0.2-4.0 micron channel)

Spectral region (5% points)	0.2-4.8 microns
Field of view (-6 db points)	2.8°
Optical entrance aperture	1.72 in. diam
Effective system f/no.	0.93
System input noise	0.59 μvolts rms
System gain	$3.9 \cdot 10^3$ (rms to dc)
Responsivity	$1.6 \cdot 10^5$ volts/watt/cm^2
NEPD	$1.52 \cdot 10^{-8}$ watts/cm^2
Time constant	0.02 sec
Target range	0 to 80% albedo
Output impedance	5.8°K
Output voltage range	0 to -6.4 volts

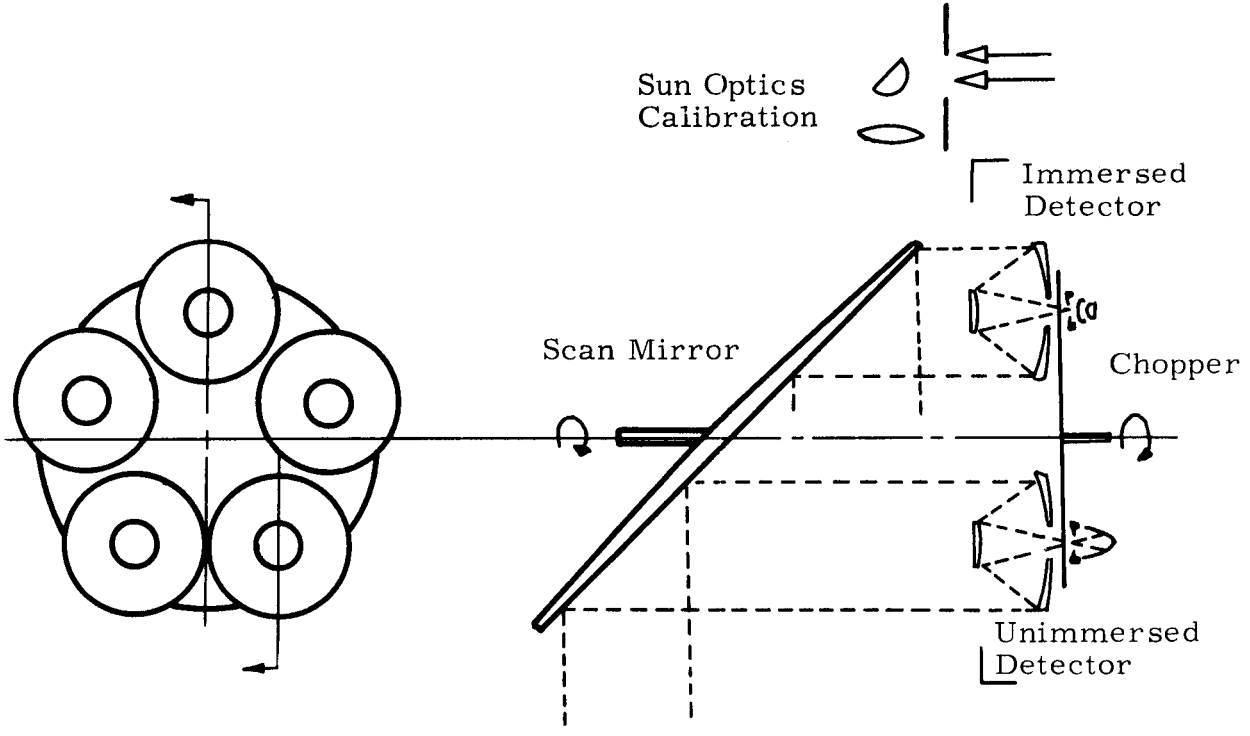

Figure 1. Optical arrangement of NIMBUS five-channel radiometer (MRIR).

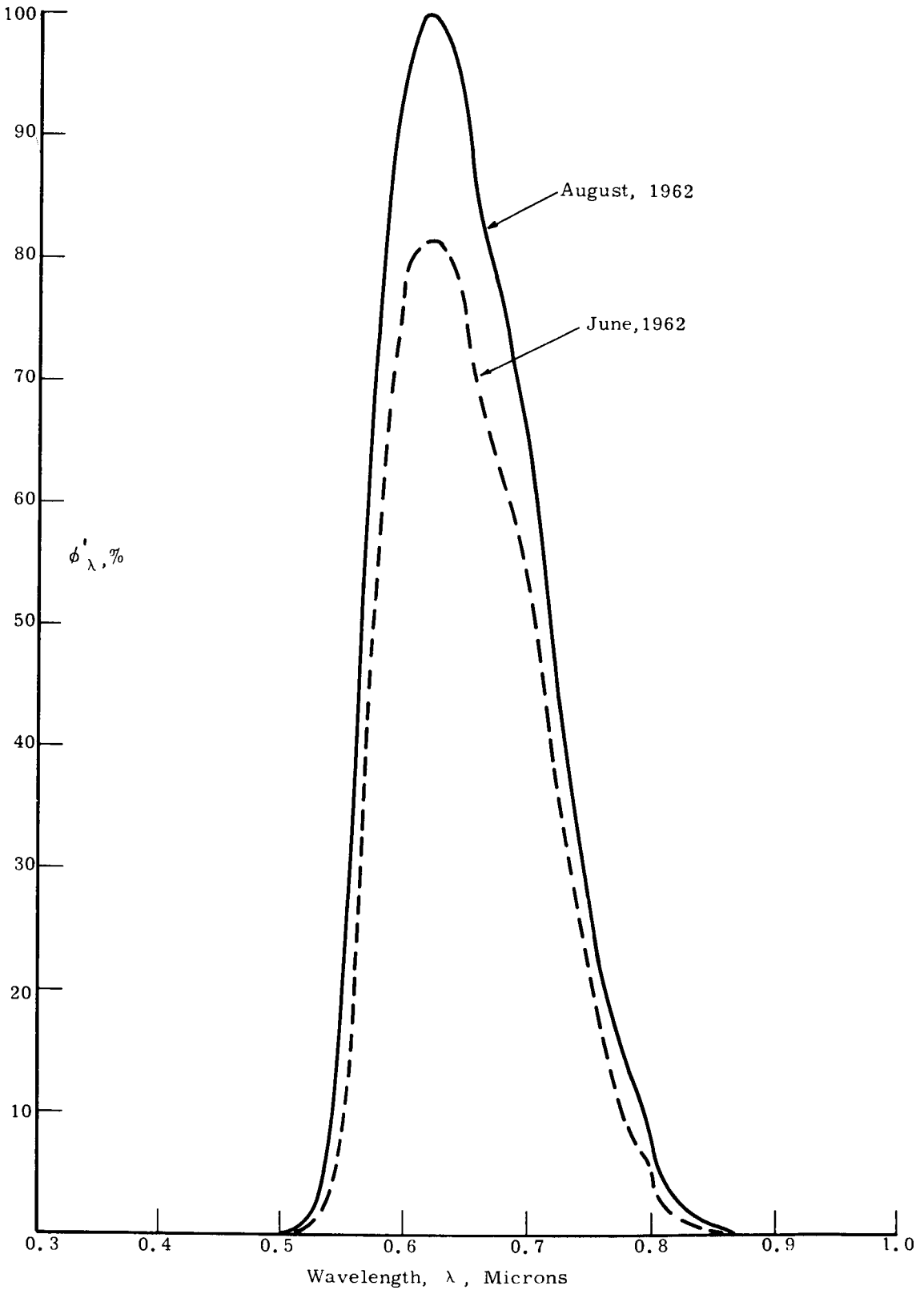

Figure 2. Relative characteristic response, ϕ'_λ, of 0.55-0.85 micron channel of F-1 MRIR.

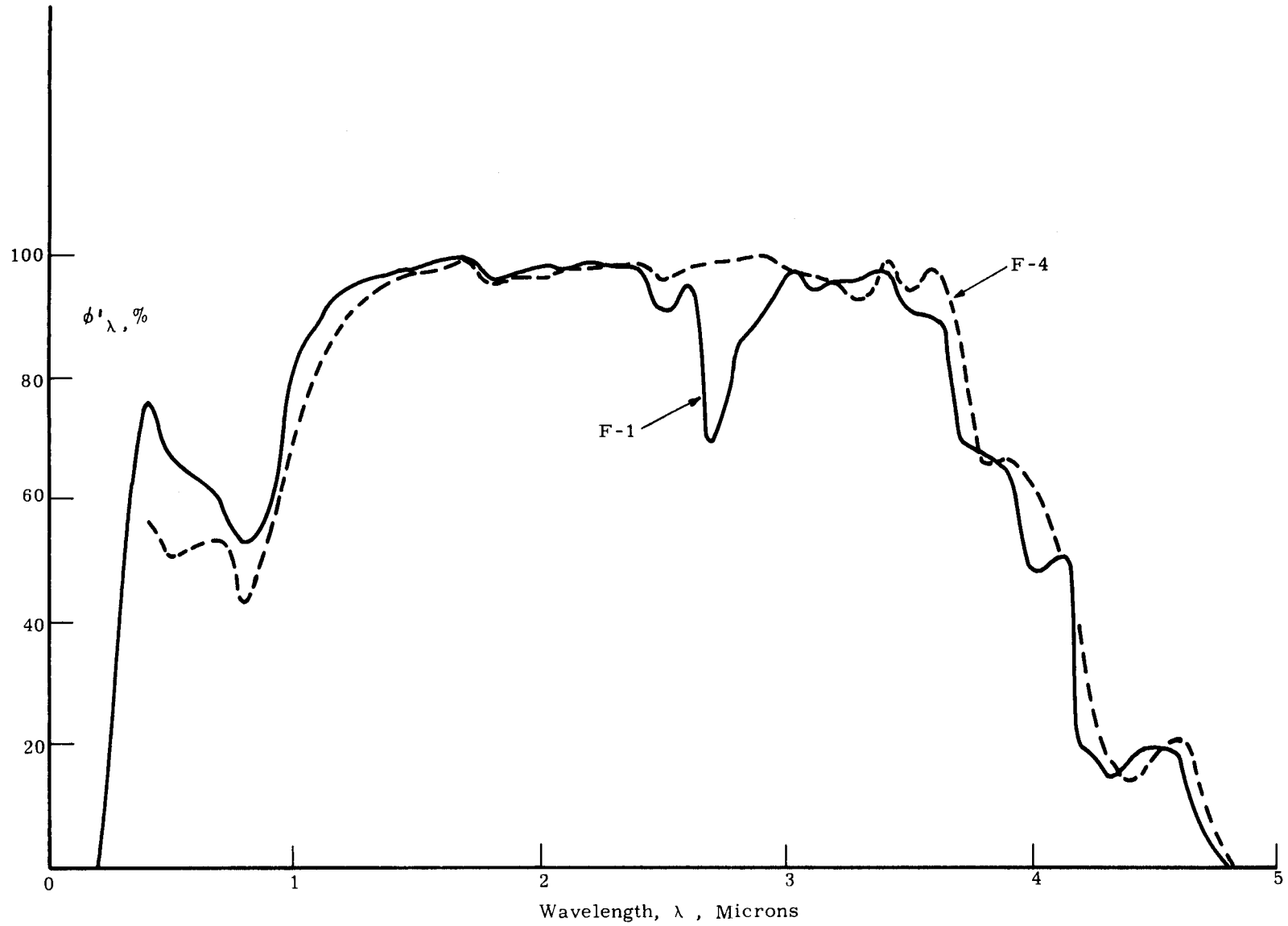

Figure 3. Relative characteristic response, ϕ'_λ, of 0.2-4.0 micron channel of F-1 and F-4 MRIR instruments.

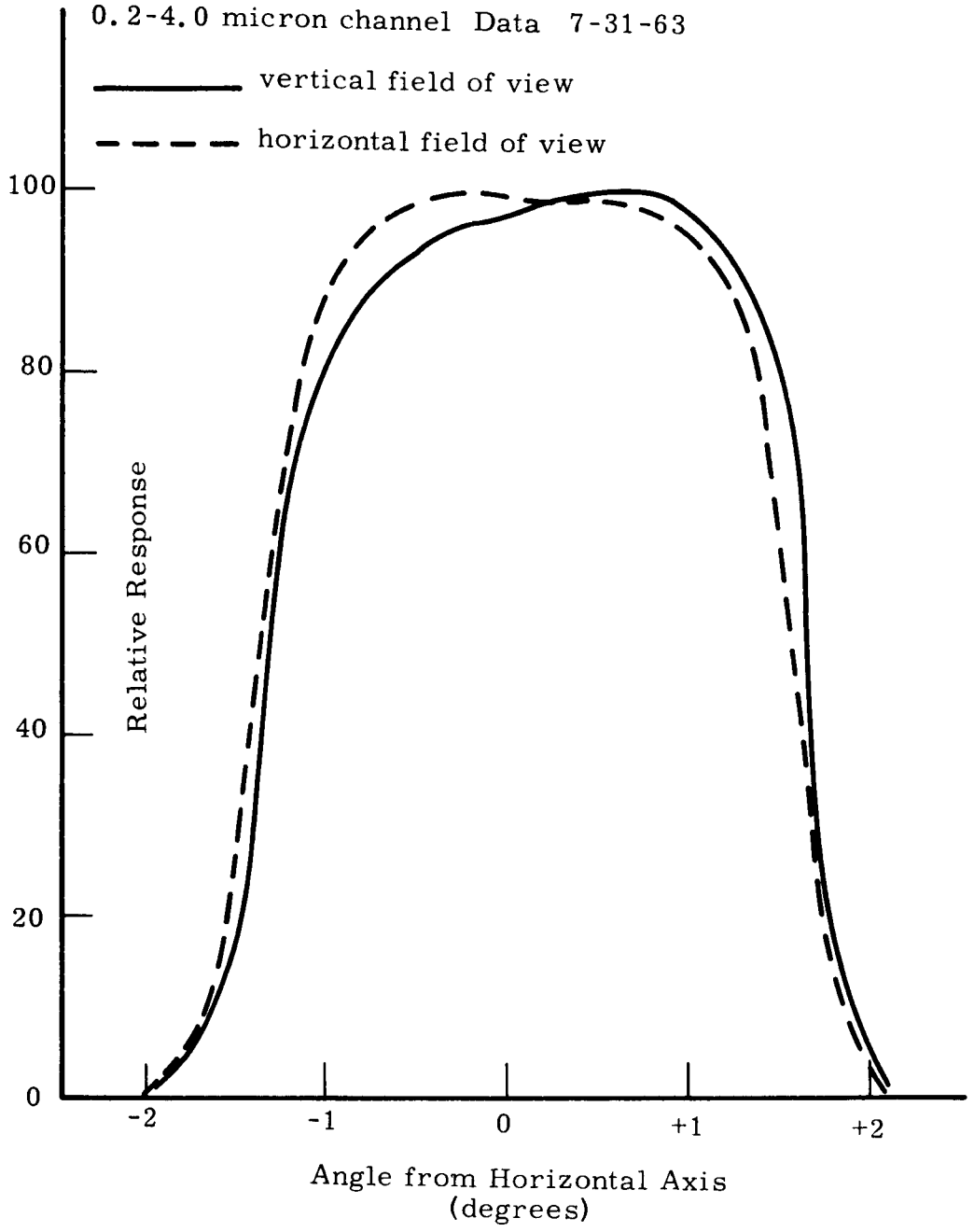

Figure 4. Field of view contours of the 0.2-4.0 micron channel of the F-4 MRIR.

3. METHOD OF CALIBRATION

The method used for the calibration of the MRIR visible channels is referred to in the literature[3] as the "near-extended source method." A diffuse source larger than the radiometer aperture, which will completely fill the radiometer field of view, is placed a short distance from the radiometer, so that the transmissivity of the medium between the source and the instrument is essentially unity. The radiant emittance of the source, assumed to be uniform over the radiometer field of view, is varied over the range of values desired. Corresponding values of source radiant emittance and radiometer output voltage are recorded. These data provide the basis for calibration curves which must be interpreted as indicated in the following discussion.

The characteristics of a perfectly diffuse calibration source are given by:

$$N_c = \int_0^\infty N_{c\lambda}\, d\lambda \quad \text{watts} \cdot \text{cm}^{-2} \cdot \text{steradian}^{-1}$$

$$W_c = \int_0^\infty W_{c\lambda}\, d\lambda \quad \text{watts} \cdot \text{cm}^{-2}$$

and the relations

$$N_c = \frac{W_c}{\pi}, \quad N_{c\lambda} = \frac{W_{c\lambda}}{\pi}$$

where

$N_{c\lambda}$ is the spectral radiance, watts $\cdot$ cm$^{-2}\cdot$ steradian$^{-1}\cdot$ micron^{-1}.
$N_{c\lambda}$ is the spectral radiant emittance, watts $\cdot$ cm$^{-2}\cdot$ micron^{-1}.
N_c is the radiance, watts $\cdot$ cm$^{-2}\cdot$ steradian^{-1}.
W_c is the radiant emittance, watts $\cdot$ cm^{-2}.

The equation which describes the output voltage of a visible channel of the radiometer when its entire field of view is uniformly illuminated by the calibration source is:

$$V_c = R' \cdot A_r \cdot \Omega \cdot N_c' \qquad (1)$$

or

$$V_c = R' \cdot A_r \cdot \Omega \cdot \frac{W_c'}{\pi}$$

where

R' is the responsivity of the channel of the radiometer averaged over the entire field of view, volts/watt.
A_r is the effective area of the radiometer aperture, cm^2.
Ω is the solid angle viewed by the radiometer, steradians.
N_c' is the "effective" radiance of the diffuse calibration source, watts $\cdot$ cm^{-2} $\cdot$ $steradian^{-1}$.
W_c' is the "effective" radiant emittance of the diffuse calibration source, watts $\cdot$ cm^{-2}.

N_c', the effective radiance, is the quantity which actually effects the radiometer. Its value is given by the integral:

$$N_c' = \int_0^\infty N_{c\lambda} \cdot \phi_\lambda \cdot d\lambda \qquad (2)$$

where

ϕ_λ is the effective spectral response of the radiometer channel.
λ is the wavelength in microns.

In the case of the perfectly diffuse source that we assumed, we also have the relation:

$$W_c' = \pi N_c' = \int_0^\infty W_{c\lambda} \cdot \phi_\lambda \cdot d\lambda$$

To simplify the discussion in the remainder of this report we will consider only the values of radiance N_c or N_c'. Values of radiant emittance W_c or W_c' can be calculated if desired and if warranted.

To summarize, the calibration procedure consists of the following steps.

(a) Vary N_c of the diffuse calibration source for which the distribution of spectral radiance is known.

(b) Record corresponding values of the radiometer output voltage V_c and the source radiance N_c.

(c) For a given value of N_c, calculate a corresponding value of N_c', using Equation (2). Values of $N_{c\lambda}$ and ϕ_λ must be known.

(d) Plot the calibration curves of V_c vs. N_c'.

This calibration procedure should be carried out at several instrument temperatures covering the range of temperatures over which the instrument may operate.

4. INTERPRETATION OF THE MRIR DATA

4.1. PERCENT REFLECTANCE

The visible channels of the MRIR radiometer are designed to obtain a measurement of the fraction of incident solar radiation which is reflected or scattered back out into space from the surface of the earth, the clouds and the atmosphere. Thus the attempt is made to interpret the radiometer readings in terms of an equivalent average "reflectivity" or "albedo" of that portion of the earth and its atmosphere lying within the radiometer field of view.

The interpretation is made as follows. Recall that the solar constant is defined to be the amount of solar radiation received at normal incidence (i.e., on a plane surface normal to the sun's rays) outside of the atmosphere at the mean earth-sun distance. The value used is 2.0 langleys $min.^{-1}$ (2 cal. cm^{-2}. $min.^{-1}$ or 0.1395 watts cm^{-2}). The solar constant can be expressed as:

$$H_s = \int_0^\infty H_{s\lambda}\, d\lambda \qquad (3)$$

where

H_s is the solar constant (irradiance), 0.1395 watts . cm^{-2}.
$H_{s\lambda}$ is the solar spectral irradiance in watts . cm^{-2}. $micron^{-1}$.

If one solar constant of radiation at normal incidence is reflected from a perfectly diffuse reflecting surface with spectral reflectance ρ_λ, the radiance of the reflecting surface will be:

$$N_s = \frac{1}{\pi}\int_0^\infty \rho_\lambda\, H_{s\lambda}\, d_\lambda$$

and the reflectance of the surface, averaged over all wavelengths will be:

$$\bar{\rho} = \frac{\frac{1}{\pi}\int_0^\infty \rho_\lambda\, H_{s\lambda}\, d\lambda}{\frac{1}{\pi}\int_0^\infty H_{s\lambda}\, d\lambda} \qquad (4)$$

This average reflectance is a weighted average with weighting function taken to be the spectral distribution of the solar radiation.

Where the surface is received by the visible channel of the MRIR radiometer, the radiometer voltage will be:

$$V_s = R' \cdot A_r \cdot \Omega \cdot N'_s$$

where N'_s is the effective radiance of the reflected solar constant, i.e.,

$$N'_s = \frac{1}{\pi} \int_0^\infty \rho_\lambda \, H_{s\lambda} \, \phi_\lambda \, d\lambda$$

For $\rho_\lambda = 1$ (i.e., 100% reflectance), then we would have:

$$N'_s(100\%) = \int_0^\infty H_{s\lambda} \, \phi_\lambda \, d\lambda$$

For $\rho_\lambda \neq 1$, we may calculate an "effective" average reflectance of the surface:

$$\bar{\rho}' = \frac{\frac{1}{\pi} \int_0^\infty \rho_\lambda \, H_{s\lambda} \, \phi_\lambda \, d\lambda}{\frac{1}{\pi} \int_0^\infty H_{s\lambda} \, \phi_\lambda \, d\lambda} \qquad (5)$$

The average reflectance $\bar{\rho}'$ thus obtained is a weighted average with weighting function taken to be the product of spectral distribution of the solar radiation multiplied by the instrument response function.

The calibration curve of the visible channel of the MRIR may be given in terms of percent reflectance by taking that value of N'_c equal to $N'_s(100\%)$ as representing 100% reflectance, for radiation normally incident upon the surface viewed. Further a radiometer voltage reading V_c corresponding to a value of $N'_c = 0.5 \, N'_s(100\%)$ represents a reflectance of 50% for normally incident radiation. Similarly, in general, we define the percent reflectance of solar radiation, as measured by the visible channel of the MRIR radiometer by:

$$\bar{\rho}' = \frac{N'_c}{N'_s(100\%)} = \frac{\int_0^\infty N_{c\lambda} \, \phi_\lambda \, d\lambda}{\frac{1}{\pi} \int_0^\infty H_{s\lambda} \, \phi_\lambda \, d\lambda} \qquad (6)$$

Finally, to correct for angles of incidence other than 90°, it is necessary to divide the value of reflectance obtained by cos Z, where Z is the zenith angle of the incident radiation.

To summarize then, the interpretation of radiometer readings as percent reflectance is made by changing the radiometer calibration curves to the form of $N_c'/N_s'(100\%)$ vs. V_c. For normal incidence, a given radiometer reading corresponds to a reflectance equal to the value of $N_c'/N_s'(100\%)$ obtained from this curve. For other angles of incidence of the solar rays it is necessary to divide by cos Z, where Z is the solar zenith angle. Thus:

$$\bar{\rho}' = \frac{N_c'}{N_s'(100\%) \cdot \cos Z}$$

$$= \frac{\int_0^\infty N_{c\lambda}\, \theta_\lambda \, d\lambda}{\cos Z \cdot \frac{1}{\pi} \int_0^\infty H_{s\lambda} \cdot \theta_\lambda \, d\lambda} \qquad (7)$$

One final correction to be made is a correction for variation in values of $H_{s\lambda}$. Values of $H_{s\lambda}$ used in drawing calibration curves are values for the sun at its mean distance from the earth. Variations of values of $H_{s\lambda}$ during a year are as great at ±3.3% and should be corrected for.

4.2. THE POSSIBILITY OF ERROR IN THE INTERPRETATION

4.2.1. Weighted Average Reflectance

The values of percent reflectance measured by the visible channel of the MRIR differ from the actual reflectance which we desire to measure as follows:

For normal incidence, we want to measure:

$$\bar{\rho} = \frac{\frac{1}{\pi} \int_0^\infty \rho_\lambda \, H_{s\lambda} \, d\lambda}{\frac{1}{\pi} \int_0^\infty H_{s\lambda} \, ds} \qquad (5)$$

We actually measure:

$$\bar{\rho}' = \frac{\frac{1}{\pi}\int_0^\infty \rho_\lambda H_{s\lambda} \Phi_\lambda \, d\lambda}{\frac{1}{\pi}\int_0^\infty H_{s\lambda} \Phi_\lambda \, d\lambda} = \frac{\int_0^\infty N_{c\lambda} \Phi_\lambda \, d\lambda}{\frac{1}{\pi}\int_0^\infty H_{s\lambda} \Phi_\lambda \, d\lambda} \qquad (7)$$

In addition to calibration errors, which relate to the substitution of

$$\int_0^\infty N_{c\lambda} \Phi_\lambda \, d\lambda$$

for

$$\int_0^\infty \rho_\lambda H_{s\lambda} \Phi_\lambda \, d\lambda \, ,$$

we have the error in interpretation due to the fact that we have measured a weighted average reflectance using the weighting function $H_{s\lambda} \Phi_\lambda$ instead of the function $H_{s\lambda}$.

Weighting functions for the visible channels of the F-1 and F-4 MRIR radiometers are shown in Figures 5 and 6. The weighting function $N_{s\lambda} \Phi'_\lambda$ for the narrow band channel of the F-1 MRIR is limited to the range 0.55 to 0.85 micron and emphasizes the range of 0.58 to 0.7 micron. The weighting function $H_{s\lambda} \Phi_\lambda$ for the wide band channel of the F-4 MRIR places less emphasis on the wavelength region below 1 micron than the $H_{\lambda s}$ weighting function would. Since the response of the wide band channel is essentially the same for both the F-1 and F-4 radiometers, only one curve has been shown in Figure 6.

It is obvious that the reflectances measured with the 0.55-0.75 micron channel of the radiometer cannot be interpreted as 0.2-4 micron reflectances, except possibly in very special cases. Also the difference in emphasis of the 0.2-4.0 micron $H_{\lambda s} \Phi_\lambda$ weighting function from the desired $H_{\lambda s}$ weighting function may lead to significant errors in certain cases. Examples will be given in Section 8.2 of this report.

4.2.2. Directional Effects

The quantity $\bar{\rho}'$, measured by the radiometer is the bi-directional reflectance illustrated in Figure 7.

In this figure, ds is an element of the reflecting surface, (θ_1, Φ_1) are the zenith and azimuth angles of the incident ray, and (θ_2, Φ_2) are zenith and azimuth angles of a reflected ray.

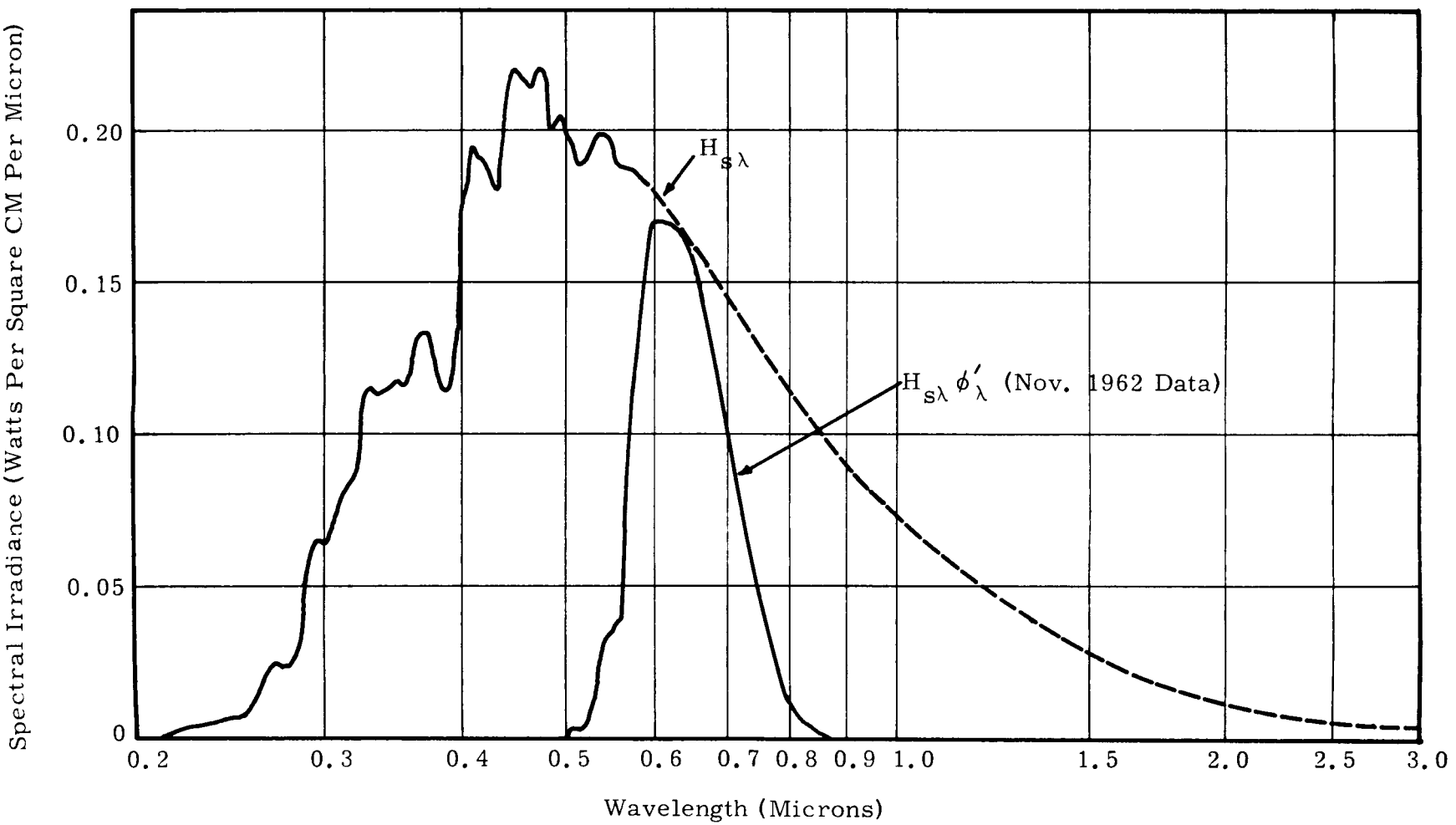

Figure 5. Weighting function, $H_{s\lambda}\phi'_{\lambda}$, for 0.55-0.85 micron channel of F-1 radiometer.

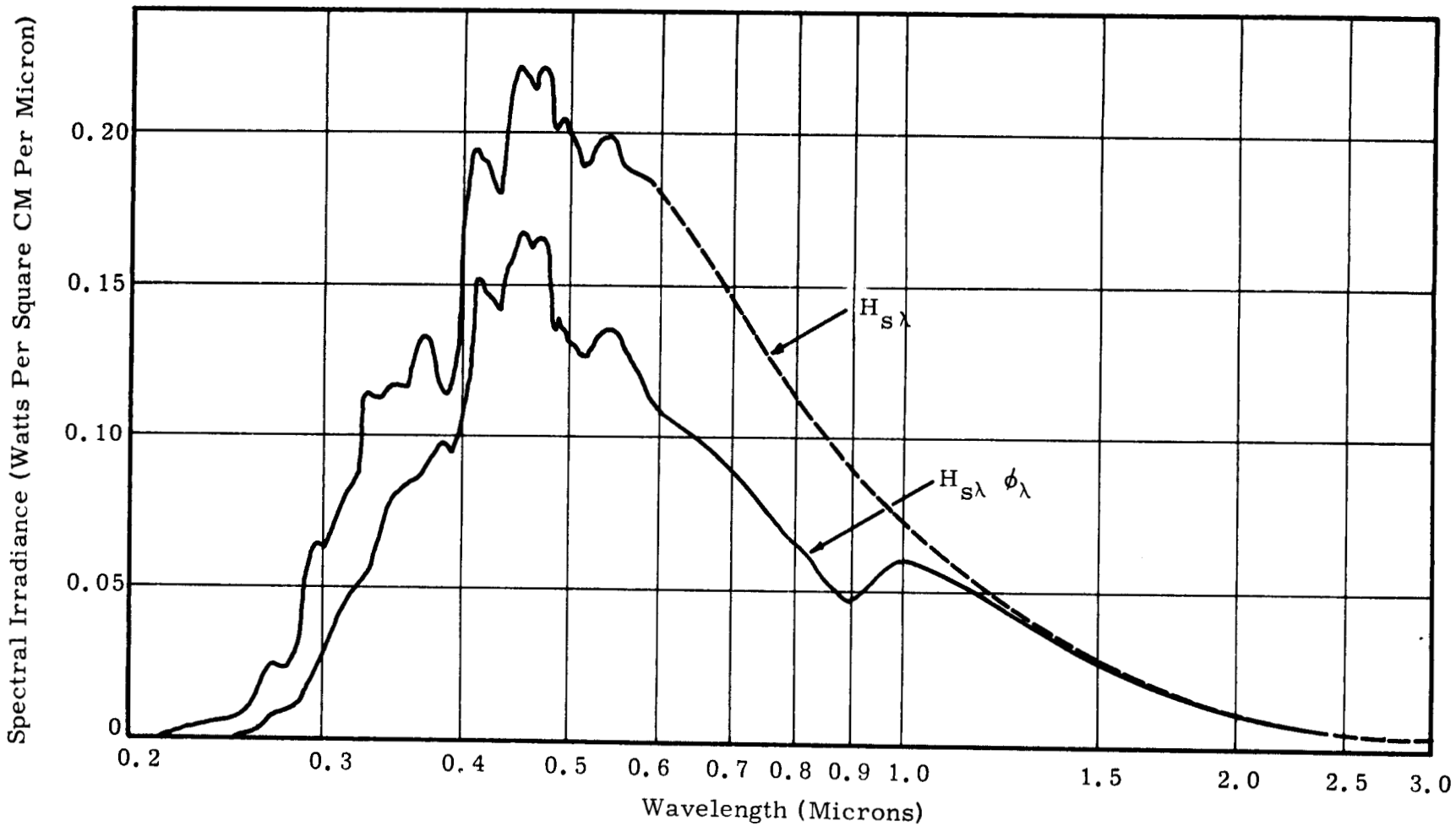

Figure 6. Weighting function, $H_{s\lambda}\phi_\lambda$, for 0.2-4.0 micron channel of F-4 radiometer.

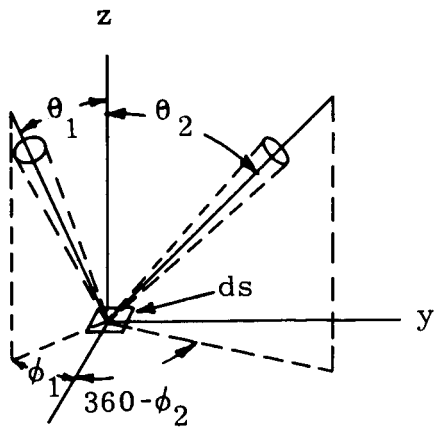

Figure 7. Bi-directional reflectance.

The quantity $\rho(\theta_1,\phi_1,\theta_2,\phi_2)$ is called the bi-directional reflectance. The total (hemispherical) reflectance of the surface for radiation incident from the direction (θ_1,ϕ_1) is called the directional reflectance:

$$r(\theta_1,\phi_1) = \frac{1}{\pi}\int_{\phi_2=0}^{2\pi}\int_{\theta_2=0}^{\pi/2} \rho(\theta_1,\phi_1,\theta_2,\phi_2)\ \sin\theta_2\ \cos\theta_2\ d\theta_2\ d\phi_2 \qquad (8)$$

If the surface is a perfectly diffuse reflector then $\rho(\theta_1,\phi_1,\theta_2,\phi_2) = \rho$, a constant, and

$$r(\theta_1,\phi_1) = \rho$$

If the reflecting surface is not diffuse then, it is necessary to measure $\rho(\theta_1,\phi_1,\theta_2,\phi_2)$ over the hemisphere (i.e., all angles θ_2,ϕ_2) for a large number of incident angles, in order to make a correct interpretation. The characteristics of the reflectance and scattering of solar radiation by the earth and its atmosphere is of the non-diffuse type and therefore the assumption of diffuse reflectance may result in significant error.

Errors in interpretation of NIMBUS MRIR data due to neglect of directional reflectance characteristics will be discussed more completely in another report.

5. DESCRIPTION OF CALIBRATION SOURCES

5.1. SOURCE CHARACTERISTICS

The calibration provides values of the integral

$$\int_0^\infty N_{c\lambda}\, \phi_\lambda\, d\lambda$$

corresponding to radiometer voltage readings. Thus it is necessary to know accurately the values of $N_{c\lambda}$ over the spectral range of the channel (0.2-4 microns). In addition the source should have uniform radiance $N_{c\lambda}$ over the entire area within the radiometer field of view. The intensity of the source should be variable in magnitude so that values of the integral covering the range of 0 to 100% reflectance (or greater) can be obtained. At any intensity setting, the source should be stable for a length of time suitable for the calibration.

5.2. THE UNIVERSITY OF MICHIGAN CALIBRATION SOURCES

5.2.1. Introduction

Three sources have been used at The University of Michigan for the calibration of the visible channels of the F-1 and F-4 MRIR's. The basic configurations are similar for all three of these sources. Radiation from a lamp of a suitable type is allowed to reflect diffusely from a specially prepared surface.

In general, the characteristics of the reflected radiation are determined as follows. The relative spectral distribution of the reflected light $\psi_{c\lambda}$ is determined by comparison with the known spectral distribution of a secondary standard lamp calibrated by the National Bureau of Standards. The total radiance of the target:

$$\int_0^\infty N_{c\lambda}\, d\lambda$$

is determined by an Eppley thermopile which has been calibrated by comparison to a secondary standard thermopile. The absolute values of the spectral radiance $N_{c\lambda}$ are then calculated from:

$$N_{c\lambda} = k_n \psi_{c\lambda}$$

where k is obtained from:

$$k_n \int_0^\infty \psi_{c\lambda} \, d\lambda = \int_0^\infty N_{\lambda c} \, d\lambda \qquad (9)$$

The diffuse nature of the reflection of radiation from the reflecting surface is established by measurements made at various reflection angles. The characteristics must be established at all levels of intensity which are used in the calibration run.

5.2.2. Carbon Arc—MgO Reflector

The first source for the MRIR calibration consisted of a Strong Engineering Company UHI carbon arc with MgO coated flat reflector plate. The arrangement is shown schematically in Figure 8. The radiation from the carbon arc is reflected by an elliptical mirror, passes through an opening in the baffle system,is incident upon the MgO reflector plate and reflected into the MRIR. The diffuse nature of the reflectance of an MgO reflector has been well established.[4]

Because of the poor stability of the carbon arc, the intensity of the reflected radiation is continuously monitored during the calibration by the Eppley thermopile. The baffles are used to prevent radiation from reaching the MRIR or Eppley thermopile by reflection from objects other than the MgO plate.

The intensity of the radiation falling on the MRIR is varied by changing the angle θ and thus changing the angle of incidence of the radiation on the flat plate.

The relative spectral radiance of this source is given in Table II and Figure 9. Although it was possible to use this source for calibration of the MRIR, several characteristics, i.e., its basic instability and very high power dissipation made it difficult to use.

Although the carbon arc system is built with a rough servo control to maintain the position of the rods and thus the arc as carbon burns off of the end of the rod, the arc itself moves around slightly with resulting intensity and spectral changes of the radiation being used for calibration.

The very high power dissipation (10 kilowatts) of the carbon arc resulted in a general heating of the apparatus and indeed of the room itself. This gradual change of thermal radiation environment with time made it difficult to maintain accuracy in the calibration procedure.

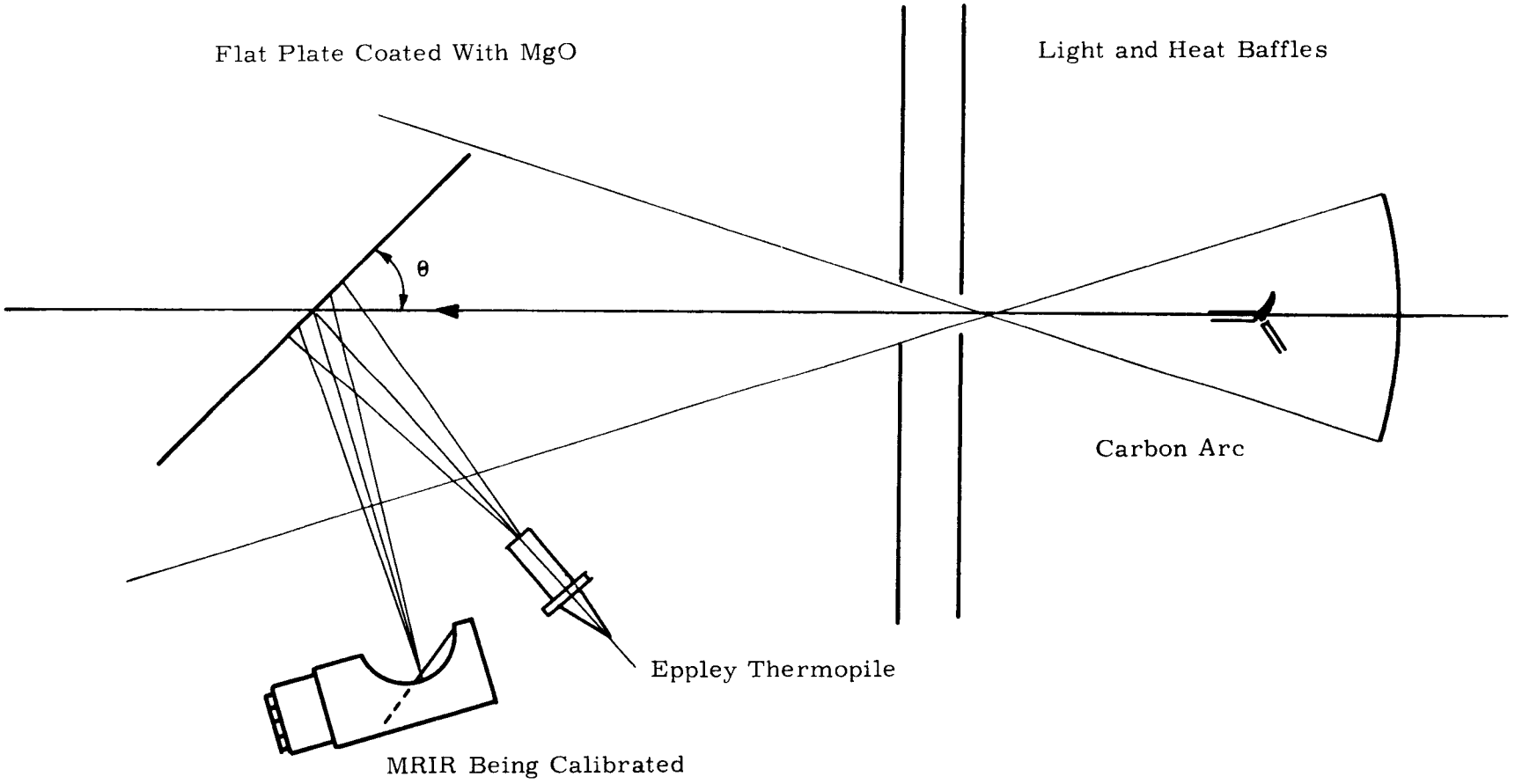

Figure 8. Carbon arc—MgO reflector calibration source.

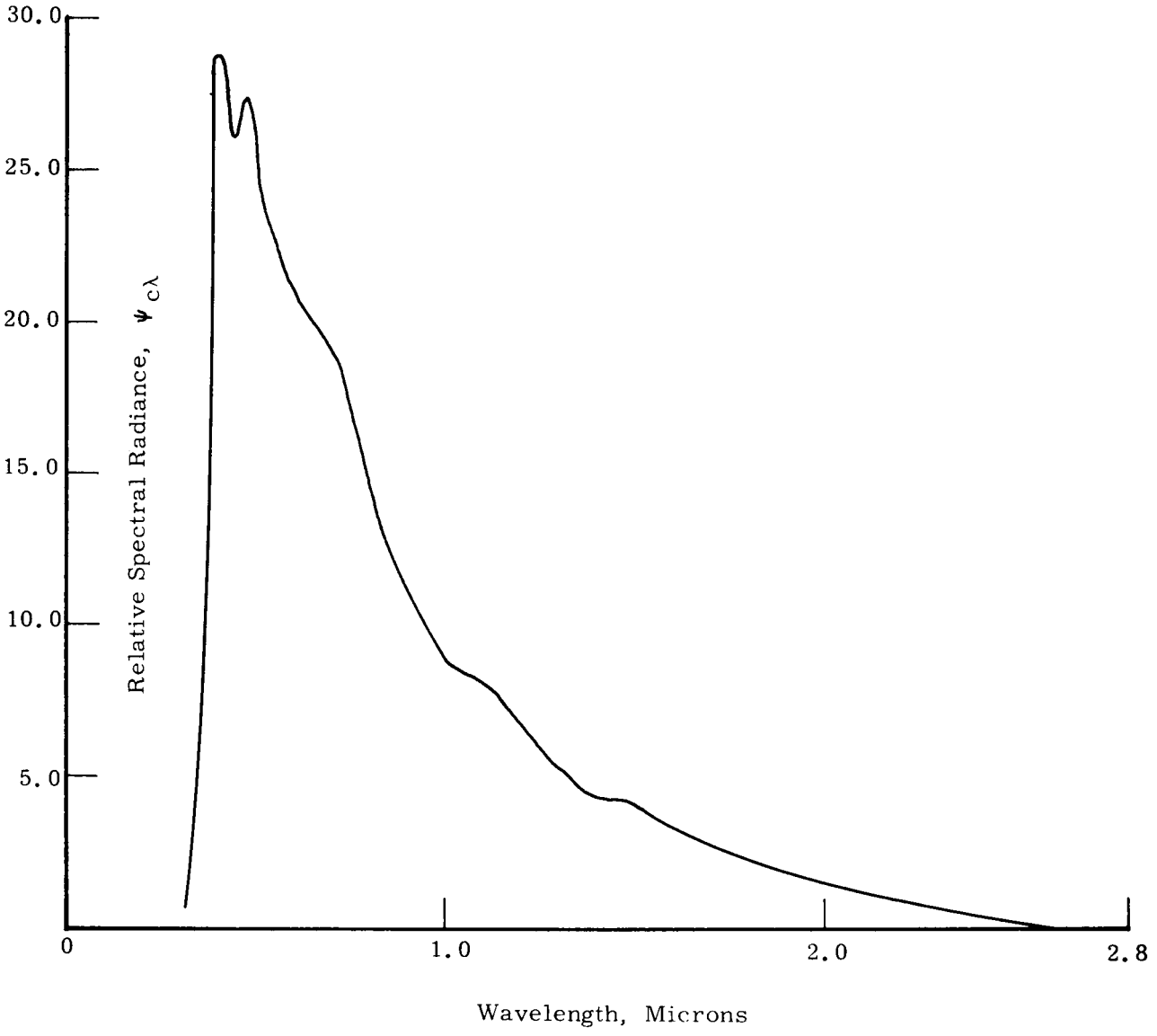

Figure 9. Relative spectral radiance of carbon arc—MgO reflector calibration source.

TABLE II

RELATIVE SPECTRAL RADIANCE OF CARBON ARC AND MgO REFLECTOR CALIBRATION SOURCE

λ Wavelength, micron	Relative Spectral Emittance, $\psi_{c\lambda}$	λ Wavelength, micron	Relative Spectral Emittance, $\psi_{c\lambda}$	λ Wavelength, micron	Relative Spectral Emittance, $\psi_{c\lambda}$
0.24	0	0.76	16.8	1.40	4.4
0.28	0	0.78	15.8	1.44	4.3
0.32	1.1	0.80	14.7	1.48	4.2
0.36	7.6	0.82	13.7	1.52	3.9
0.40	28.8	0.84	12.9	1.56	3.6
0.44	26.2	0.86	12.3	1.60	3.4
0.48	27.3	0.88	11.8	1.64	3.1
				1.68	2.8
0.50	26.3	0.92	10.8	1.72	2.6
0.52	23.8	0.96	9.9	1.76	2.4
0.54	22.9	1.00	9.0	1.80	2.3
0.56	22.3	1.04	8.6	1.84	2.1
0.58	21.5	1.08	8.3	1.88	2.0
0.60	21.0	1.12	7.9	1.92	1.8
0.62	20.6	1.16	7.4	1.96	1.6
0.64	20.2	1.20	6.7	2.00	1.5
0.66	19.9	1.24	6.1		
0.68	19.5	1.28	5.5	2.20	0.9
0.70	19.2	1.32	5.1	2.40	0.4
0.72	18.6	1.36	4.6	2.60	0
0.74	17.8				

5.2.3. Tungsten Filament Lamp—MgO Reflector

The arrangement of the second source used for MRIR calibration at The University of Michigan is shown schematically in Figure 10. Radiation from a 2000 watt tungsten filament lamp is allowed to reflect from the flat MgO reflector plate. The intensity of the calibration source is varied by changing the distance R between the lamp filament and the reflector plate surface.

The spectral radiance of this source was determined as noted above in Section 5.2.1 and then checked as follows. The spectral distribution of the irradiance of the lamp at R = 1 meter was determined by comparison with several working standards of radiance. Data on the spectral reflectivity of a MgO coated plate were obtained from the literature and extended by measurements in our laboratory.

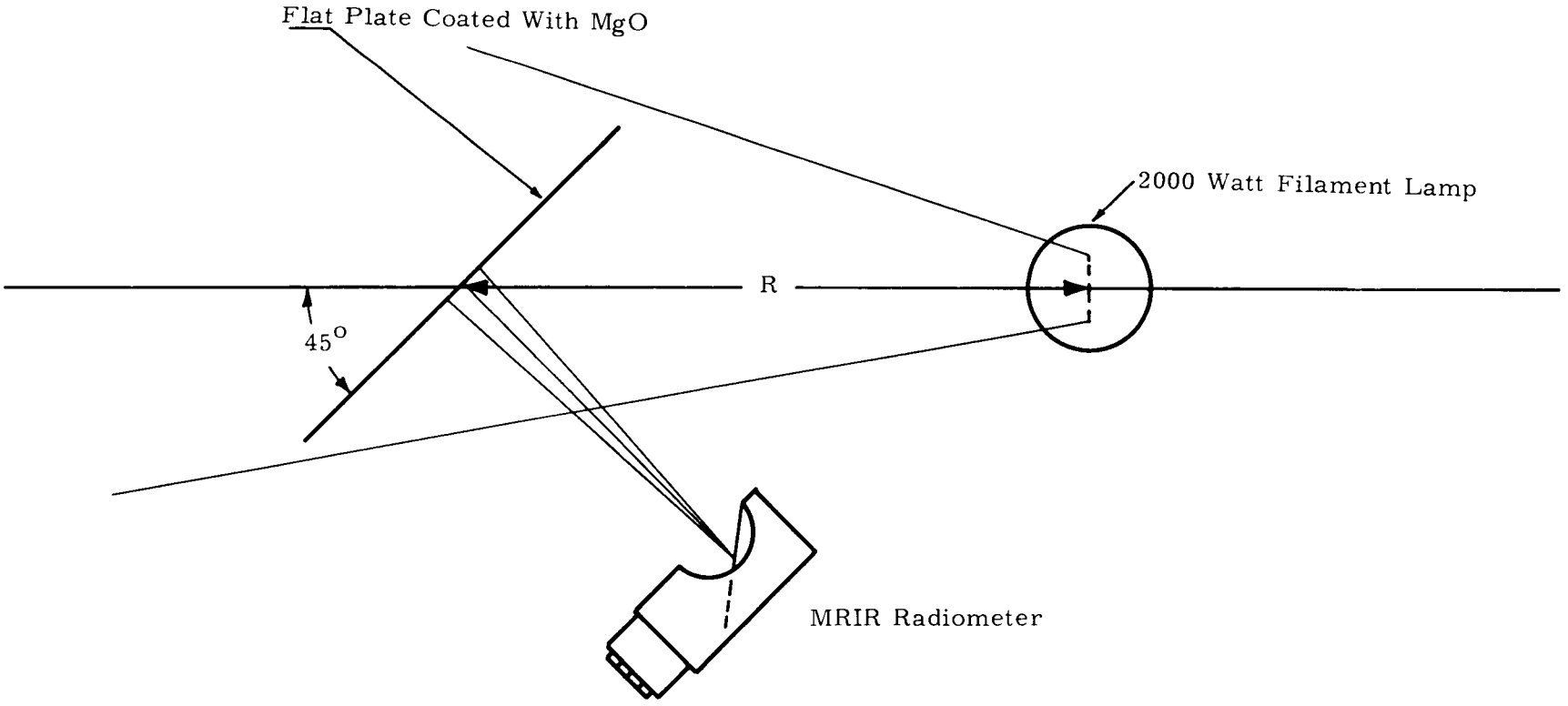

Figure 10. Tungsten filament lamp—MgO reflector calibration source.

The spectral radiance of the source was then calculated from the relation

$$N_\lambda = \frac{H_\lambda \cdot \rho_\lambda \cdot \cos 45^\circ}{R^2} \text{ watts} \cdot m^{-2} \cdot \text{steradian}^{-1} \qquad (10)$$

where

N_λ = the spectral radiance of the MgO reflector.
H_λ = the spectral irradiance of the MgO reflector by the lamp at 1 meter distance.
ρ_λ = the bi-directional reflectance of the MgO reflector.
R = the distance of the lamp from the MgO reflector in meters.

The factor cos 45° enters into the equation because of the 45° angle between the normal to the MgO reflector and the direction of incident radiation from the lamp.

Results obtained by this second technique agree with results obtained by the first technique within about 5%.

The relative spectral radiance of this source as determined by the first technique are given in Table III and Figure 11.

Excess power dissipation and associated heating was still a problem with this source, and maximum albedo values obtained were lower than desired. In addition the MgO coating on the flat plate was extremely delicate. In spite of extreme care, the coating would not last any great length of time. Accordingly a new source was designed to eliminate these difficulties.

5.2.4. Hemisphere Source

The third source built for calibration of the MRIR is shown schematically in Figure 12. Radiation from ten lamps located on the circumference of the hemisphere undergoes multiple reflections in the hemisphere before passing through the exit hole. All portions of the inside surface are brush coated with Burch sphere paint No. 2210 over Burch No. 2201-S undercoat.

The lamps mounted around the circumference of the hemisphere are 150 watts each, General Electric No. 1958 incandescent quartz-iodine. The intensity of radiation emitted by the hemisphere is varied by turning on the number of lamps in units of two (diametrically located). Usually 5 steps of 2, 4, 6, 8, 10 lamps are used.

The relative spectral radiance of this source is given in Table IV and Figure 13.

TABLE III

RELATIVE SPECTRAL RADIANCE OF 2000-WATT TUNGSTEN LAMP AND MgO REFLECTOR CALIBRATION SOURCE

λ Wavelength, micron	Relative Spectral Emittance, $H_\lambda \rho_\lambda$	λ Wavelength, micron	Relative Spectral Emittance, $H_\lambda \rho_\lambda$	λ Wavelength, micron	Relative Spectral Emittance, $H_\lambda \rho_\lambda$
0.20	0	1.56	71.3	2.92	9.4
0.24	0.10	1.60	67.8	2.96	8.5
0.28	0.40	1.64	64.5	3.00	7.8
0.32	1.10	1.68	61.6	3.04	6.9
0.36	1.8	1.72	58.7	3.08	6.3
0.40	4.6	1.76	55.6	3.12	5.9
0.44	7.3	1.80	52.7	3.16	5.3
0.48	10.6	1.84	49.6	3.20	5.0
0.52	15.6	1.88	46.9	3.24	4.5
0.56	22.0	1.92	44.5	3.28	4.1
0.60	30.6	1.96	42.3	3.32	3.9
0.64	42.1	2.00	38.5	3.36	3.7
0.68	53.2	2.04	38.3	3.40	3.4
0.72	62.3	2.08	36.6	3.44	3.2
0.76	70.9	2.12	35.1	3.48	3.0
0.80	78.1	2.16	33.3	3.52	2.8
0.84	84.4	2.20	31.9	3.56	2.6
0.88	89.6	2.24	30.2	3.60	2.3
0.92	93.9	2.28	28.8	3.64	2.1
0.96	96.7	2.32	27.4	3.68	2.0
1.00	99.1	2.36	26.3	3.72	1.9
1.04	100.4	2.40	25.1	3.76	1.8
1.08	100.3	2.44	23.6	3.80	1.7
1.12	99.6	2.48	22.1	3.84	1.7
1.16	98.7	2.52	20.5	3.88	1.5
1.20	97.3	2.56	19.4	3.92	1.3
1.24	95.8	2.60	17.9	3.96	1.1
1.28	93.4	2.64	16.7	4.00	1.0
1.32	90.7	2.68	15.4	4.04	0.80
1.36	87.9	2.72	14.3	4.08	0.60
1.40	84.7	2.76	13.1	4.12	0.40
1.44	81.5	2.80	12.1	4.16	0.20
1.48	78.2	2.84	11.1	4.20	0
1.52	74.9	2.88	10.1		

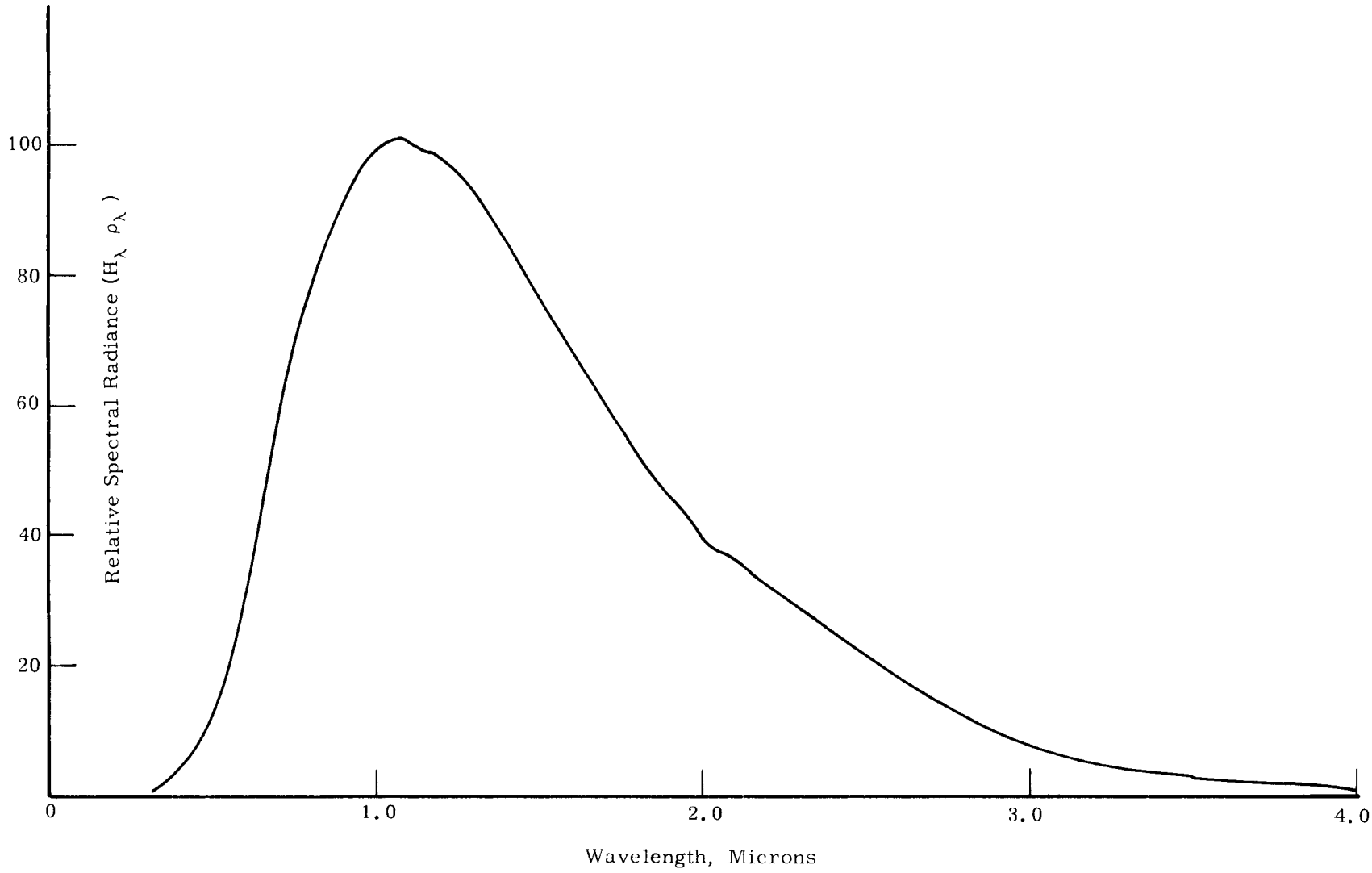

Figure 11. Relative spectral radiance of 2000 watt lamp—MgO reflector calibration source.

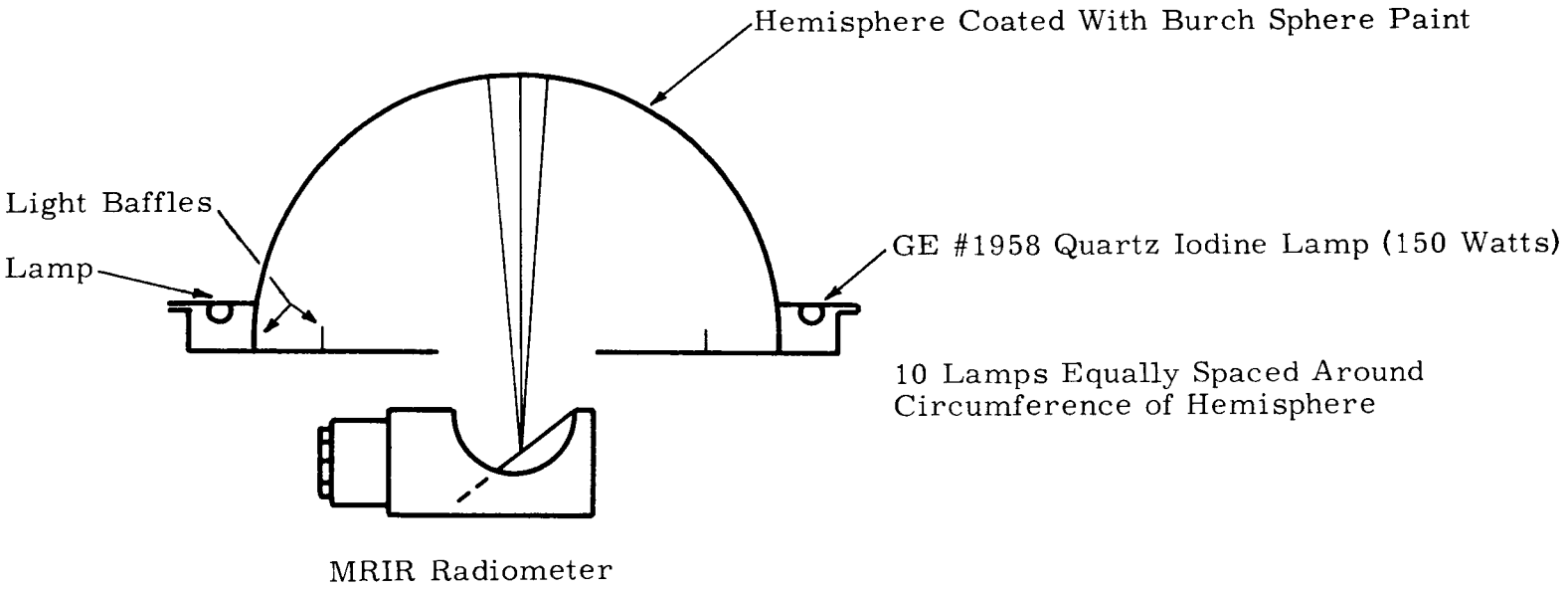

Figure 12. Hemisphere source.

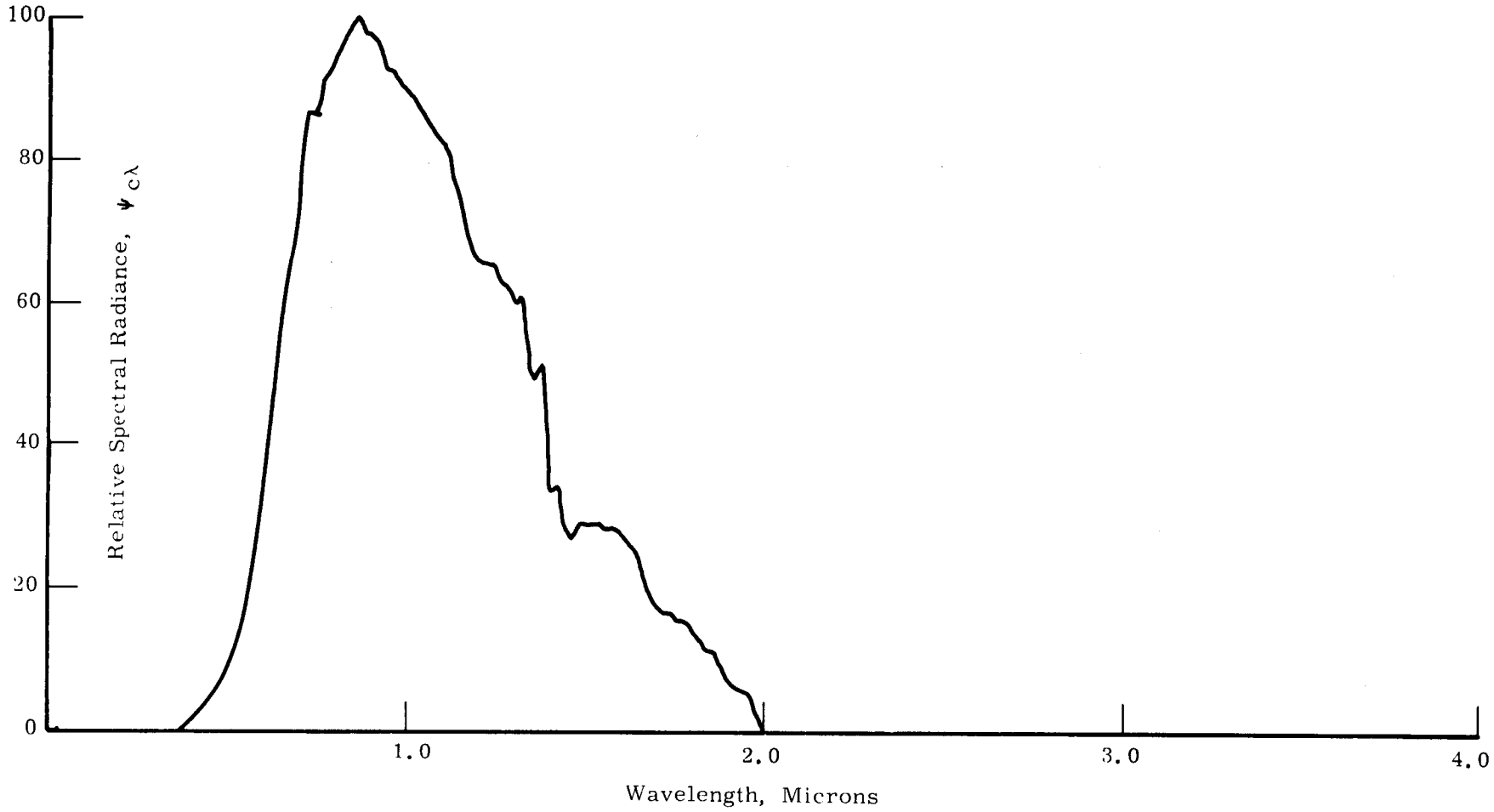

Figure 13. Relative spectral radiance of hemisphere calibration source.

TABLE IV

RELATIVE SPECTRAL RADIANCE OF HEMISPHERE CALIBRATION SOURCE

λ Wavelength, micron	Relative Spectral Emittance, $\psi_{c\lambda}$	λ Wavelength, micron	Relative Spectral Emittance, $\psi_{c\lambda}$	λ Wavelength, micron	Relative Spectral Emittance, $\psi_{c\lambda}$
0.38	0.69	0.94	92.5	1.48	28.9
0.40	1.39	0.96	92.2	1.50	29.6
0.42	2.17	0.98	90.3	1.52	29.0
0.44	3.65	1.00	89.6	1.54	29.0
0.46	4.97	1.02	88.4	1.56	28.5
0.48	6.93	1.04	87.1	1.58	28.4
0.50	8.99	1.06	85.0	1.60	27.7
0.52	12.50	1.08	83.3	1.62	26.5
0.54	15.70	1.10	82.3	1.64	25.3
0.56	20.30	1.12	78.2	1.66	22.1
0.58	25.10	1.14	75.7	1.68	19.6
0.60	34.90	1.16	70.4	1.70	17.6
0.62	46.10	1.18	67.7	1.72	16.7
0.64	53.0	1.20	65.5	1.74	16.7
0.66	63.0	1.22	65.7	1.76	15.8
0.68	67.5	1.24	65.8	1.78	15.4
0.70	75.0	1.26	62.9	1.80	14.5
0.72	86.4	1.28	62.2	1.82	13.7
0.74	86.3	1.30	60.0	1.84	11.7
0.76	90.8	1.32	61.1	1.86	11.7
0.78	92.5	1.34	54.2	1.88	9.14
0.80	94.9	1.36	49.2	1.90	7.40
0.82	96.9	1.38	51.3	1.92	6.46
0.84	99.0	1.40	33.7	1.94	5.93
0.86	100.0	1.42	34.5	1.96	5.78
0.88	97.6	1.44	28.6	1.98	3.00
0.90	97.3	1.46	26.9	2.00	0
0.92	95.4				

This source is relatively easy to use for calibration of the MRIR. Maximum power dissipation is only 1500 watts and this power is only used a fraction of the time.

5.3. SANTA BARBARA CALIBRATION SOURCE

The source used at the Santa Barbara Research Corporation[2] is shown in Figure 14. The size of the source is significantly smaller than those used at The University of Michigan. Indeed it is made small enouth to be used inside of a vacuum system along with black body sources for calibration of the thermal channels of the MRIR.

The General Electric Company No. 212 photo enlarger lamp is the basic source of radiation. It is used with an additional diffuser, lens and plastic filters as shown in Figure 14. In addition several mirrors, not shown in the schematic diagram are used to direct the light to the MRIR under calibration.

The intensity (and spectral distribution) of the lamp are varied by changing the voltage applied to the lamp. Curves of this calibration source radiance for several lamp voltages are shown in Figure 15. Note that the relative spectral distribution changes with lamp voltage.

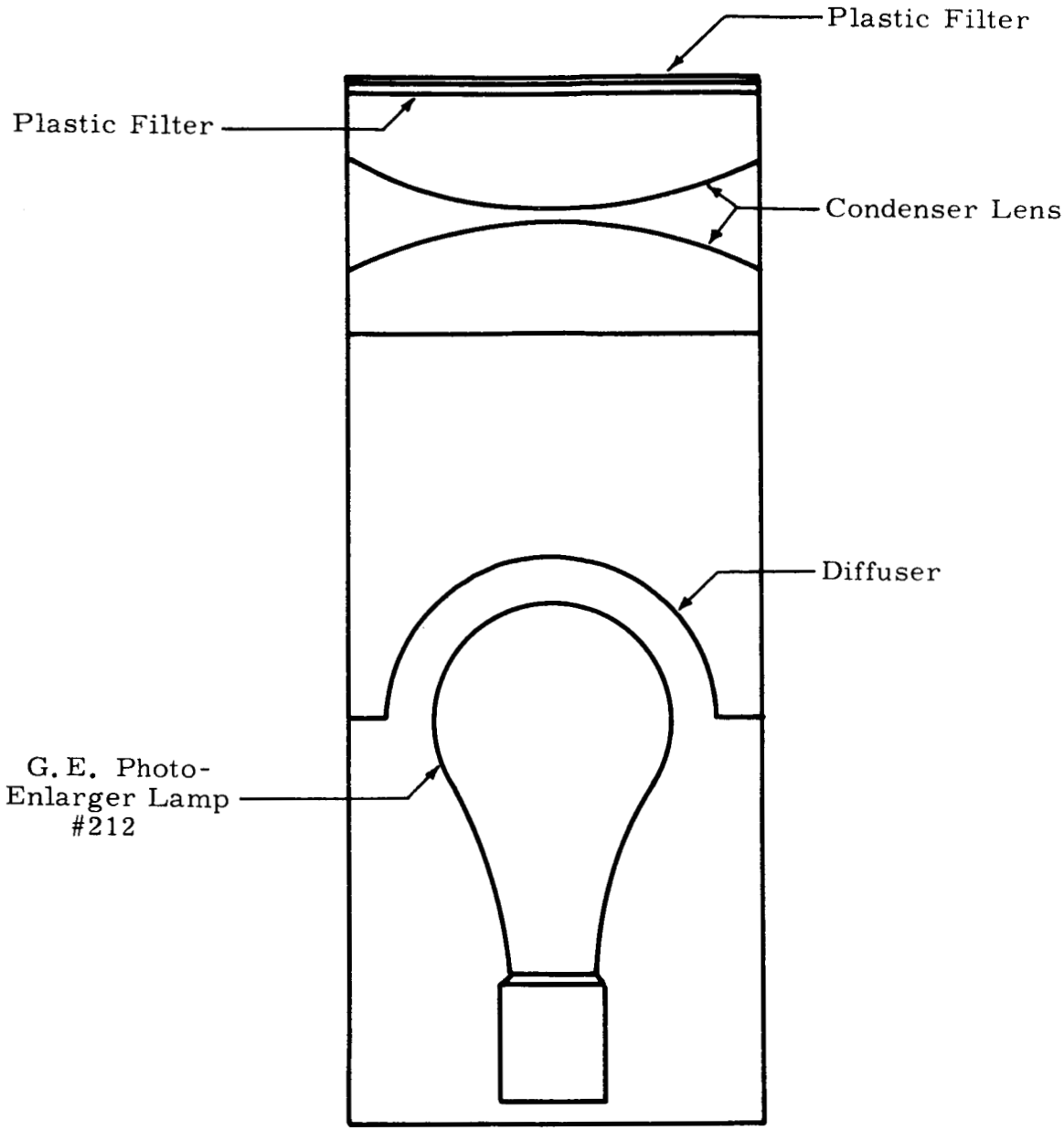

Figure 14. SBRC calibration source.

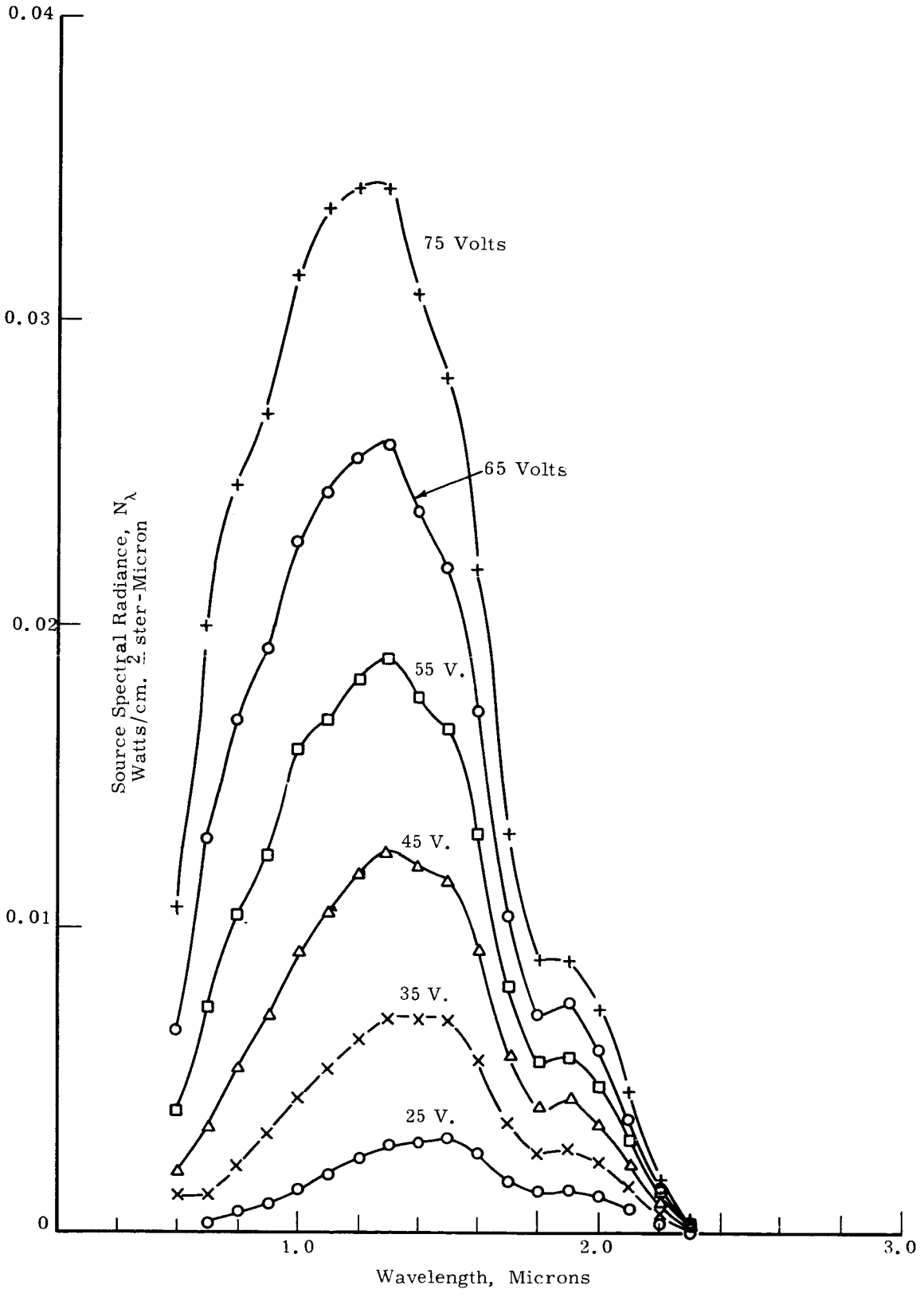

Figure 15. Spectral radiance of SBRC calibration source.

6. IN-FLIGHT CALIBRATIONS

6.1. THE DIRECT SUN SIGNAL CALIBRATION TECHNIQUE

Because of the pronounced deterioration of the TIROS 5-channel radiometer which was noticed on satellite flights of this instrument,[5] provisions have been made for in-flight checks of calibration of the MRIR radiometer.

The arrangement for check of calibration of the 0.2-4 micron channel is shown schematically in Figure 1. The NIMBUS satellite is flown with such orientation that the axis of the scan mirror lies in the orbital plane which is lined up with the sun. During a certain portion of the orbit when the axis of the MRIR is aligned within 6° of the sun, solar radiation will enter the small opening located in the MRIR housing and be reflected down into the scan mirror cavity. When the scan mirror looks vertically upward into the housing this "direct" solar signal is reflected from the scan mirror into the optics of the 0.2-4 micron channel.

The output of the radiometer for this solar calibrate signal can be written as:

$$V_{sc} = R' \int_{\lambda_1}^{\lambda_2} H_{s\lambda}\, \phi_\lambda\, \phi_\lambda^{sc}\, d\lambda \qquad (11)$$

where ϕ_λ^{sc} is a factor which represents the attenuation of the "direct solar signal" in the optical path from the opening of the housing to the scan mirror. Changes in sensitivity due to change in angle within the 6° acceptance angle for solar radiation must be included in this factor.

This direct solar signal check of calibration can be of considerable help in monitoring deterioration of the 0.2-4 micron channel over a period of time provided:

(1) The orbital plane of the satellite does contain the sun.

(2) The orientation of the MRIR direct solar calibrate port is accurately known, since the calibrate signal is a function of angle within the field of view.

A problem arises, however, in monitoring any possible change in the 0.2-4 micron channel in the time between the last check before launch until the first direct solar calibrate signal in orbit. To predict accurately what the first solar calibrate signal will be requires an accurate prelaunch calibration of the direct solar calibrate optics.

6.2. SURFACE CALIBRATION OF THE DIRECT SUN SIGNAL OPTICS

For this calibration the instrument is taken outside on a clear day and allowed to view the sun. The amplitude of this direct sun signal is recorded. A correction factor for the attenuation of the direct solar radiation is then calculated and applied to the recorded sun signal.

In the direct sun signal calibrations at SBRC a single reading is taken with the sun at a high angle. The correction factor is then calculated from the data of solar spectral irradiance at sea level for varying optical air masses taken from the hand book of Geophysics. This data is reproduced in Figure 16. If $H_{s\lambda}$ is the solar irradiance at the top of the atmosphere and $H_{m\lambda}$ is the solar irradiance at sea level, then the correction factor is taken to be:

$$F = \frac{\sum_{\lambda} H_{s\lambda}\, \phi_{\lambda}\, \Delta\lambda}{\sum_{\lambda} H_{m\lambda}\, \phi_{\lambda}\, \Delta\lambda} \qquad (12)$$

Values of $H_{m\lambda}$ were obtained from the curves of Figure 16 by interpolation.

In the direct sun signal calibrations of the F-4 MRIR at Michigan, data was taken on several clear days for many different sun angles. Correction factors were prepared from solar irradiance data taken from the handbook of Geophysics with atmospheric attenuation calculated for Elterman's clear standard atmosphere.[6] The correction factor was calculated from

$$F = \frac{\sum_{\lambda} H_{s\lambda} \cdot \phi_{\lambda}\, \Delta\lambda}{\sum_{\lambda} H_{s\lambda}\, \phi_{\lambda}\, T_{\lambda}^{m}\, \Delta\lambda}$$

where T_{λ}^{m} is the atmospheric transmission through the atmosphere with optical path length m. From Elterman's report:

$$T_{\lambda}^{m} = \exp\left[-\tau_{\lambda}' \cdot m\right] \qquad (13)$$

where the values of extinction optical thickness τ_{λ}' were obtained from Elterman's tables. Values of F were calculated for the F-4 MRIR for optical path lengths of 1, 1.5, 2, 3, 4, and 5 (zenith angles of 0, 48.3°, 60°, 70.6°, 75.5°, and 78.7°, respectively). Details of the calculations are shown in Table V.

The values of F were plotted against m (see Figure 17). This graph can be used to obtain correction factors for solar zenith angles of 0 to 78° (according to Elterman's clear standard atmosphere).

The results of direct sun signal calibrations made on the surface at SBRC and at The University of Michigan, and on a balloon flight are discussed in Section 8.3.

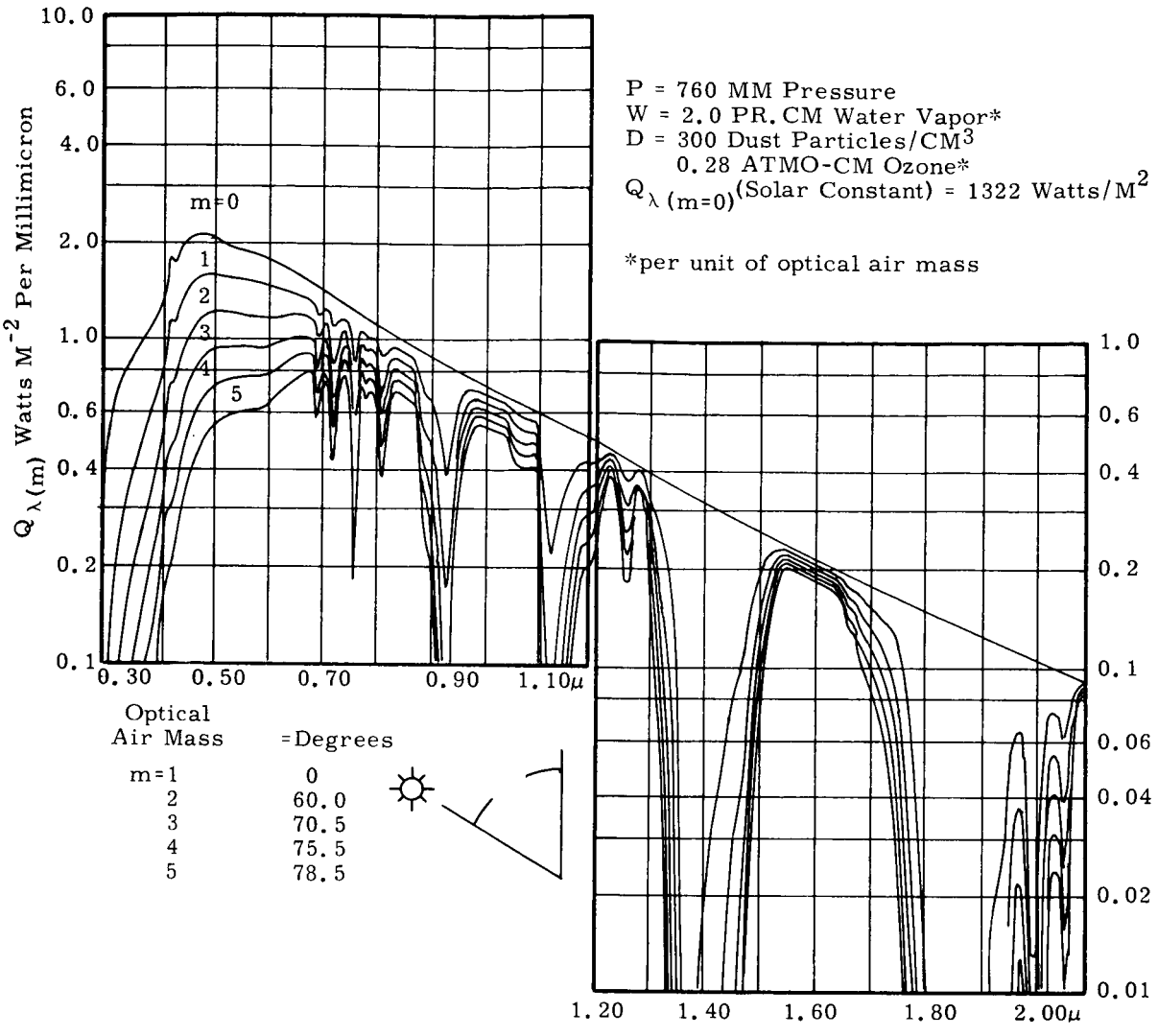

Figure 16. Solar spectral irradiance curves at sea level with varying optical air masses.

TABLE V

CALCULATION OF CORRECTION FACTORS FOR DIRECT SUN SIGNAL CALIBRATION OF F-4 MRIR

λ	$H_{s\lambda}\phi_\lambda\Delta\lambda$	T_λ^1	$H_{s\lambda}\phi_\lambda T^{1}\cdot\Delta\lambda$	$T_\lambda^{1.5}$	$H_{s\lambda}\phi_\lambda T_\lambda^{1.5}\cdot\Delta\lambda$	$H_{s\lambda}\phi_\lambda T_\lambda^{2}\cdot\Delta\lambda$	$H_{s\lambda}\phi_\lambda T_\lambda^{3}\cdot\Delta\lambda$	$H_{s\lambda}\phi_\lambda T_\lambda^{4}\cdot\Delta\lambda$	$H_{s\lambda}\phi_\lambda T_\lambda^{5}\cdot\Delta\lambda$
0.2	0.86	---	---	---	---	---	---	---	---
0.25	8.76	---	---	---	---	---	---	---	---
0.30	27.03	0.25	6.8	0.125	3.9	1.7	0.4	0.1	---
0.35	35.00	0.48	16.8	0.331	11.6	8.1	3.9	1.9	0.9
0.40	52.21	0.59	30.8	0.454	23.7	18.2	10.7	6.3	3.7
0.45	55.06	0.67	36.9	0.549	30.3	24.7	16.5	11.1	7.4
0.50	48.83	0.715	34.8	0.604	29.5	24.9	17.8	12.7	9.1
0.55	49.58	0.725	35.9	0.616	30.6	26.0	18.8	13.6	9.9
0.60	45.84	0.77	35.2	0.675	30.9	27.1	20.9	16.1	12.4
0.65	42.54	0.79	33.6	0.704	30.0	26.6	21.0	16.6	13.1
0.70	37.64	0.815	30.6	0.734	27.6	24.9	20.3	16.5	13.5
0.75	27.97	0.825	23.1	0.75	21.0	19.1	15.8	13.0	10.8
0.80	24.93	0.835	20.8	0.763	19.0	17.4	14.5	12.1	10.1
0.85	25.68	0.84	21.7	0.768	19.7	18.2	15.3	12.9	10.8
0.90	26.83	0.85	22.8	0.786	21.1	19.4	16.5	14.0	11.9
0.95	27.00	0.855	23.1	0.793	21.4	19.7	16.8	14.4	12.3
1.00	50.69	0.86	43.6	0.800	40.5	37.4	32.2	27.7	23.8
1.10	44.98	0.86	38.7	0.80	35.9	33.3	28.6	24.6	21.2
1.20	38.48	0.862	33.1	0.802	28.4	28.5	24.6	21.2	18.3
1.30	32.01	0.865	27.7	0.807	25.8	24.0	20.8	18.0	15.6
1.40	26.57	0.87	23.1	0.814	21.6	20.1	17.5	15.2	13.2
1.50	22.42	0.875	19.6	0.820	18.4	17.2	15.1	13.2	11.6
1.60	18.70	0.88	16.4	0.828	15.5	14.4	12.7	11.2	9.8
1.70	15.40	0.885	13.6	0.835	12.9	12.0	10.6	9.4	8.3
1.80	12.37	0.89	11.0	0.842	10.4	9.8	8.7	7.7	6.9
1.90	10.54	0.89	9.4	0.842	8.8	8.4	7.4	6.7	5.9
2.00	8.94	0.895	8.0	0.848	7.6	7.2	6.5	5.8	5.2
2.10	7.71	0.895	6.9	0.848	6.6	6.2	5.6	5.0	4.5
2.20	6.68	0.896	6.0	0.849	5.7	5.4	4.8	4.3	3.9
2.30	5.77	0.898	5.2	0.849	4.9	4.7	4.2	3.8	3.4
2.40	4.90	0.90	4.4	0.855	4.2	4.0	3.6	3.2	2.9
2.50	4.28	0.901	3.9	0.856	3.6	3.5	3.2	2.9	2.6
2.60	3.82	0.902	3.4	0.857	3.3	3.1	2.8	2.5	2.3
2.70	3.39	0.903	3.1	0.859	2.9	2.8	2.5	2.3	2.0
2.80	3.01	0.904	2.7	0.861	2.6	2.4	2.2	2.0	1.8
2.90	2.63	0.905	2.5	0.862	2.3	2.3	2.1	1.9	1.7
3.00	2.34	0.906	2.1	0.864	2.0	1.9	1.7	1.5	1.4
3.10									
	861.4		657.3		584.2	524.6	426.7	351.4	292.2

$$F_1 = \frac{\sum H_{s\lambda}\phi_\lambda\Delta\lambda}{\sum H_{s\lambda}\phi_\lambda T^{1}\cdot\Delta\lambda} = \frac{861.4}{657.3} = 1.28$$

$$F_2 = \frac{861.4}{584.2} = 1.47$$

$$F_3 = \frac{861.4}{524.6} = 1.64$$

$$F_4 = \frac{861.4}{426.7} = 2.02$$

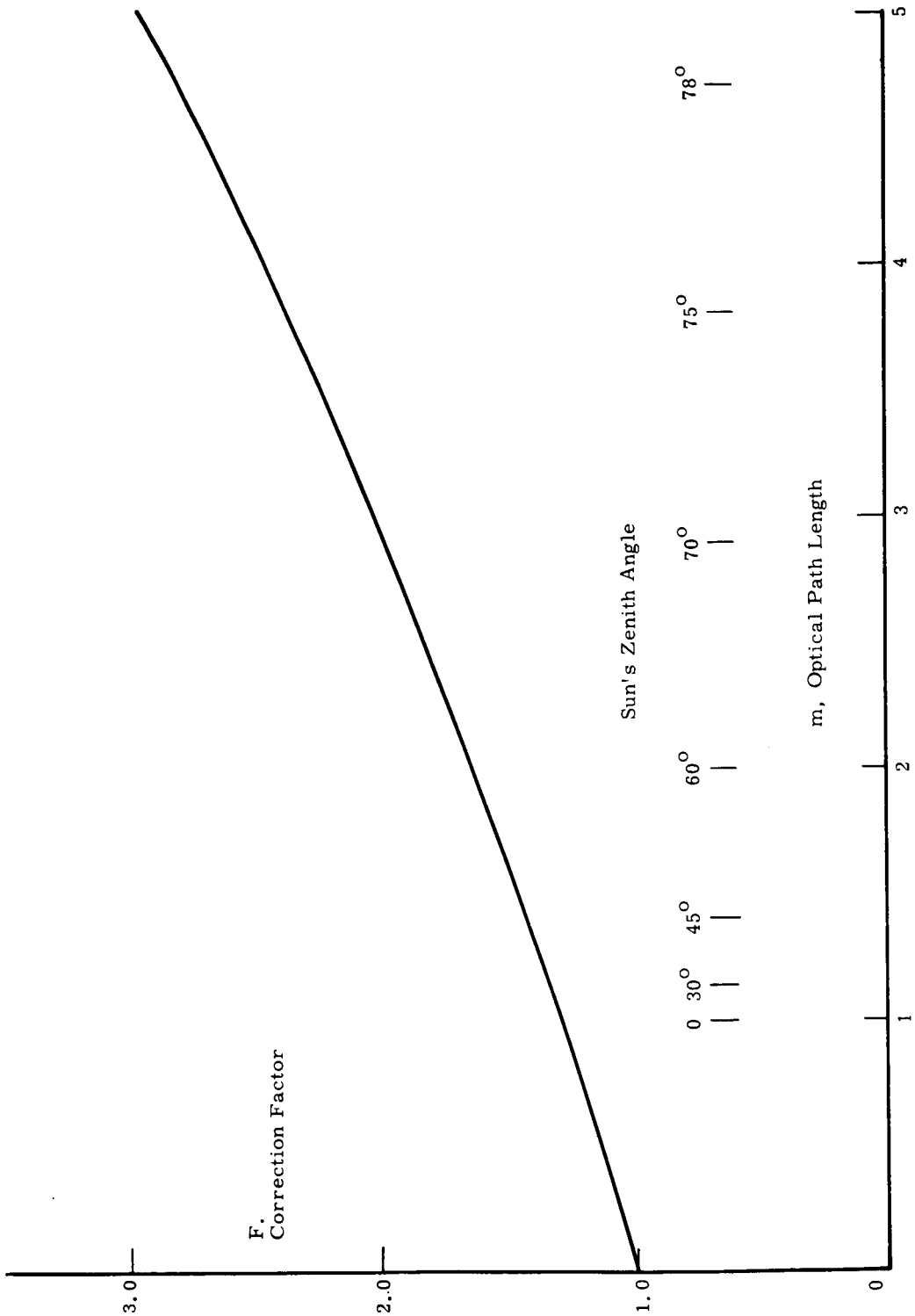

Figure 17. Correction factors for F-4 MRIR direct solar calibrate signals.

7. CALIBRATIONS OF THE F-1 MRIR

7.1. SANTA BARBARA CALIBRATION DATA

Calibrations of the F-1 MRIR were made at SBRC in November, 1962, and in June, 1964. These data are summarized in Reference 7. Both calibrations involved 2 sets of measurements made at the different combinations of scanner and electronic module temperatures; i.e.:

Set 1		Set 2	
Scanner Temperature, °C	Electronic Temperature, °C	Scanner Temperature, °C	Electronic Temperature, °C
50	25	50	50
25	25	0	0
0	25		

For the 0.55-0.85 micron channel, the calibration changed between November, 1962, and June, 1964. Further tests of the instrument at SBRC indicated that this change was due to a decrease in transmission of the 0.55-0.85 micron filter, which had suffered an apparent polymerization of the balsam cement which bonds two elements of the filter. The data are shown in Figures 18 and 19. The change in calibration is shown by comparison of the (25,25) curves for the two calibrations in Figure 20.

The 0.2-4 micron channel showed no change in calibration over this time period. The data are shown in Figures 21 and 22. The two (25,25) curves are shown for comparison in Figure 23. It can be seen that they agree within experimental error.

7.2 THE UNIVERSITY OF MICHIGAN CALIBRATION DATA

Calibrations of the F-1 MRIR were performed at The University of Michigan as follows:

(a) Carbon Arc and MgO Reflector—February, 1963.

(b) Lamp and MgO Reflector—August, 1963.

(c) Hemisphere Source—April and May, 1964.

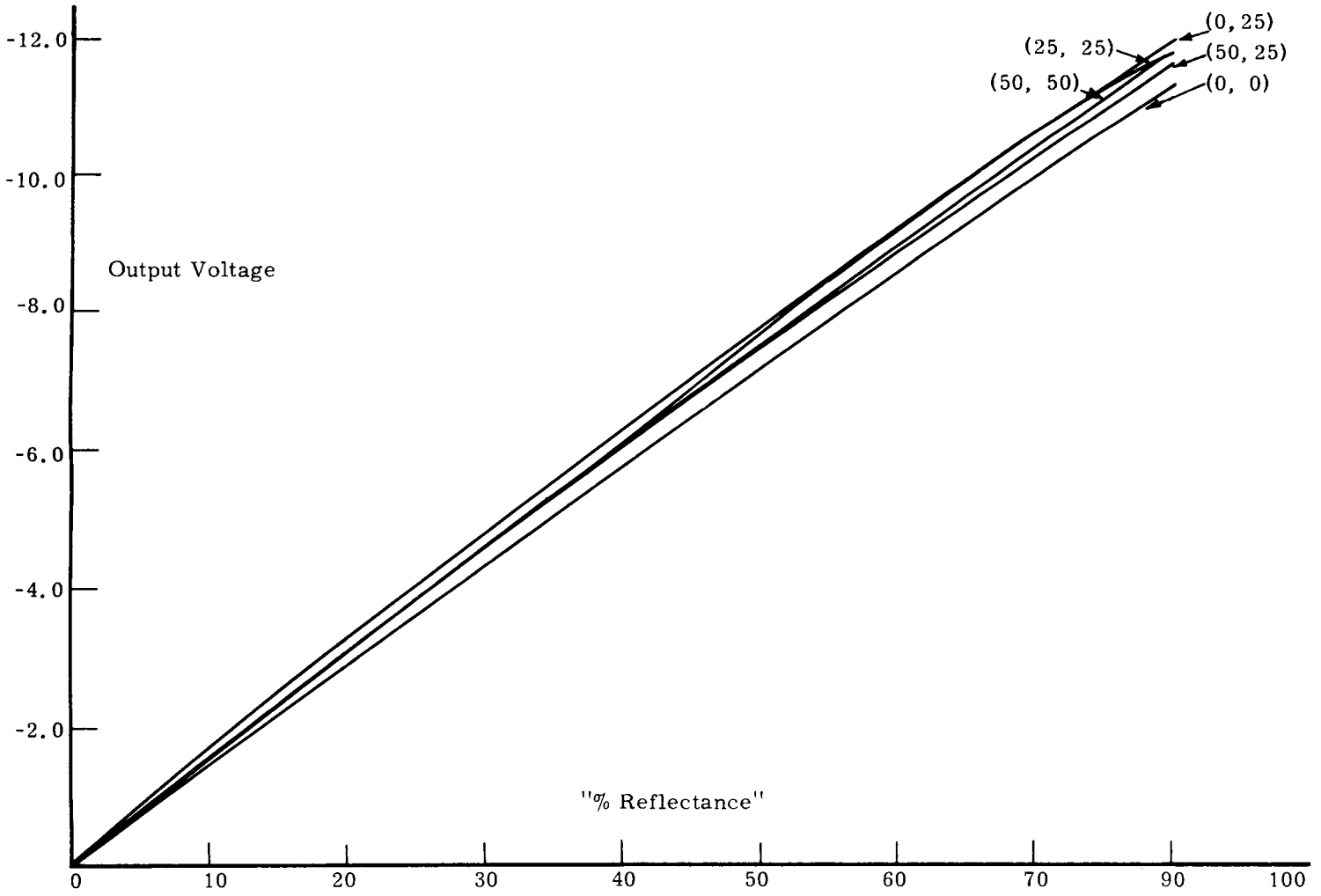

Figure 18. F-1 MRIR calibration data—SBRC data, November 1962, 0.55-0.85 micron channel.

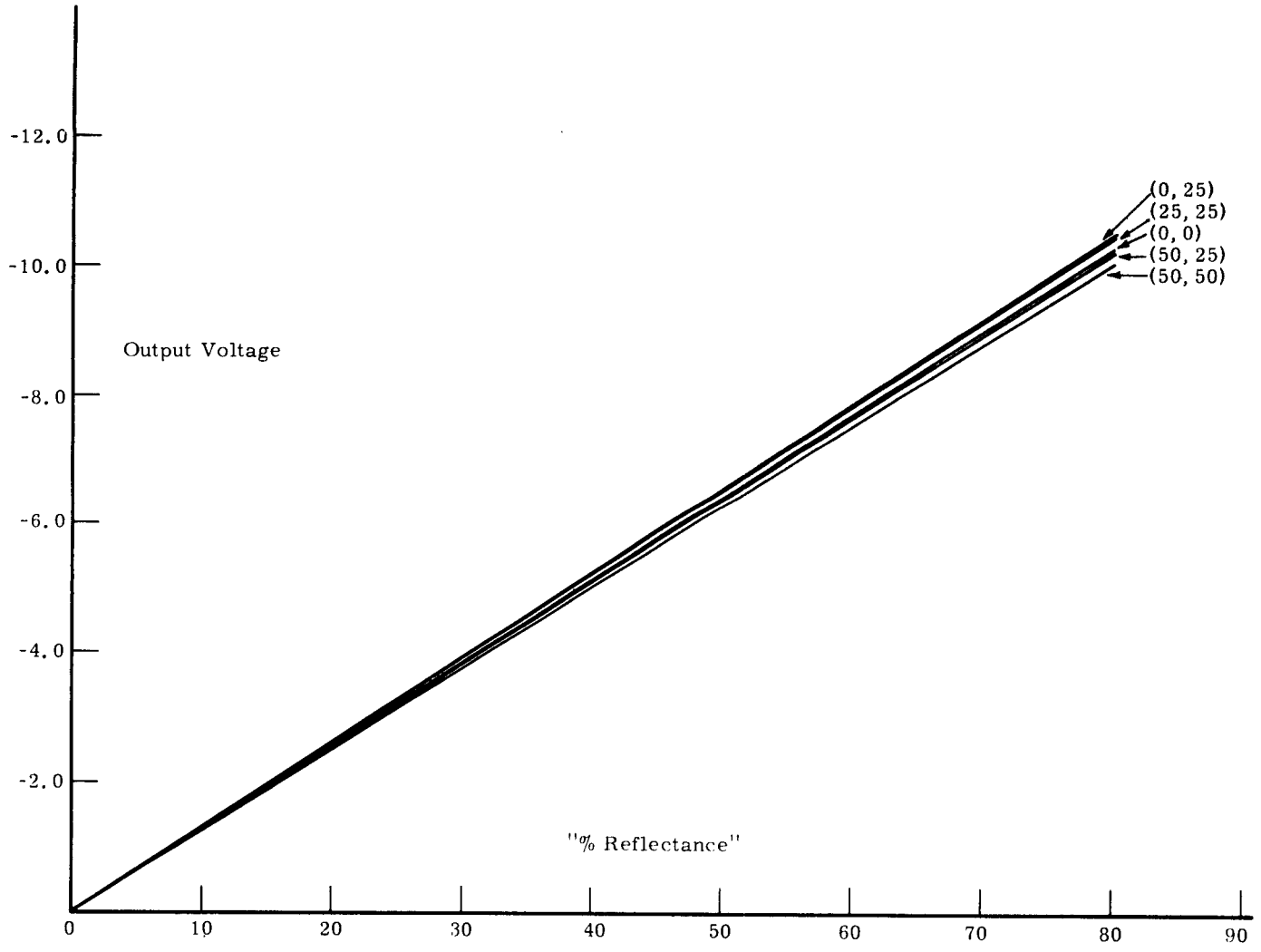

Figure 19. F-1 MRIR calibration data—SBRC data, June 1964, 0.55-0.85 micron channel.

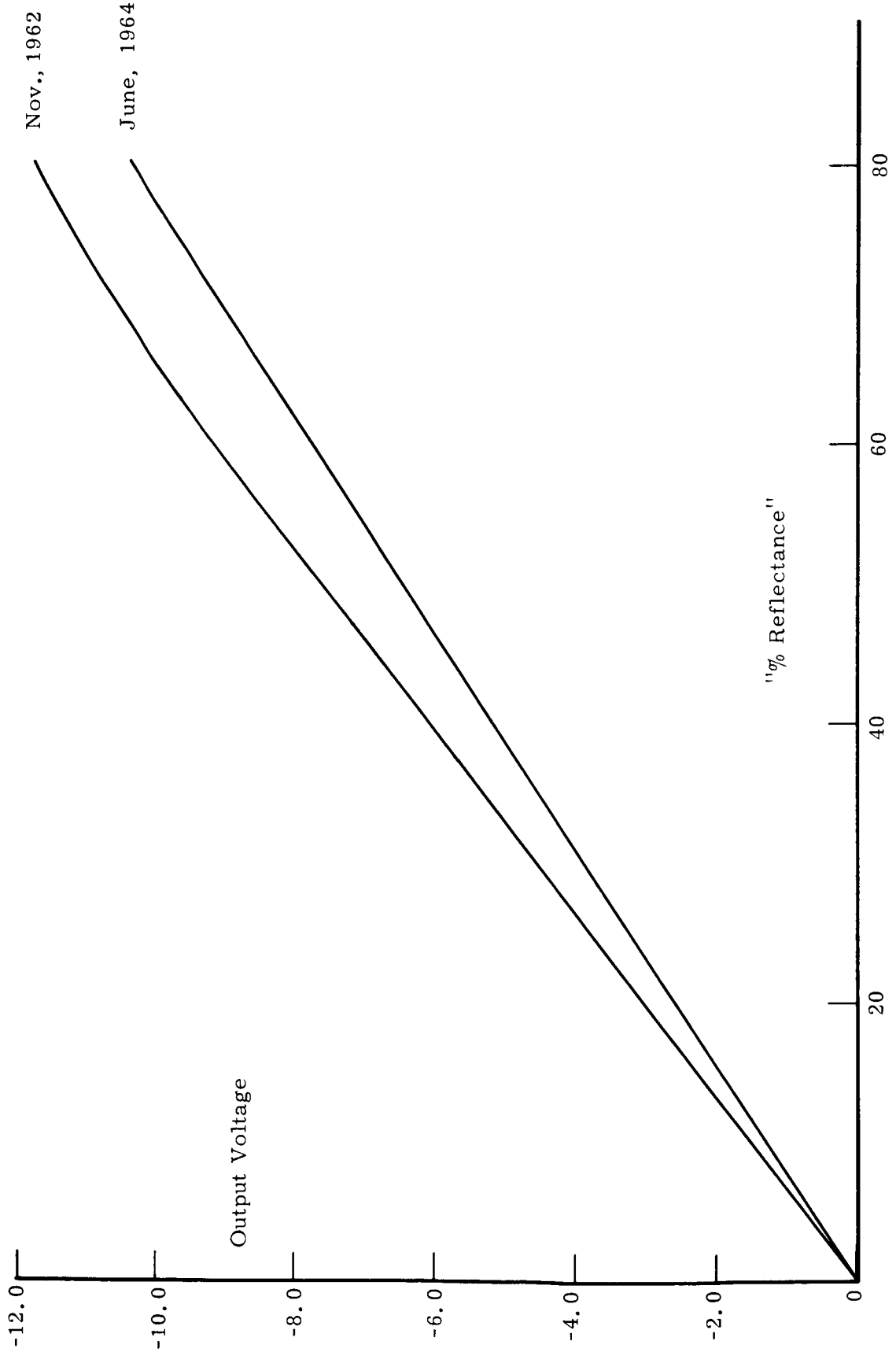

Figure 20. F-1 MRIR calibration data—SBRC data, 0.55-0.85 micron channel, scanner temperature = 25°C, electronic temperature = 25°C.

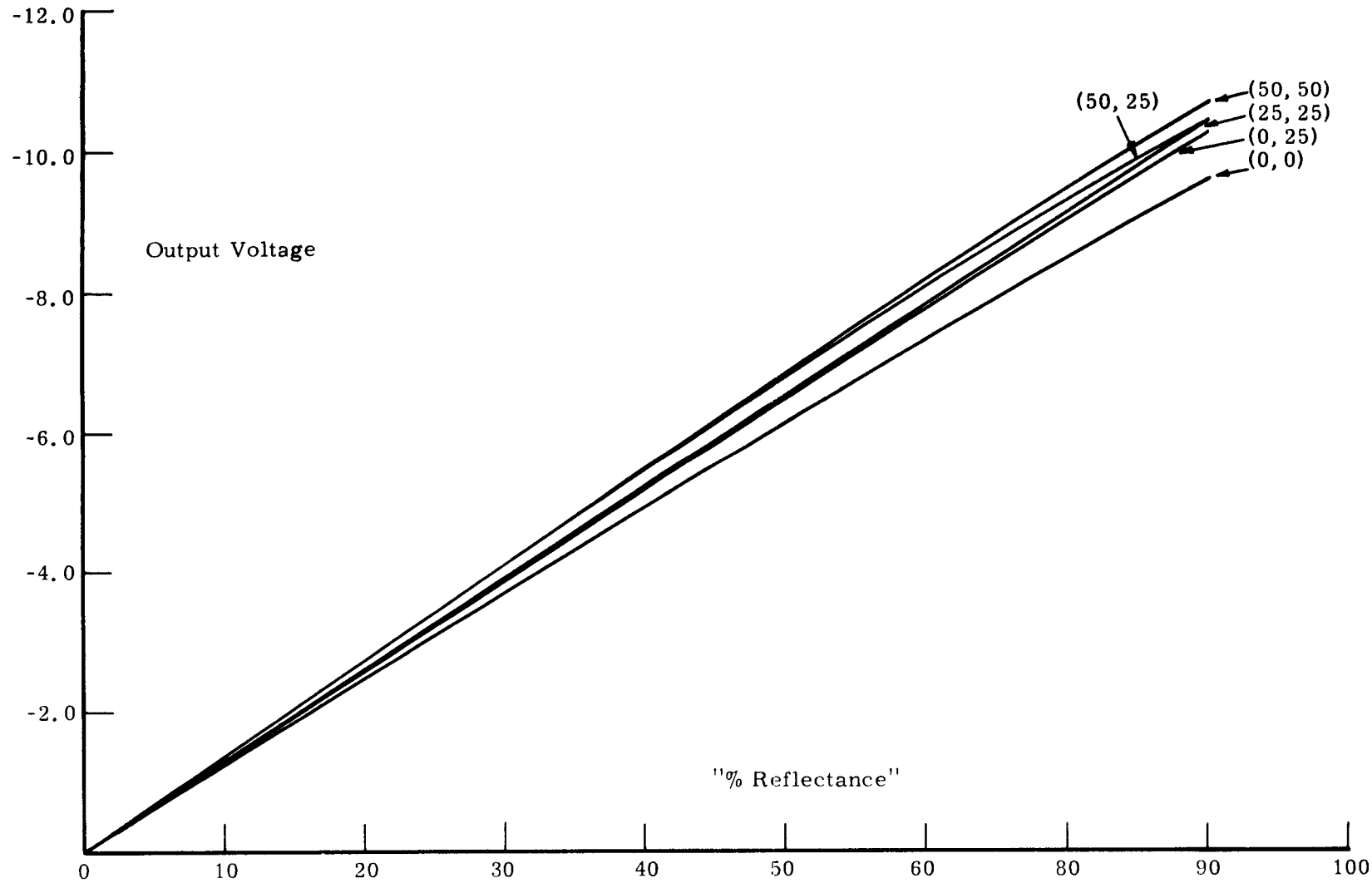

Figure 21. F-1 MRIR calibration data—SBRC data, November 1962, 0.2-4.0 micron channel.

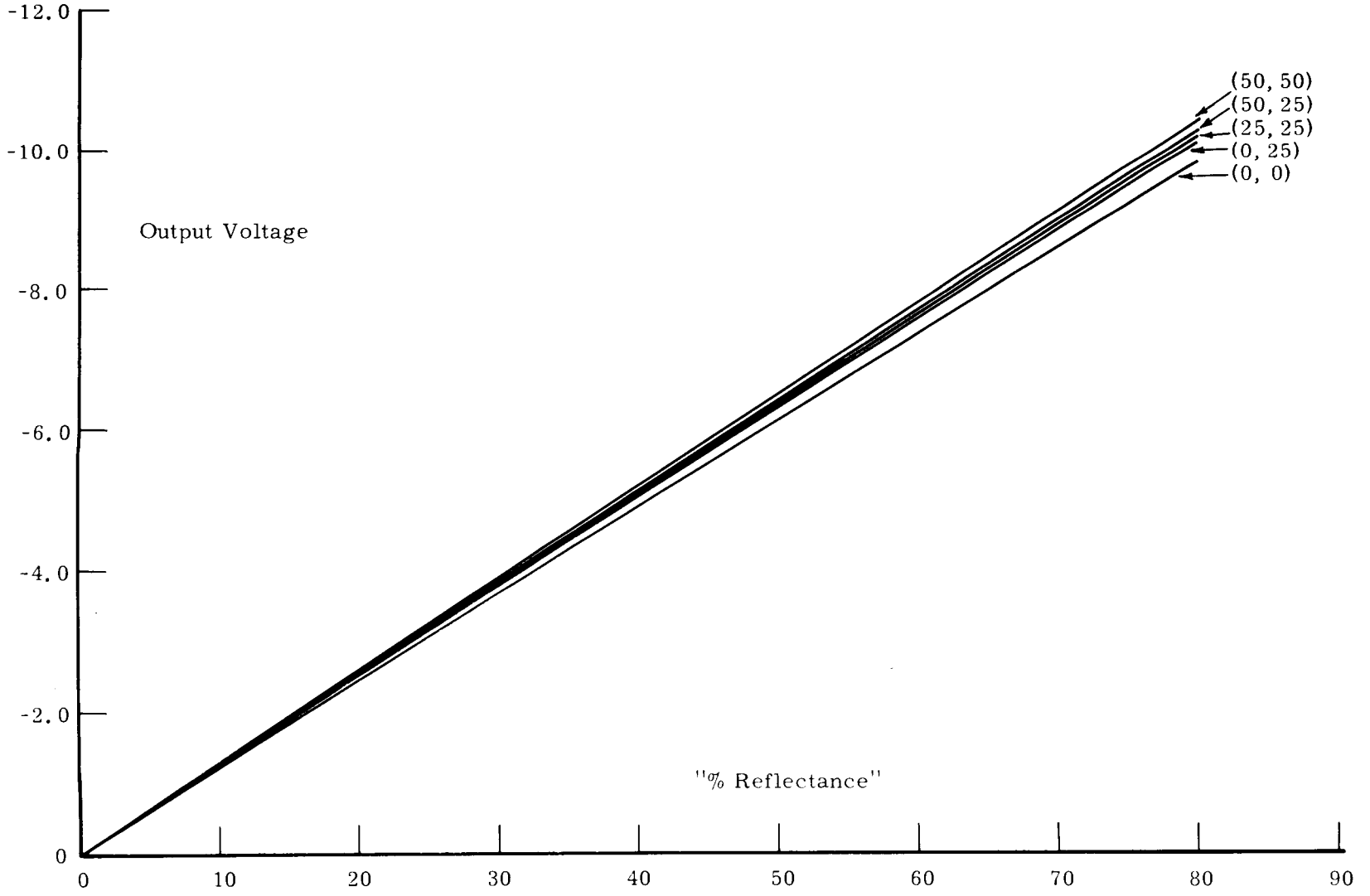

Figure 22. F-1 MRIR calibration data—SBRC data, June 1964, 0.2-4.0 micron channel.

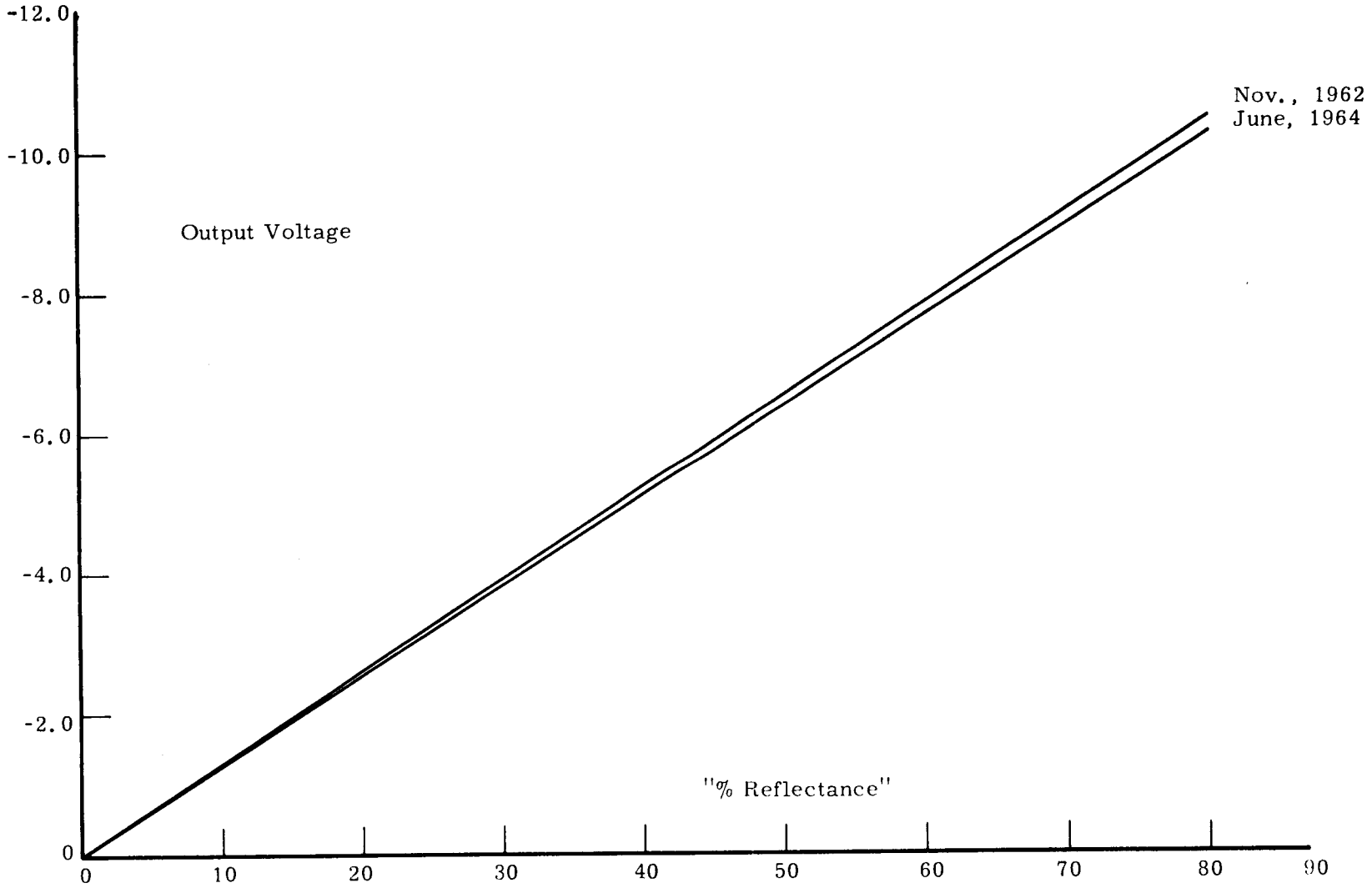

Figure 23. F-1 MRIR calibration data—SBRC data, 0.2-4.0 micron channel, scanner temperature = 25°C, electronic temperature = 25°C.

The response of a channel of the MRIR is given by

$$\Phi_i = k_r \Phi_i'$$

values of Φ_i', the relative response of the 0.55-0.85 micron and 0.2-4 micron channels of the F-1 MRIR are shown in Figures 2 and 3. The constants k_r are not known for these two channels, however it will be seen that they are not required for calibrations in terms of percent reflectance.

Recall that the spectral radiance of a source is given by:

$$N_{ci} = k_n \Psi_{ci}$$

and

$$N_c = \sum_{\lambda} k_n \Psi_{ci} \Delta\lambda_i = k_n \sum \Psi_{ci} \Delta\lambda_i$$

and that the effective radiance of a source is written as:

$$N_c' = k_r k_n \sum_i \Phi_i' \Psi_{ci} \Delta\lambda_i \qquad (14)$$

The spectral irradiance of the sun is H_{si} (see Figure 5) and thus the effective radiance of a target with 100% diffuse reflectance is

$$N_s' = \frac{k_r}{\pi} \sum_i \Phi_i' H_{si} \qquad (15)$$

Values of Φ_i', H_{si}, Ψ_{ci} and $\Phi_i' N_{si}$ and $\Phi' \Psi_{ii}$ are given for the sun and all three sources for the 0.55-0.85 micron channel in Table VI. Similar data for the 0.2-4 micron channel is given in Table VII. Curves of $\Phi' H_{si}$ and $\Phi_i' \Psi_{ci}$ are given in Figures 24 through 31.

The calibration data taken in February, 1963, with the carbon arc—MgO Reflector Source are shown in Table VIII.

Percent reflectance is computed from:

$$\bar{\rho}' = \frac{k_r k_n \sum_i \Phi_i' \Psi_{ci} \Delta\lambda_i}{\frac{k_r}{\pi} \sum_i \Phi_i' H_{si}} = \frac{k_n \sum_i \Phi_i' \Psi_{ci} \Delta\lambda_i}{\frac{1}{\pi} \sum_i \Phi_i' H_{si}}$$

k_n is computed from:

$$k_n = \frac{N_c}{\sum_i \Psi_{ci} \Delta\lambda_i}$$

S

TABLE VI

CALCULATION OF EFFECTIVE SPECTRAL RADIANCE
OF SUN AND CALIBRATION SOURCES FOR 0.55-0.85 MICRON CHANNEL OF F-1 MRIR

λ, microns	ϕ_i'	Sun		Carbon Arc and Mgo Reflector		Lamp and MgO Reflector		Hemisphere with Burch Paint	
		H_{si}, watts/m^2	$H_{si}\phi_i'$	ψ_{ci}	$\psi_{ci}\phi_i'$	$k_n\psi_{ci}$, watts/m^2 μ	$k_n\psi_{ci}\phi_i'$	ψ_{ci}	$\psi_{ci}\phi_i'$
0.51	0.005	19.45	0.097						
0.52	0.010	19.25	0.193	23.8	0.238	17.12	0.171	12.5	0.125
0.53	0.030	19.55	0.586						
0.54	0.085	19.80	1.683	22.9	1.947	20.21	1.718	15.7	1.335
0.55	0.210	19.49	4.093						
0.56	0.385	19.10	7.354	22.3	8.586	23.07	8.882	20.3	7.816
0.57	0.625	19.07	11.919						
0.58	0.760	19.09	14.508	21.5	16.340	27.35	20.786	25.1	19.076
0.59	0.865	19.00	16.435						
0.60	0.940	18.36	17.258	21.0	19.740	32.10	30.174	34.9	32.806
0.61	0.980	17.83	17.473						
0.62	1.000	17.48	17.480	20.6	20.600	38.05	38.05	46.1	46.1
0.63	0.99	17.11	16.939						
0.64	0.955	16.75	15.996	20.2	19.291	44.23	42.246	53.0	50.615
0.65	0.910	16.50	15.015						
0.66	0.838	16.32	13.676	19.9	16.676	49.94	41.850	63.0	52.794
0.67	0.800	16.03	12.824						
0.68	0.760	15.60	11.856	19.5	14.820	55.88	42.469	67.5	51.3
0.69	0.700	15.17	10.619						
0.70	0.655	15.06	9.825	19.2	12.576	60.64	39.719	75.0	49.125
0.71	0.575	14.73	8.470						
0.72	0.485	14.30	6.936	18.6	9.021	65.40	31.719	86.4	41.904
0.73	0.415	14.05	5.831						
0.74	0.345	13.69	4.723	17.8	6.141	70.15	24.202	86.3	29.774
0.75	0.280	13.53	3.788						
0.76	0.215	13.28	2.855	16.8	3.612	74.43	16.002	90.8	19.522
0.77	0.180	12.75	2.295						
0.78	0.140	12.45	1.743	15.8	2.212	78.47	10.986	92.5	12.950
0.79	0.115	12.23	1.406						
0.80	0.080	11.99	0.959	14.7	1.176	82.04	6.563	94.9	7.592
0.81	0.045	11.74	0.528						
0.82	0.030	11.52	0.346	13.7	0.411	85.61	2.568	96.9	2.847
0.83	0.020	11.23	0.225						
0.84	0.013	10.86	0.154	12.9	0.168	88.70	1.153	99.0	1.287
0.85	0.008	10.61	0.085						
0.86	0.005	10.36	0.052	12.3	0.062	91.55	0.458	100.0	0.500
			256.225		153.617		359.710		427.468

TABLE VII

CALCULATION OF EFFECTIVE SPECTRAL RADIANCE
OF SUN AND CALIBRATION SOURCES FOR 0.2-4.0 MICRON CHANNEL OF F-1 MRIR

λ, microns	ϕ_i'	Sun		Carbon Arc and MgO Reflector		Lamp and MgO Reflector		Hemisphere with Burch Paint	
		H_{si} watts/m^2	$\phi_i' H_{si}$	ψ_{ci}	$\phi_i' \psi_{ci}$	$k_n \psi_{ci}$	$k_n \phi_i' \psi_{ci}$	ψ_{ci}	$\phi_i' \psi_{ci}$
0.3	0.41	62.79	25.74	0.55	0.23	0.75	0.31	---	---
0.4	0.76	156.34	118.82	28.80	21.89	4.60	3.50	1.39	1.06
0.5	0.67	203.54	136.37	26.30	17.62	13.10	8.78	8.99	6.02
0.6	0.64	181.84	116.38	21.00	13.44	30.60	19.58	34.90	22.34
0.7	0.59	148.80	88.38	19.20	11.33	57.75	34.07	75.00	44.25
0.8	0.53	120.21	63.71	14.70	7.79	78.10	41.39	94.90	50.30
0.9	0.59	95.08	56.10	11.30	6.67	91.75	54.13	97.30	57.41
1.0	0.825	74.78	61.69	9.00	7.43	99.10	81.76	89.60	73.92
1.1	0.89	58.09	51.70	8.10	7.21	99.95	88.96	82.30	73.25
1.2	0.94	47.60	44.74	6.70	6.30	97.30	91.46	65.50	61.57
1.3	0.957	38.18	36.54	5.30	5.07	92.05	88.09	60.00	57.42
1.4	0.97	30.87	29.94	4.40	4.27	84.70	82.16	33.70	32.69
1.5	0.977	25.17	24.59	4.05	3.96	76.55	74.79	29.60	28.92
1.6	0.99	20.68	20.47	3.40	3.37	67.80	67.12	27.70	27.42
1.7	0.993	17.13	17.01	2.70	2.68	60.15	59.73	17.60	17.48
1.8	0.96	14.29	13.72	2.30	2.21	52.70	50.59	14.50	13.92
1.9	0.968	12.00	11.62	1.90	1.84	45.70	44.24	7.40	7.16
2.0	0.977	10.15	9.92	1.50	1.46	38.50	37.61	---	---
2.1	0.975	8.63	8.41	1.20	1.17	35.85	34.95		
2.2	0.983	7.39	7.26	0.90	0.88	31.90	31.36		
2.3	0.98	6.36	6.23	0.65	0.64	28.00	27.44		
2.4	0.974	5.50	5.36	0.40	0.39	25.10	24.45		
2.5	0.905	4.78	4.33	0.20	0.18	21.30	19.28		
2.6	0.945	4.18	3.95	---	---	17.90	16.92		
2.7	0.625	3.66	2.29			14.85	9.28		
2.8	0.85	3.22	2.74			12.10	10.29		
2.9	0.90	2.84	2.56			9.75	8.78		
3.0	0.96	2.54	2.44			7.80	7.49		
3.1	0.94	2.24	2.11			6.10	5.73		
3.2	0.95	1.99	1.89			5.00	4.75		
3.3	0.957	1.81	1.73			4.00	3.83		
3.4	0.969	1.62	1.57			3.40	3.29		
3.5	0.908	1.46	1.33			2.90	2.63		
3.6	0.895	1.31	1.17			2.30	2.06		
3.7	0.700	1.18	0.83			1.95	1.37		
3.8	0.675	1.07	0.72			1.70	1.15		
3.9	0.645	0.97	0.63			1.40	0.90		
4.0	0.482	0.90	0.43			1.00	0.48		
4.1	0.500	0.84	0.42			0.50	0.25		
4.2	0.195	0.77	0.15			---	---		
4.3	0.152	0.71	0.11						
4.4	0.177	0.65	0.12						
4.5	0.191	0.58	0.11						
4.6	0.175	0.50	0.09						
4.7	0.060	0.44	0.03						
4.8	---	0.43	--						
4.9	---	0.42	--						
5.0	---	--	--						

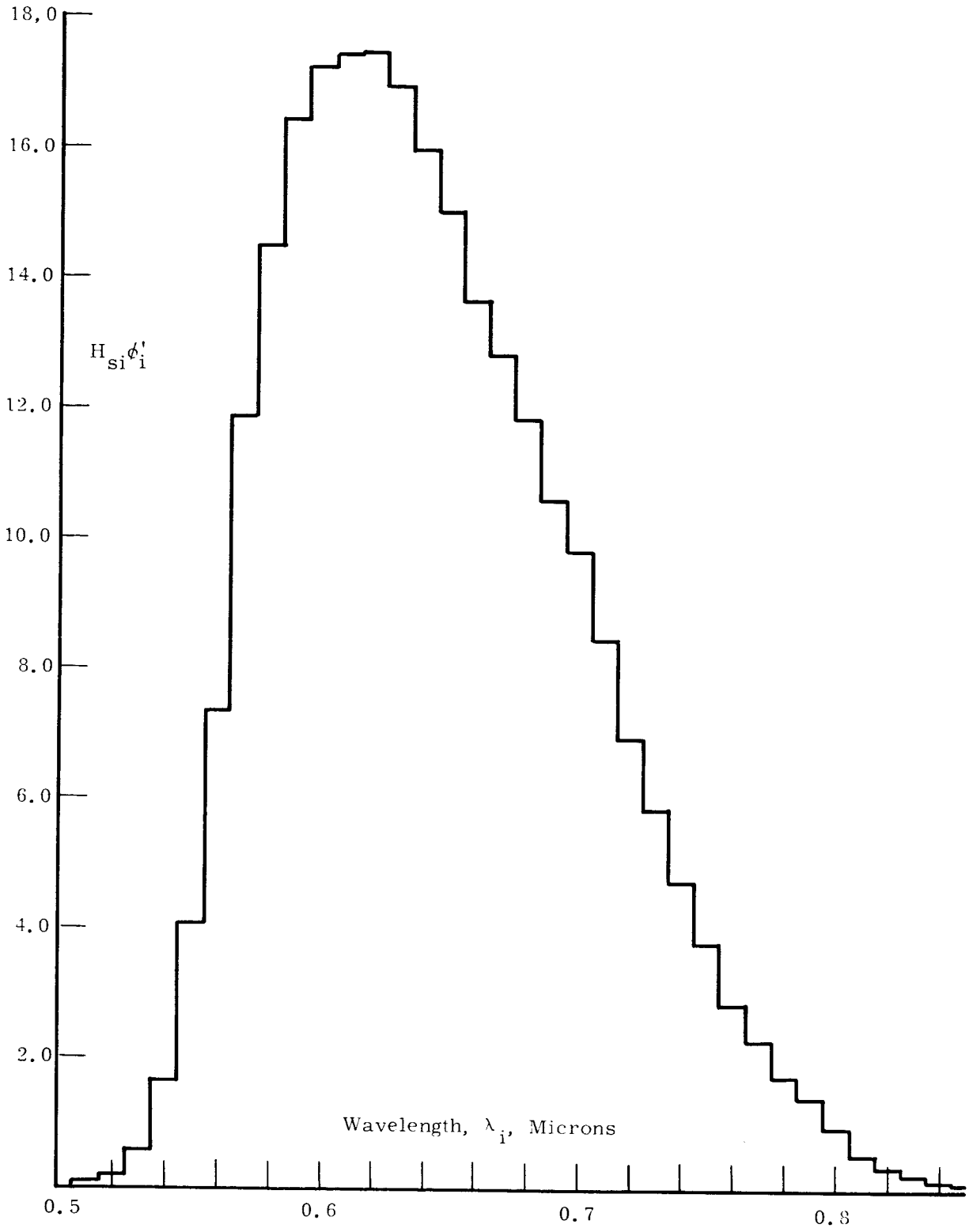

Figure 24. Effective spectral irradiance of sun, $H_{si}\phi_i'$ for 0.55-0.85 micron channel of F-1 MRIR.

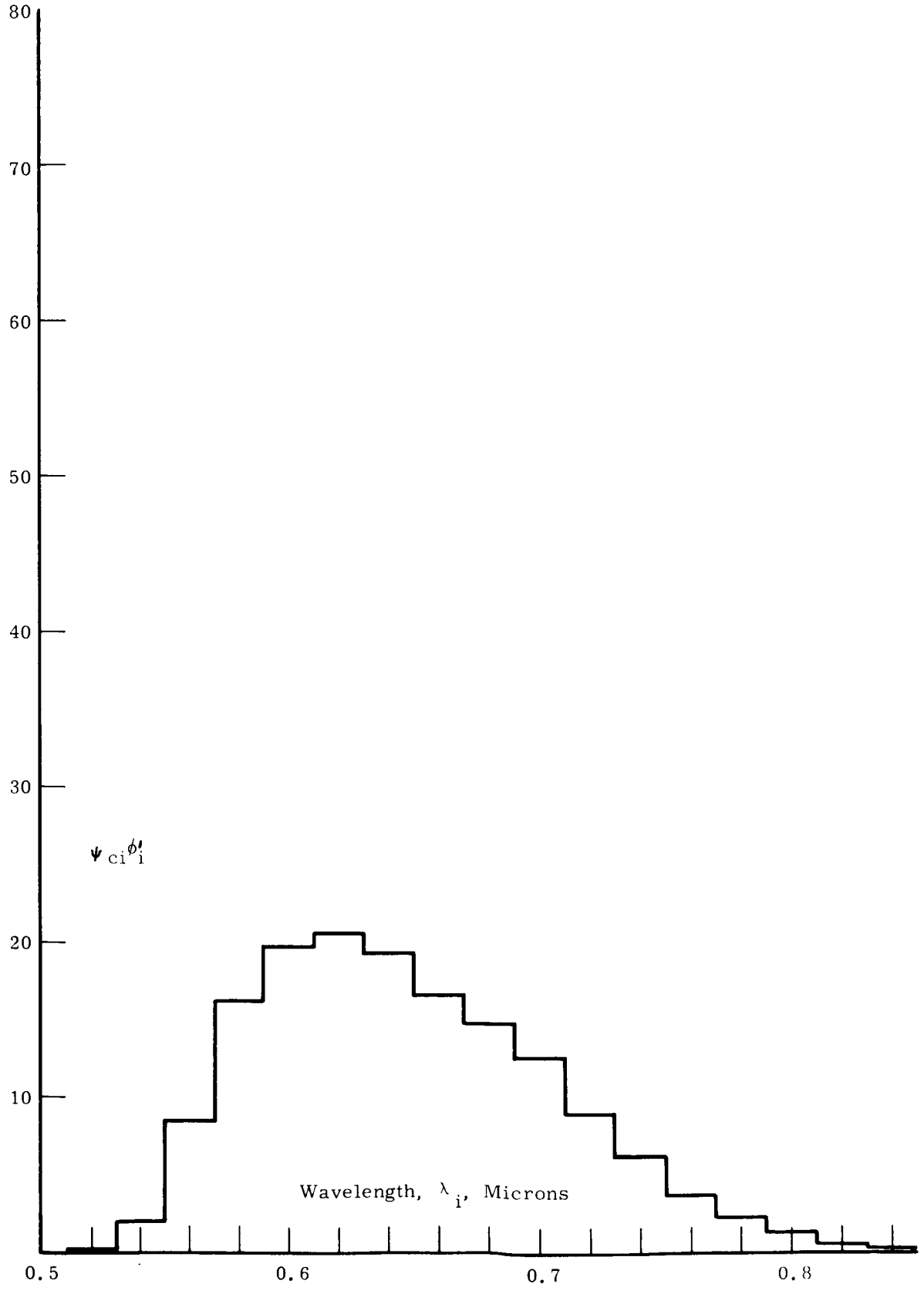

Figure 25. $\phi'_i\psi_{ci}$ for carbon arc—MgO reflector and 0.55-0.85 micron channel of F-1 MRIR.

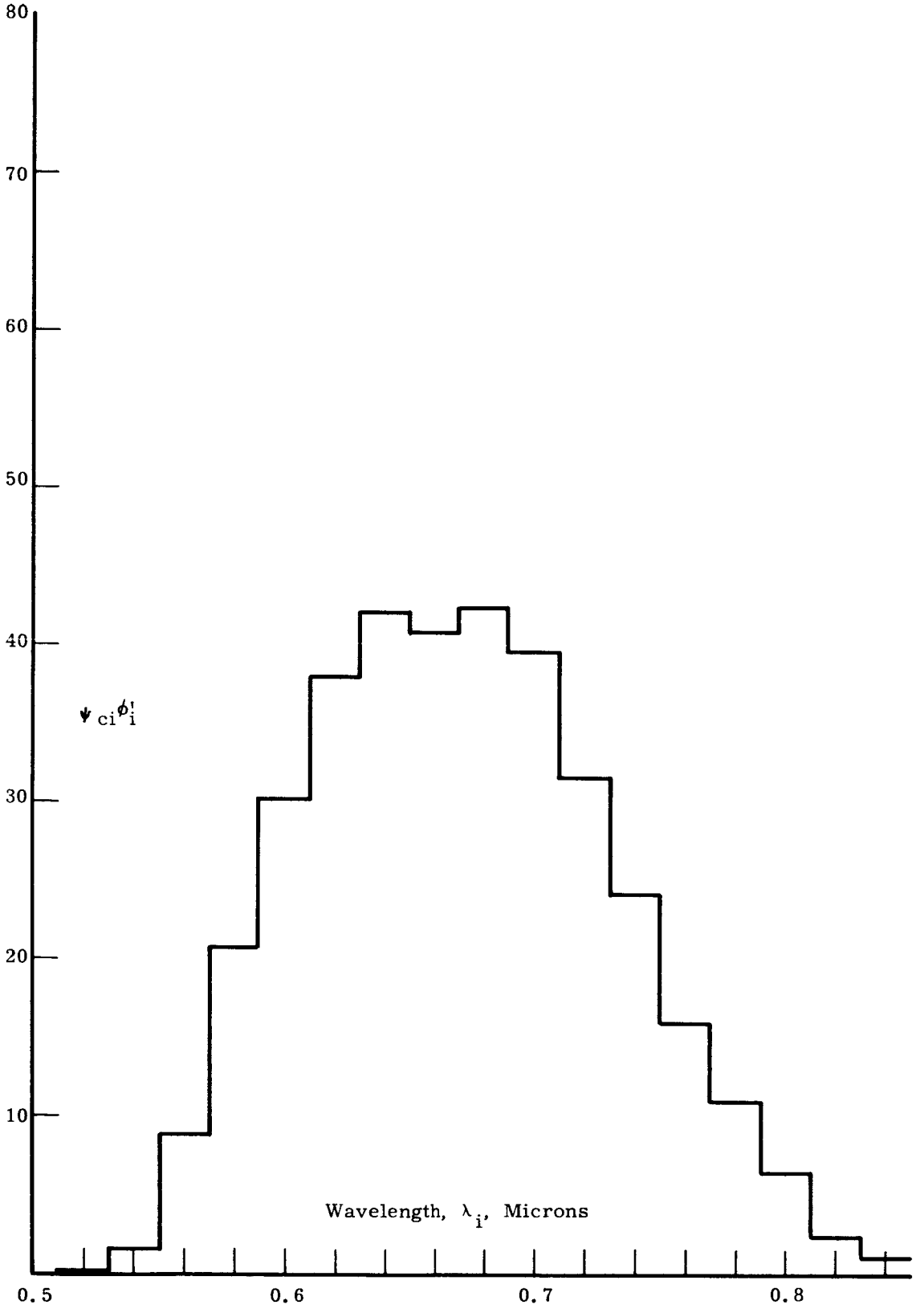

Figure 26. $k_n\phi_i'\psi_{ci}$ for lamp—MgO reflector and 0.55-0.85 micron channel of F-1 MRIR.

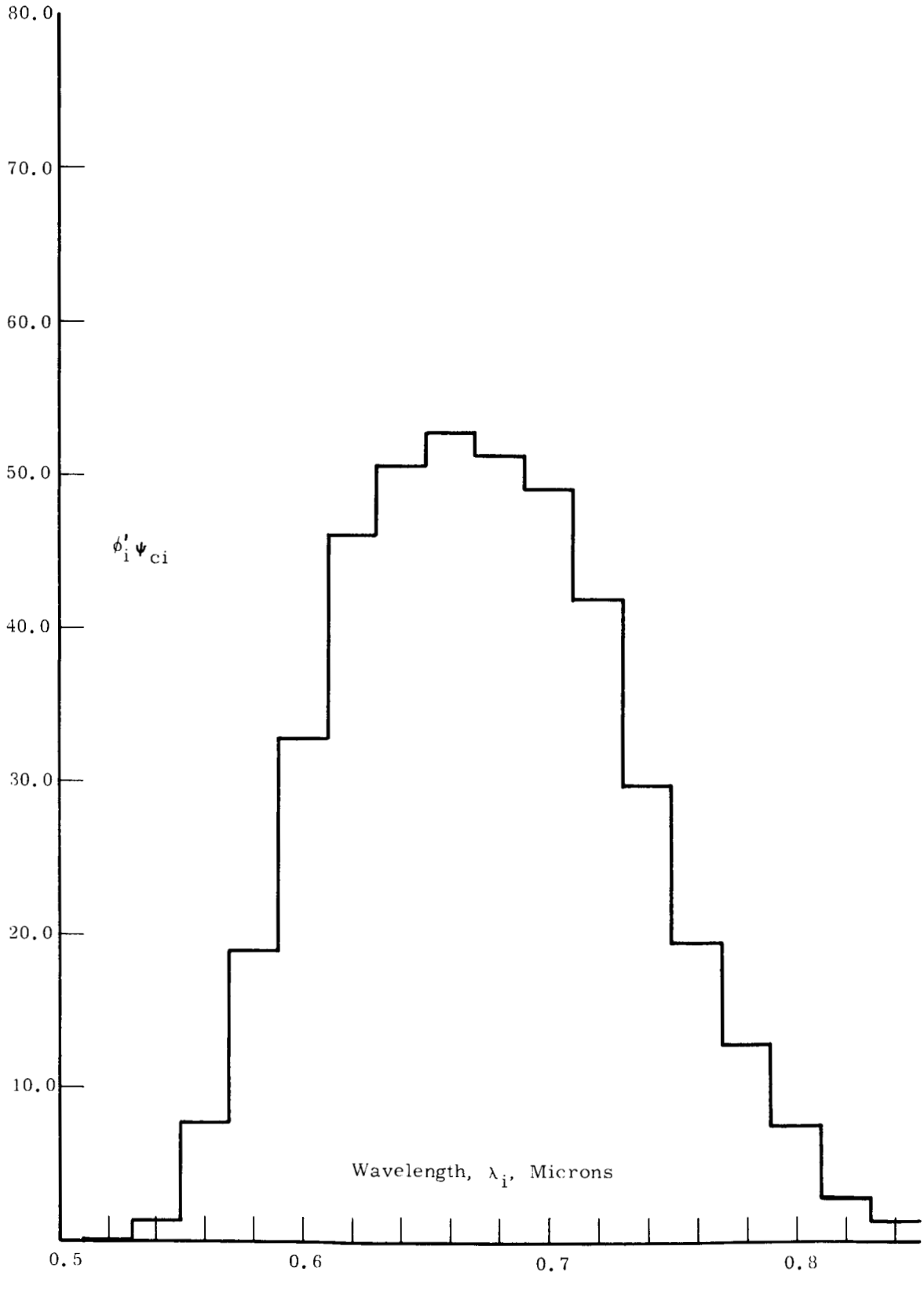

Figure 27. $\phi_i' \psi_{ci}$ for hemisphere source and 0.55-0.85 micron channel of F-1 MRIR.

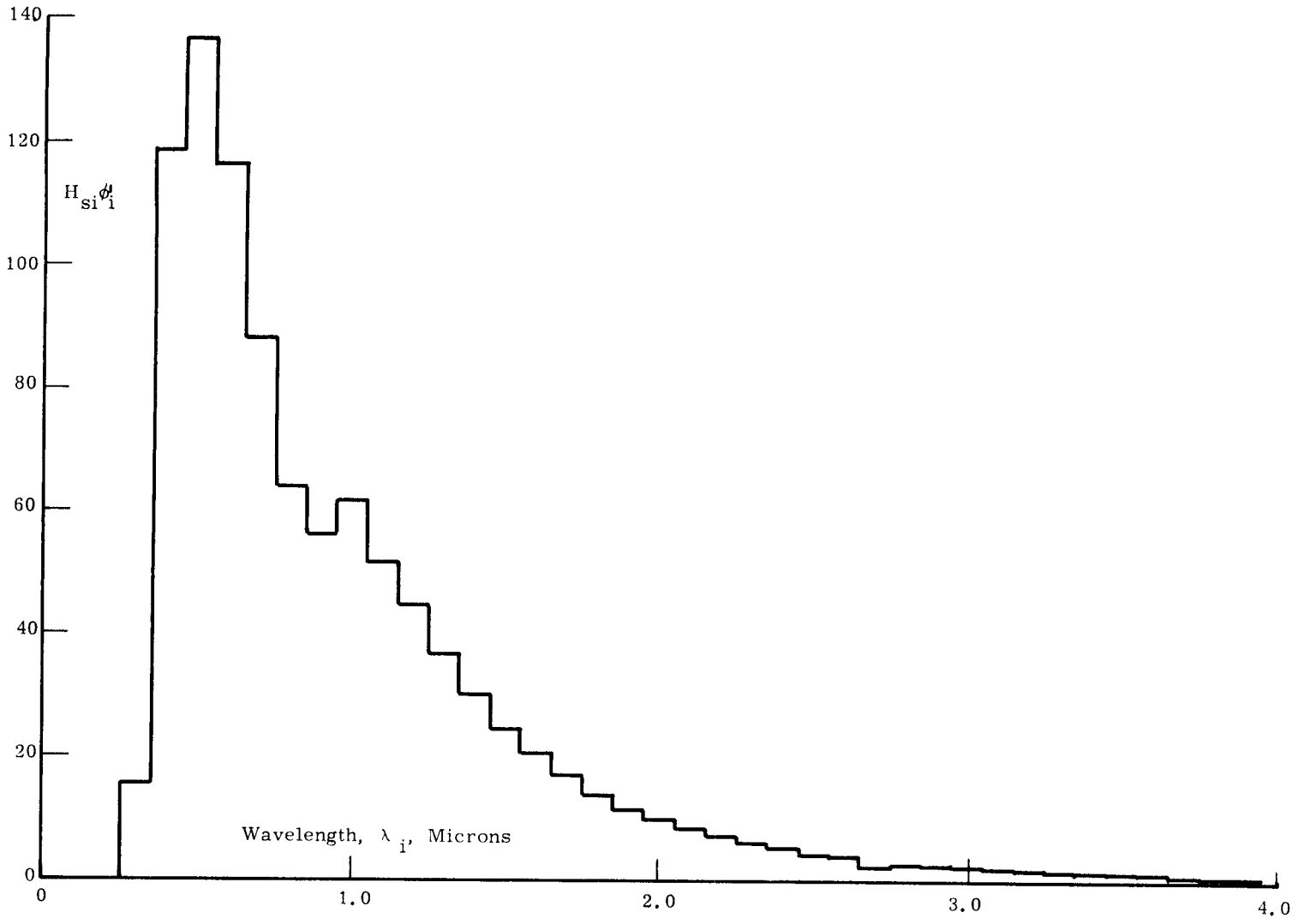

Figure 28. Effective spectral irradiance of sun, $H_{si}\phi_i^!$ for 0.2-4.0 micron channel of F-1 MRIR.

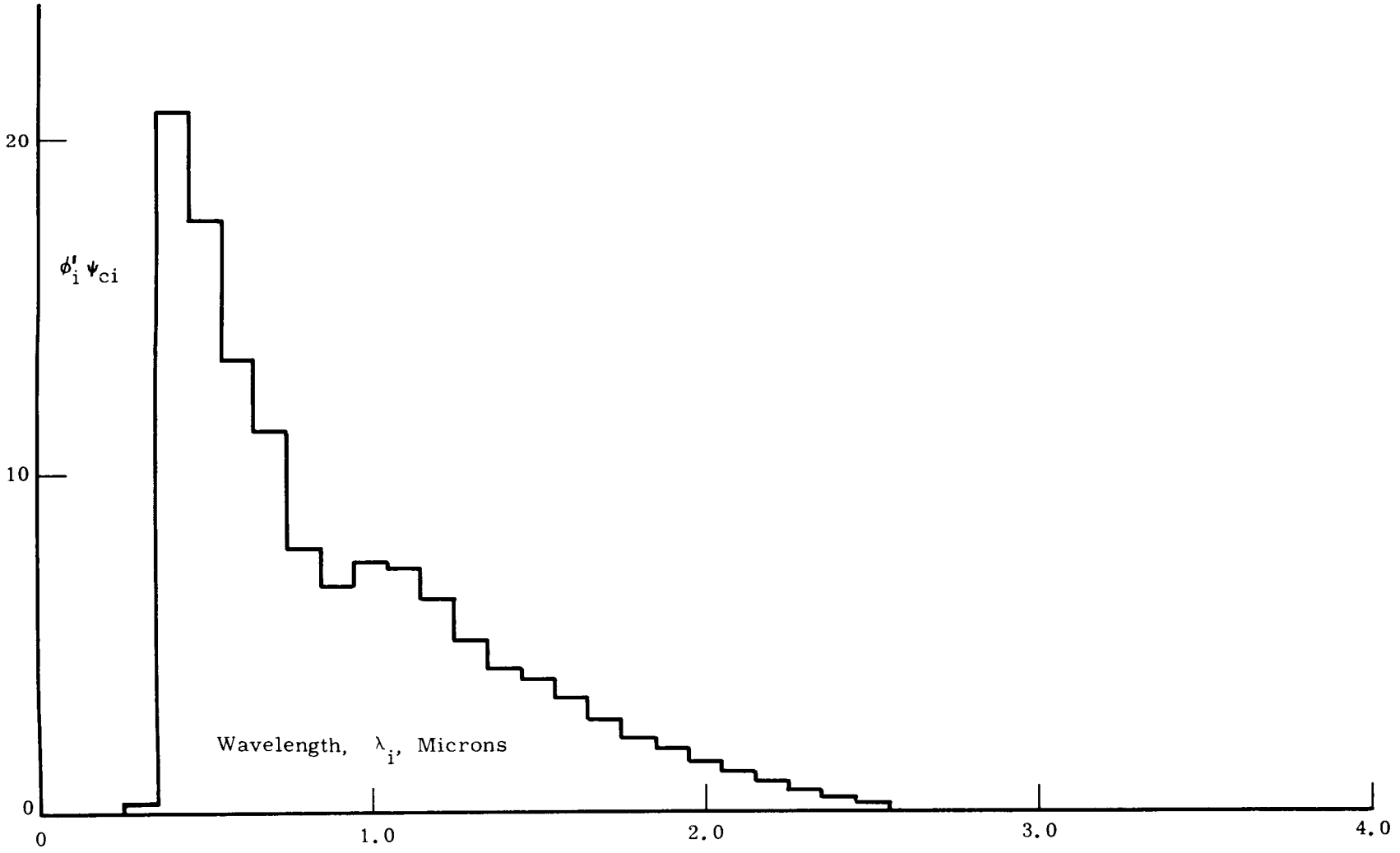

Figure 29. $\phi_i' \psi_{ci}$ for carbon arc—MgO reflector and 0.2-4.0 micron channel of F-1 MRIR.

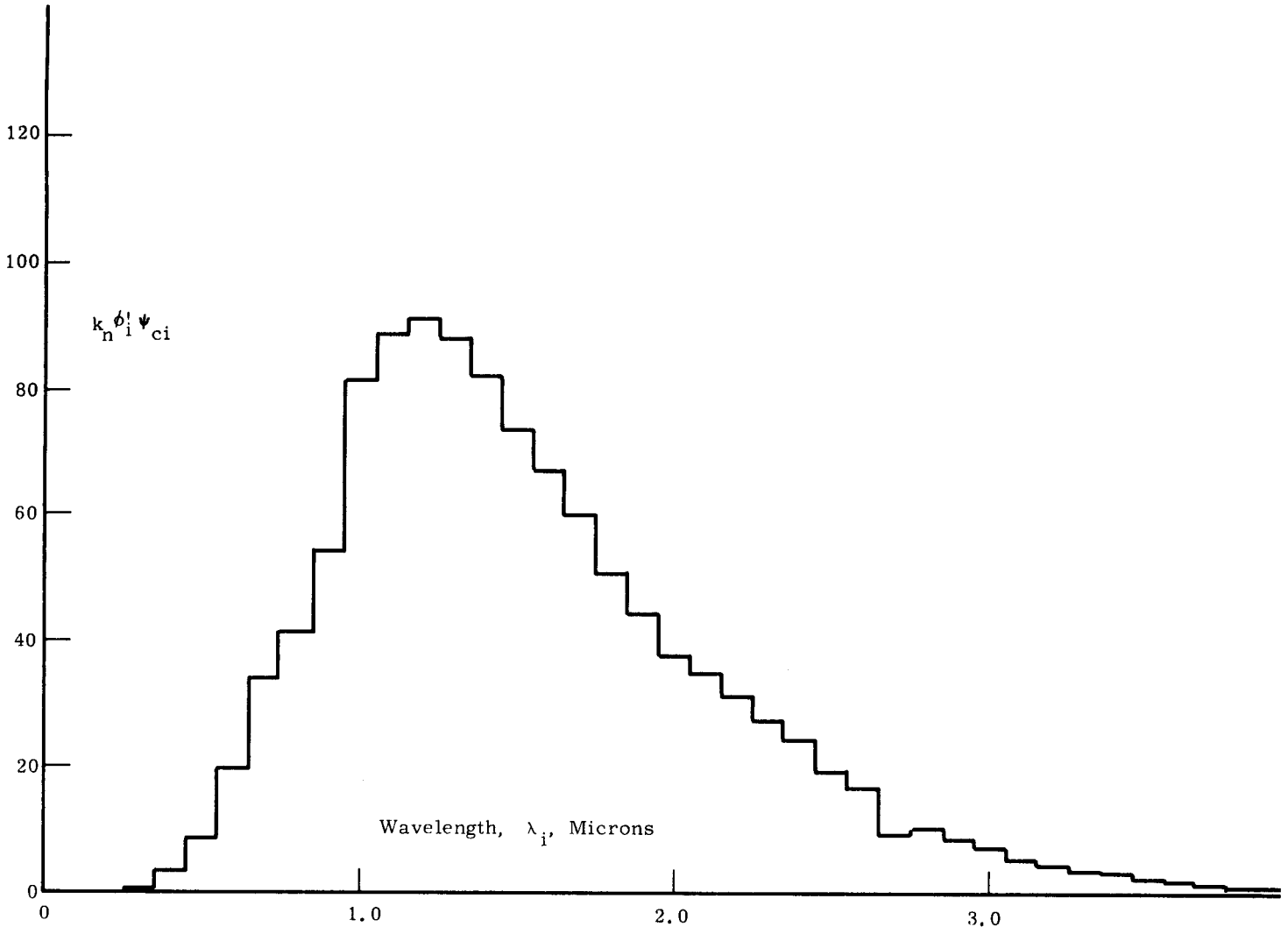

Figure 30. $k_n \phi_i' \Psi_{ci}$ for lamp—MgO reflector and 0.2-4.0 micron channel of F-1 MRIR.

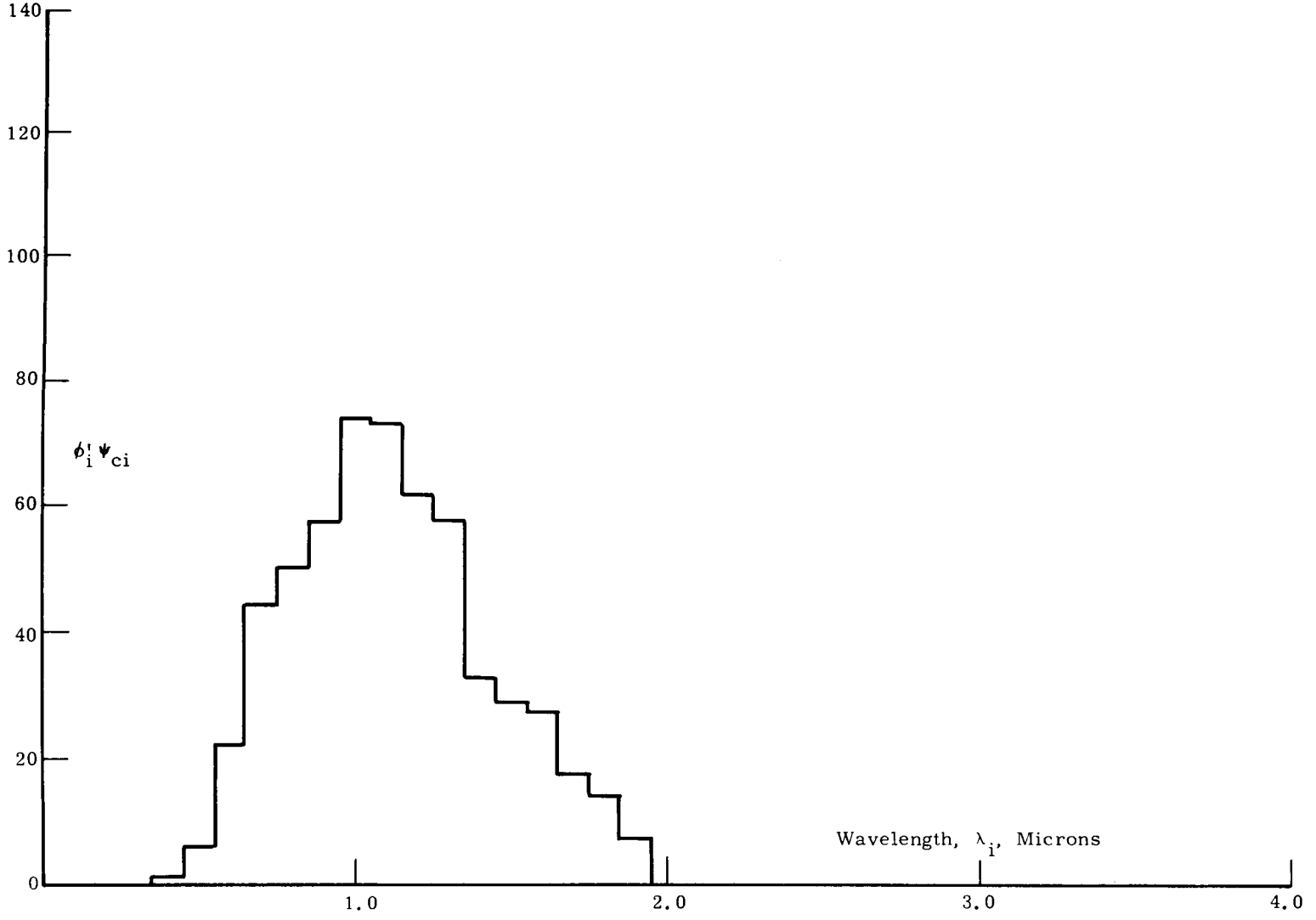

Figure 31. $\phi_i' \Psi_{ci}$ for hemisphere source and 0.2-4.0 micron channel of F-1 MRIR.

TABLE VIII

UNIVERSITY OF MICHIGAN F-1 CALIBRATION DATA

(Carbon arc-MgO reflector source—February, 1963)

W_c, Watts/m^2	N_c, Watts/m^2 sr	0.55-0.85 Micron Channel		0.2-4.0 Micron Channel	
		MRIR, Volts	$\bar{\rho}'$, % Reflectance	MRIR, Volts	$\bar{\rho}'$, % Reflectance
208	66.21	1.5	14.7	1.8	15.9
398	126.69	3.2	28.1	3.6	30.4
597	190.03	4.9	42.1	5.3	45.5
787	250.51	6.6	55.5	6.9	60.0
977	310.99	8.4	68.9	8.6	74.5
1177	374.65	10.1	83.0	10.3	84.8
1376	437.99	11.8	97.0	11.9	105.0
1575	501.34	12.8	111.0		

The necessary numerical values for the 0.55-0.85 micron channel are:

$$\sum_i \psi_{ii} \Delta\lambda_i = 17.004$$

$$\frac{1}{\pi} \sum_i \phi'_i H_{si} = 81.56$$

$$\sum_i \phi'_i \psi_{ci} \Delta\lambda_i = 3.072$$

Thus:

$$\bar{\rho}' = \frac{3.072}{17.004} \cdot \frac{N_c}{81.56}$$

or

$$\bar{\rho}'(\%) = \frac{307.2}{17.004 \cdot 81.56} N_c = 0.2215\, N_c$$

The necessary numerical values for the 0.2-4 micron channel are:

$$\frac{1}{\pi} \sum_i \phi'_i H_{si} = 314.00$$

$$\sum_i \phi'_i \psi_{ci} \Delta\lambda_i = 12.80$$

Thus:

$$\bar{\rho}' = \frac{12.80}{17.004} \cdot \frac{N_c}{314}$$

$$\bar{\rho}'(\%) = \frac{12.80}{17.004 \cdot 314} N_c = 0.2397\ N_c$$

The calibration data taken in August, 1963, with the lamp—MgO Reflector Source are shown in Table IX.

TABLE IX

UNIVERSITY OF MICHIGAN F-1 CALIBRATION DATA

(Lamp-MgO reflector source—August, 1963)

R	0.55-0.85 Micron Channel		0.2-4.0 Micron Channel	
	MRIR, Volts	$\bar{\rho}'$, % Reflectance	MRIR, Volts	$\bar{\rho}'$, % Reflectance
1.00	--	2.0	0.8	8.2
0.79	0.45	3.2	1.29	13.1
0.65	0.75	4.7	2.03	19.4
0.56	1.10	6.3	2.82	26.2
0.50	1.50	7.9	3.75	32.8
0.456	1.90	9.5	4.80	39.5
0.423	2.30	11.1	5.75	45.9
0.400	2.50	12.4	6.40	51.3
0.370	2.90	14.5	7.60	59.9

The radiance of the MgO plate, with irradiance from the lamp at 45° is:

$$N_c = \frac{0.707}{\pi} \frac{1}{R^2} \sum k_n\ \psi_{ci}\ \Delta\lambda_i \quad \text{watts/m}^2\text{-steradian}$$

and the reflectance is computed from:

$$\bar{\rho}' = \frac{k_r \cdot \frac{0.707}{\pi} \frac{1}{R^2} \sum_i k_n \psi_{ci} \phi_i' \Delta\lambda_i}{\frac{k_r}{\pi} \sum_i \phi_i H_{si}}$$

$$= \frac{.2250}{R^2} \cdot \frac{\sum_i k_n \psi_{ci} \phi_i' \Delta\lambda_i}{\frac{1}{\pi} \sum_i \phi_i' H_{si}}$$

For the 0.55-0.85 micron band

$$\sum_i k_n \phi_i' \psi_{ci} \Delta\lambda_i = 7.194$$

$$\bar{\rho}'(\%) = \frac{719.4 \cdot 0.225}{81.56 \cdot R^2} = \frac{1.985}{R^2}$$

For the 0.2-4.0 micron band

$$\sum_i k_n \phi_i' \psi_{ci} \Delta\lambda_i = 114.5$$

$$\bar{\rho}'(\%) = \frac{11450 \cdot 0.225}{314.00} \frac{1}{R^2} = \frac{8.205}{R^2}$$

The calibration data taken with the Hemisphere Source in April and May, 1964 are shown in Table X.

TABLE X

UNIVERSITY OF MICHIGAN F-1 CALIBRATION DATA

(Hemisphere source—May, 1964)

No. of Lamps	W_c, Watts/m^2	N_c, Watts/m^2 sr	0.55-0.85 Micron Channel		0.2-4.0 Micron Channel	
			MRIR, Volts	ρ', % Reflectance	MRIR, Volts	ρ', % Reflectance
2	226.29	72.03	1.45-1.61	10.2	2.03	17.8
4	443.52	141.18	3.29-3.42	20.0	4.08-4.10	34.9
6	651.71	207.45	4.93-5.07	29.4	5.84-6.00	51.3
8	859.89	273.71	6.31-6.46	38.7	7.68-7.91	67.7
10	1049.97	334.21	7.70-7.97	47.3	9.52-9.83	82.7

The % reflectance is computed from

$$\bar{\rho}' = \frac{k_r\, k_n \sum_i \phi_i'\, \psi_{ci}\, \Delta\lambda_i}{\frac{k_r}{\pi} \sum_i \phi_i'\, H_{si}} = \frac{k_n \sum_i \phi_i'\, \psi_{ci}\, \Delta\lambda_i}{\frac{1}{\pi} \sum_i \phi_i'\, H_{si}}$$

k_n is computed from:

$$k_n = \frac{N_c}{\sum_i \psi_{ci}\, \Delta\lambda_i}$$

The necessary numerical values for the 0.55-0.85 micron channel are:

$$\sum_i \psi_{ci}\, \Delta\lambda_i = 74.038$$

$$\frac{1}{\pi} \sum_i \phi_i'\, H_{si} = 81.56$$

$$\sum_i \phi_i'\, \psi_{ci}\, \Delta\lambda_i = 8.549$$

Thus:

$$\bar{\rho}' = \frac{8.549}{74.038} \cdot \frac{N_c}{81.56}$$

or

$$\bar{\rho}'(\%) = \frac{854.9}{74.038 \cdot 81.56} N_c = .14157\, N_c$$

The necessary numerical values for the 0.2-4 micron channel are:

$$\frac{1}{\pi} \sum_i \phi_i'\, H_{si} = 314.00$$

$$\sum_i \phi_i'\, \psi_{ci}\, \Delta\lambda_{i'} = 57.51$$

Thus:

$$\bar{\rho}' = \frac{57.51}{74.038} \cdot \frac{N_c}{314.00}$$

or

$$\bar{\rho}'(\%) = \frac{5751}{74.038 \cdot 314.00} N_c = 0.2474\, N_c$$

The calibration curves using the data of Tables VIII to X are plotted in Figures 32 and 33. The voltage indicated is the MRIR voltage output into a 56800 ohm load (The University of Michigan calibrations which were taken with a 52600 ohm load are corrected to a 56800 ohm load).

For the 0.2-4 micron channel, the curves of Figure 33 show excellent agreement between the February, 1963, and May, 1964 data. The August, 1963 departs from the other two sets in a strange fashion, that suggests that the $1/R^2$ law variation used for irradiance of the reflector plate by the lamp is not valid.

Figure 32 indicates complete disagreement between three University of Michigan calibrations for the 0.55-0.85 micron channel. The change of transmission of the filter of this channel due to polymerization of the balsam cement used as a bonding agent was demonstrated by SBRC. It is possible that the transmission of the channel may have been changing wildly during the time of the measurements. No other explanation for the disagreement is apparent.

Again the bend in the calibration curve for the August, 1963, data indicates that the $1/R^2$ law used in this calibration was not valid.

SBRC data taken at the same scanner and electronic temperatures have been shown for comparison. Disagreement with University of Michigan data is indicated. Probable causes of the disagreement are discussed and corrected calibration curves for the 0.2-4 micron channel are shown in Section 9.2 of this report.

7.3. DIRECT SUN SIGNAL CALIBRATIONS

The direct sun signal calibration system was installed on the F-1 MRIR, but was not adjusted or ground calibrated for use. Direct sun signals were obtained on the June 26, 1965, balloon flight, however it is not possible to judge the performance of the system because of the lack of surface calibrations.

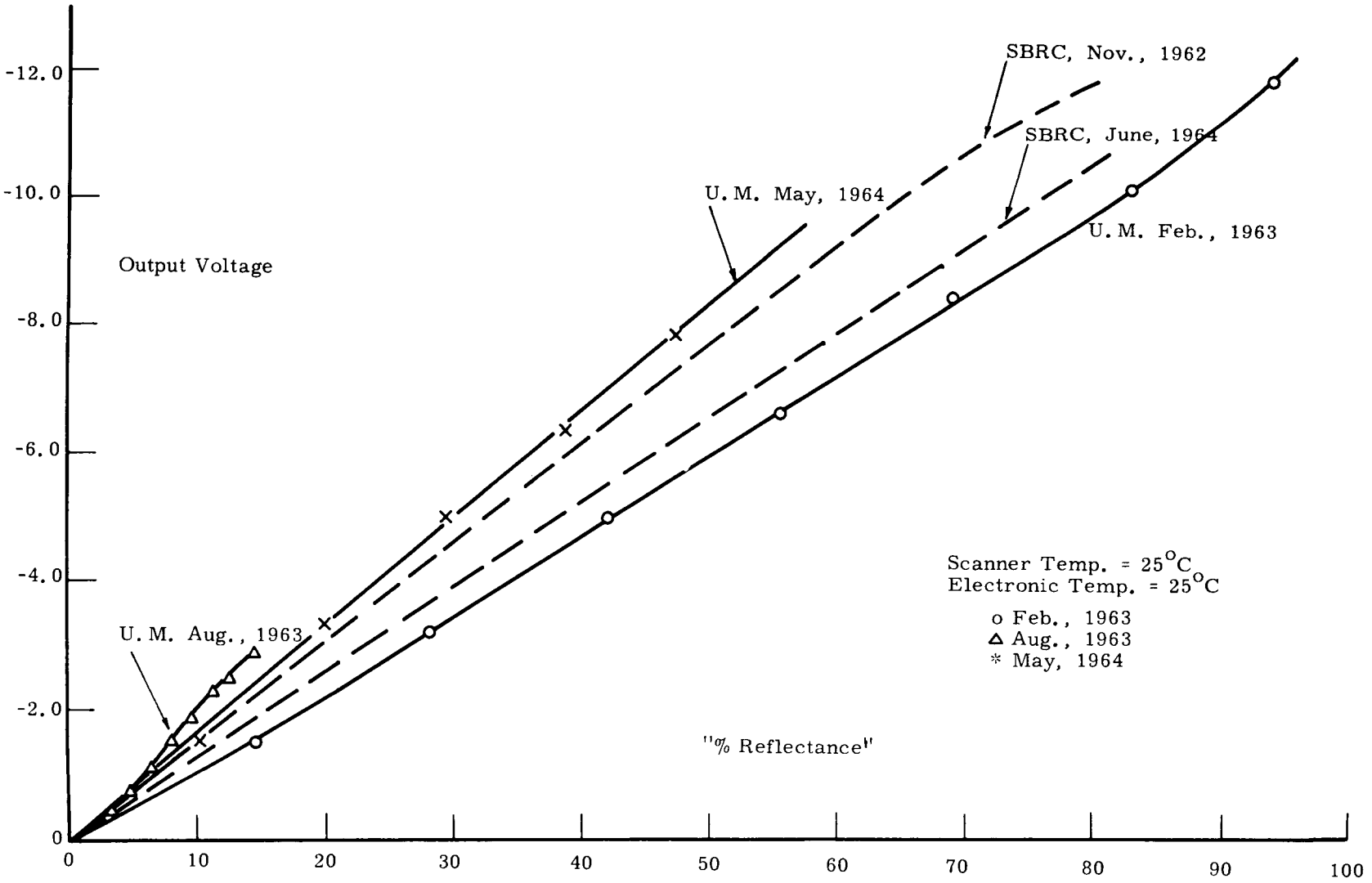

Figure 32. University of Michigan F-1 MRIR calibration data, 0.55-0.85 micron channel.

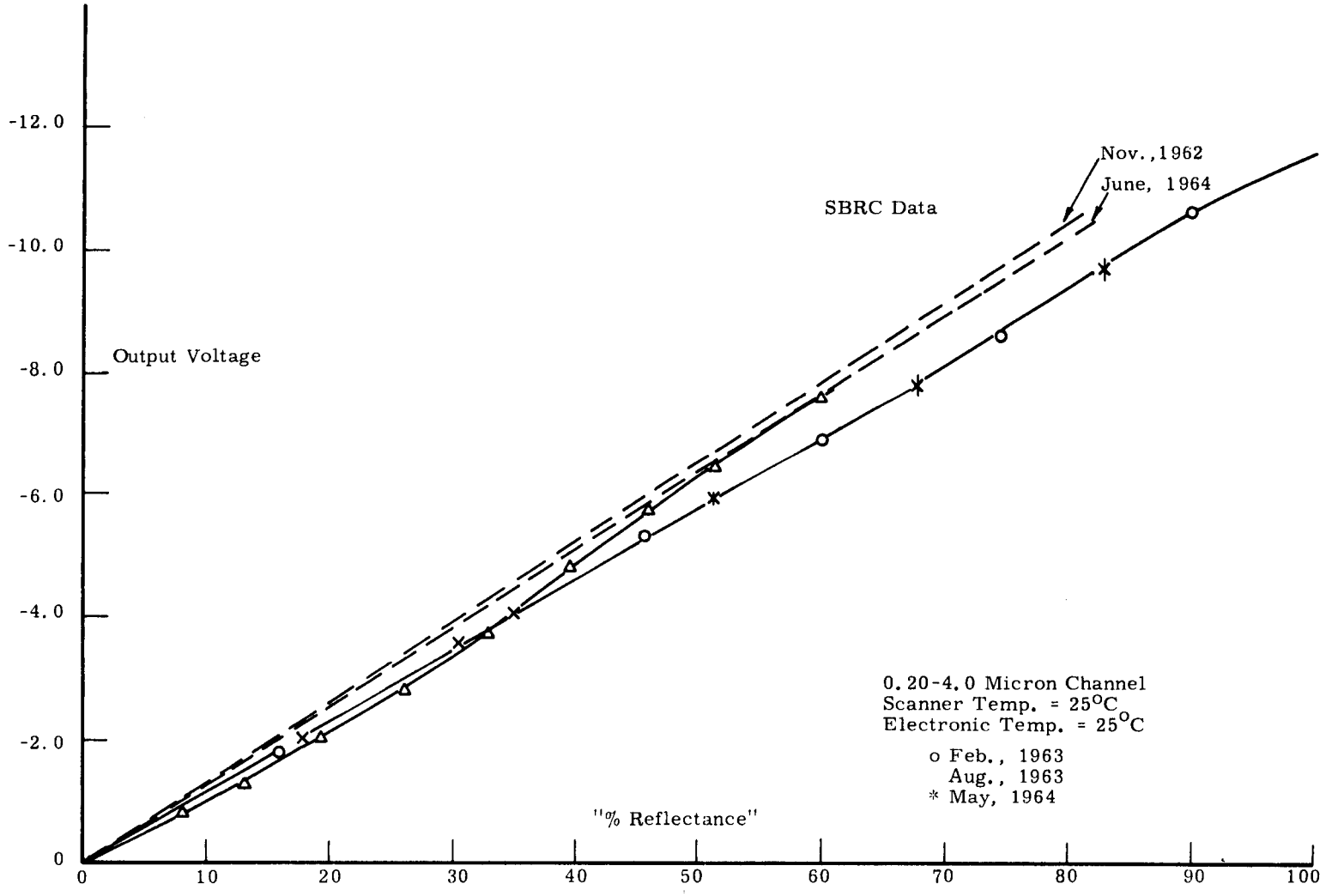

Figure 33. University of Michigan F-1 MRIR calibration data, 0.2-4.0 micron channel.

8. CALIBRATIONS OF THE F-4 MRIR

8.1. SANTA BARBARA CALIBRATION DATA

Calibrations of the F-4 MRIR were made at SBRC in November, 1964, on April 8, 1965, and in December, 1965. The November, 1964, and December, 1965, calibrations were complete sets made for 10 combinations (2 sets of 5 each) of scanner and electronic module temperatures, i.e.:

Set 1		Set 2	
Scanner Temperature, °C	Electronic Temperature, °C	Scanner Temperature, °C	Electronic Temperature, °C
50	25	50	50
40	25	40	40
25	25	25	25
10	25	10	10
0	25	0	0

The calibration on April 8, 1964, was made after a faulty chopper motor drive amplifier was replaced. This was merely a spot check of calibration with both scanner and electronic modules at 25°C.

It should be noticed that the (25,25) calibration in set 1 and (25,25) calibration in set 2 above provide an opportunity to evaluate the precision of the calibrations.

The three sets of calibration data are shown in Figures 34, 35, and 36. In Figure 34 a comparison of the two (25,25) curves, which are almost identical, indicates a very high precision for the October, 1964, calibrations. The same comparison in Figure 36, indicates a significantly degraded precision in the December, 1965, calibration, i.e., at 75% reflectance, there is a difference of 0.35 volts. Note also the much greater effects of electronic module temperature variations in the December, 1965, calibrations.

Figure 37 shows the (25,25) data for all of the SBRC calibrations. At first glance it appears that the calibration curve has changed between each calibration, i.e., it seems that the curve has moved downward between October, 1964, and April, 1965, and then back upward by December, 1965. However, it should be noticed that the apparent error established by comparison of the

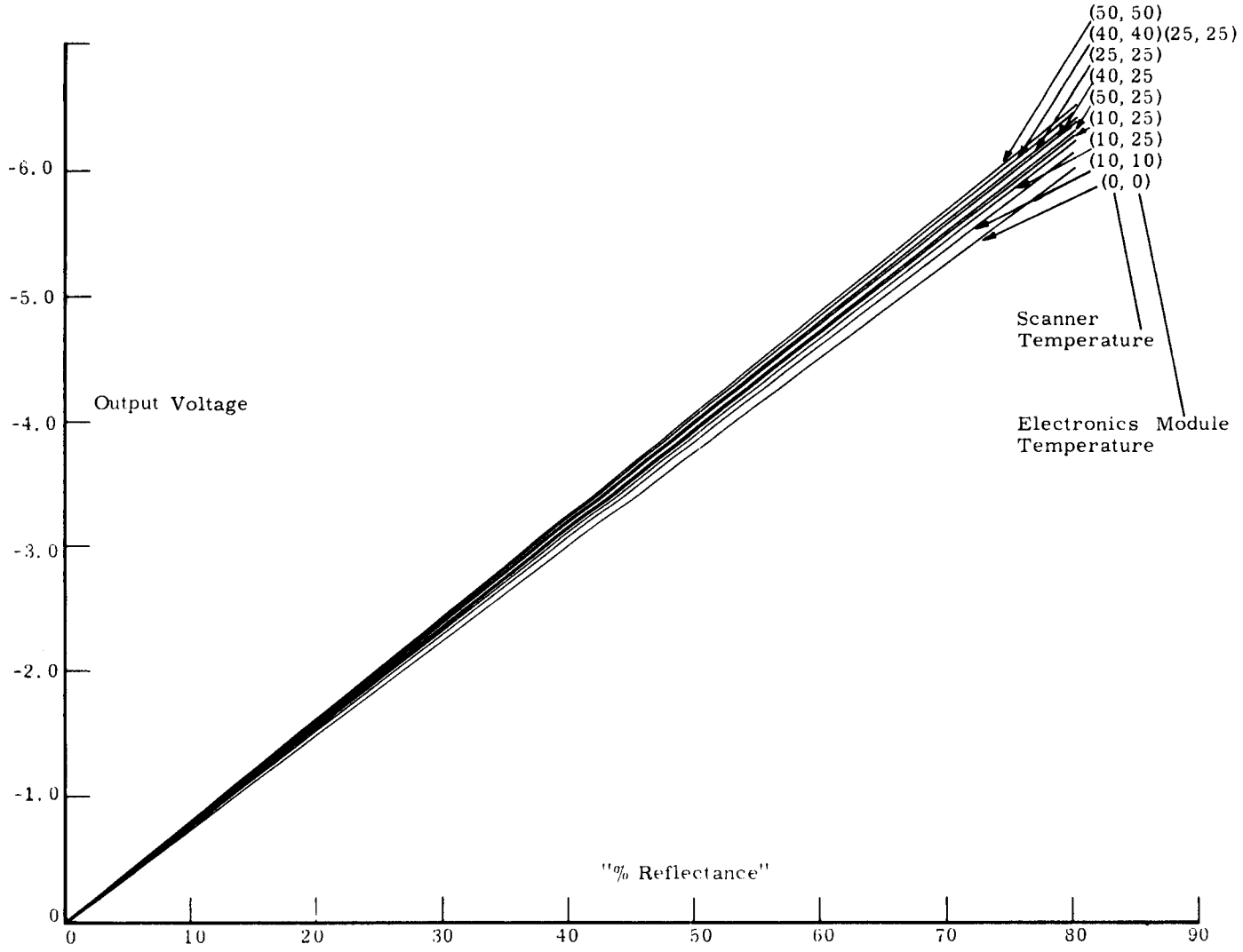

Figure 34. SBRC F-4 MRIR calibration data, 0.2-4.0 micron channel, October 1964.

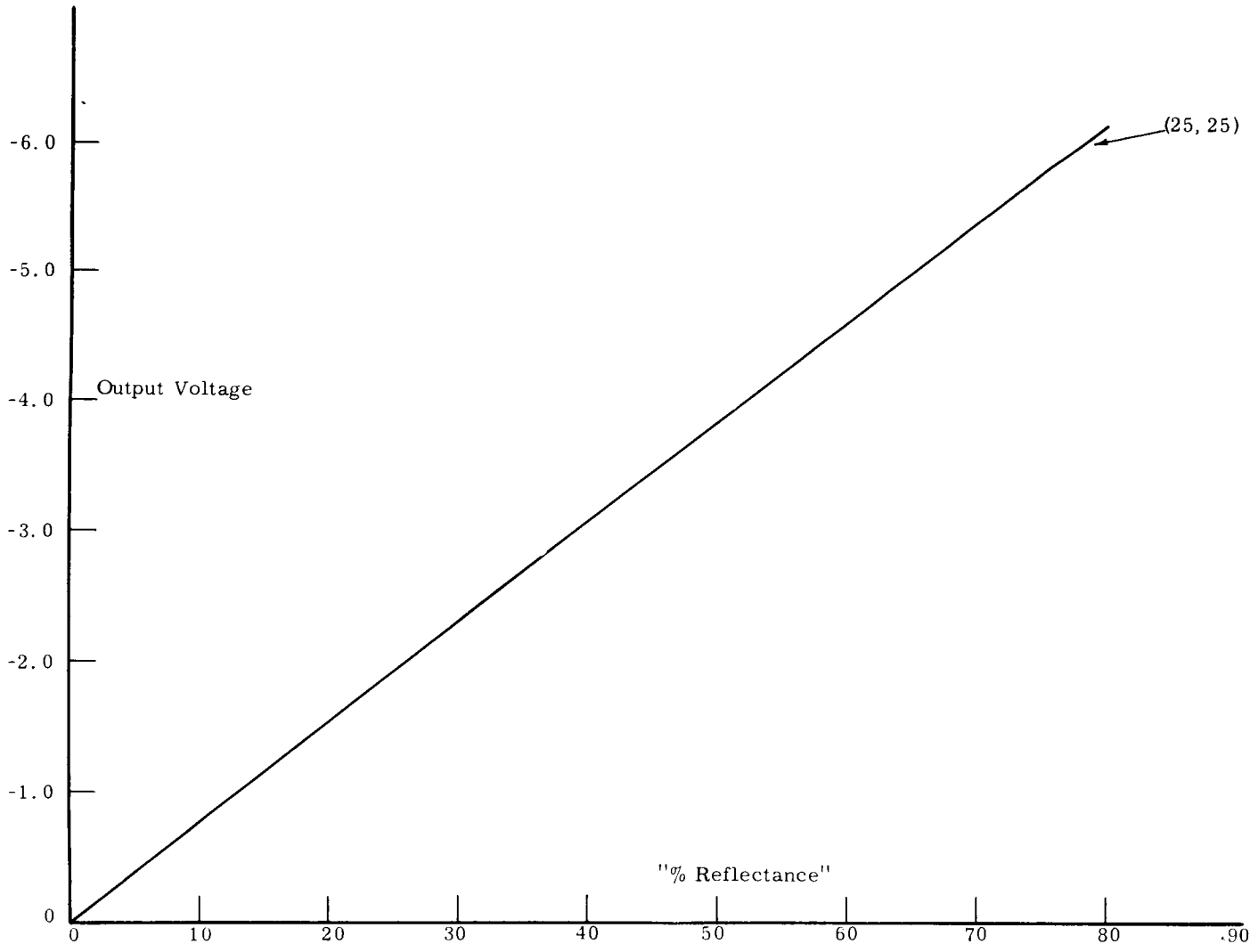

Figure 35. SBRC F-4 MRIR calibration check, 0.2-4.0 micron channel, April 1965.

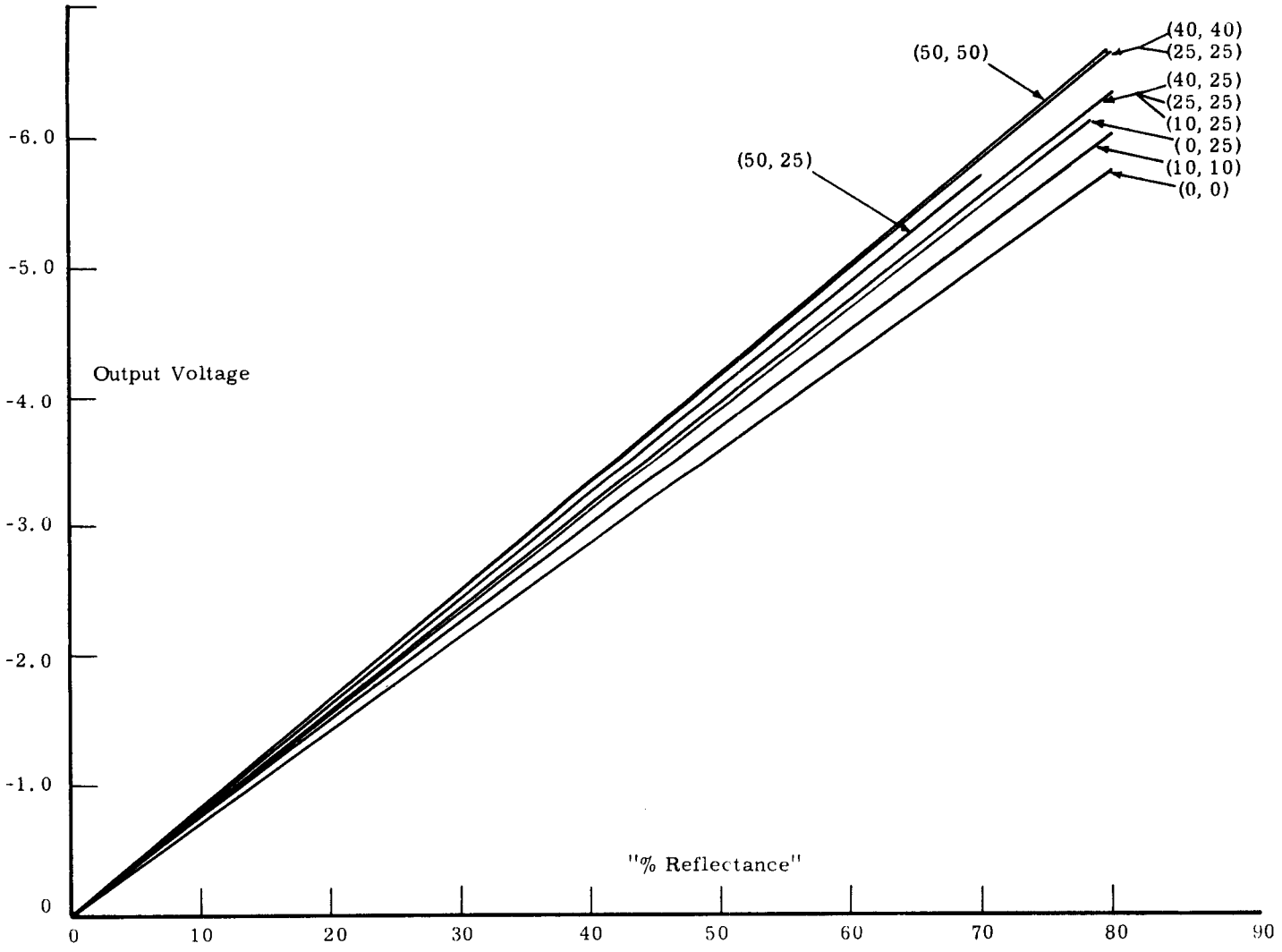

Figure 36. SBRC F-4 MRIR calibration data, 0.2-4.0 micron channel, December 1965.

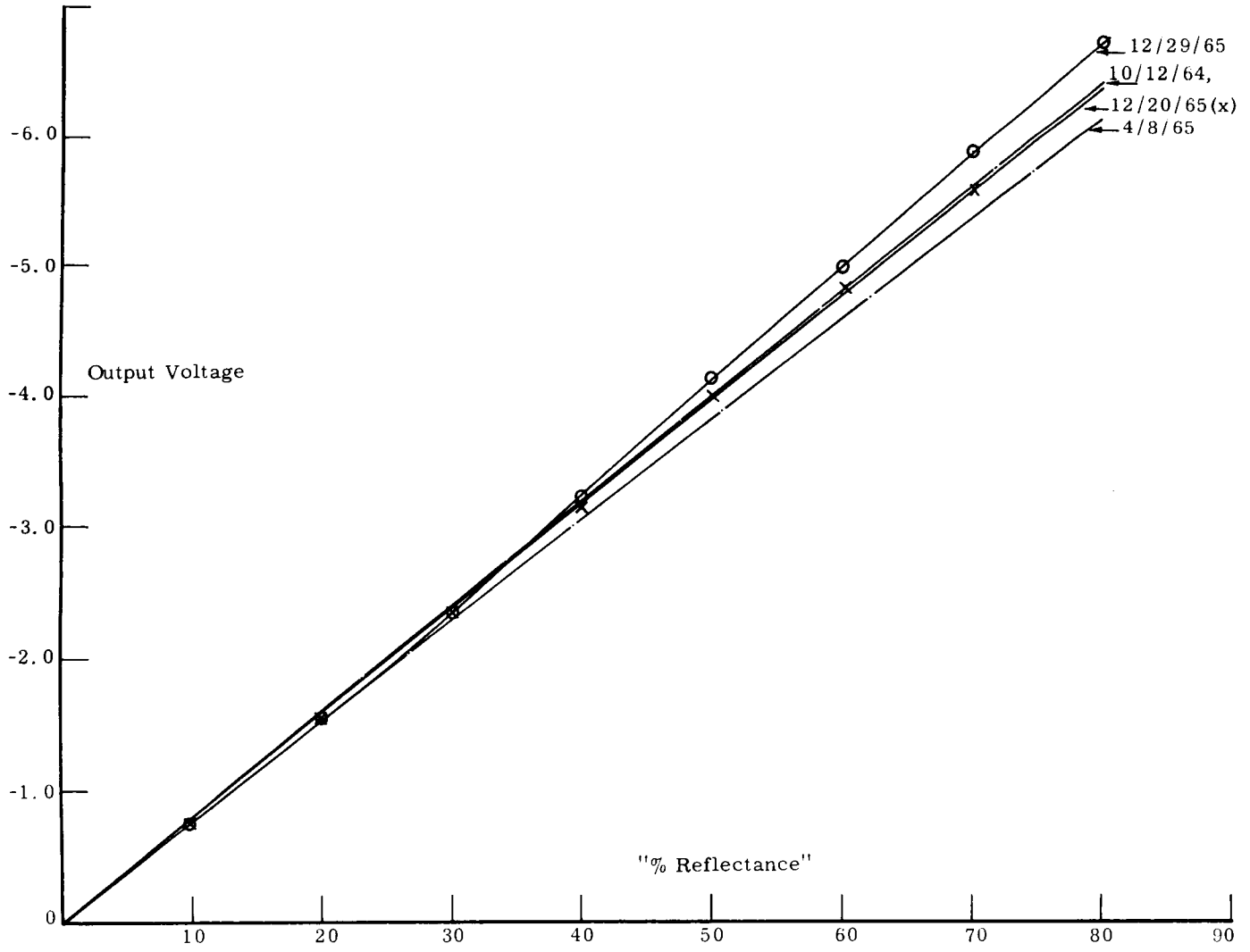

Figure 37. SBRC F-4 MRIR calibration, 0.2-4.0 micron channel, (25,25) data for November 1964, April 1965, and December 1965.

December 20, 1965, and December 29, 1965, measurements is of approximately the same magnitude as the apparent calibration shift.

Thus, it cannot be concluded that the change in calibration curves indicated on this graph indicates a shift in instrument characteristics but is merely evidence of the limit of repeatibility of the calibration data.

8.2. UNIVERSITY OF MICHIGAN CALIBRATION DATA

The calibrations of the F-4 MRIR were made with the hemisphere source.

The response of the radiometer is given by:

$$\Phi_i = 0.94\ \Phi_i'$$

where Φ_i' are values of the relative response average over small wavelength intervals, see Figure 3.

The spectral radiance and radiance of the Burch hemisphere with n lamps turned on are given by:

$$N_{ci} = k_n\ \psi_{ci} \qquad N_c = \sum_i k_n\ \psi_{ci}\ \Delta\lambda_i$$

The effective radiance of the Burch hemisphere is written as:

$$N_c' = 0.94\ k_n \sum_i \Phi_i'\ \psi_{ci}\ \Delta\lambda_i$$

The spectral irradiance of the sun is H_{si} (see Figure 5), and thus the effective radiance of a target with 100% diffuse reflectance is:

$$N_s' = \frac{0.94}{\pi} \sum_i \Phi_i'\ H_{si}$$

Values of Φ_i', H_{si}, ψ_{ci}, and the products $\Phi_i'\ H_{si}$ and $\Phi_i'\ \psi_{ci}$ are given in Table XI. Curves of $\Phi_i'\ H_{si}$ and $\Phi_i'\ \psi_{ci}$ are given in Figures 38 and 39.

The calibration data taken in 1965 and early in 1966 are shown in Table XII.

The percent reflectance is computed from

$$\overline{\rho}' = \frac{0.94\ k_n \sum_i \Phi_i'\ \psi_{ci}\ \Delta\lambda_i}{\frac{0.94}{\pi} \sum_i \Phi_i'\ H_{si}}$$

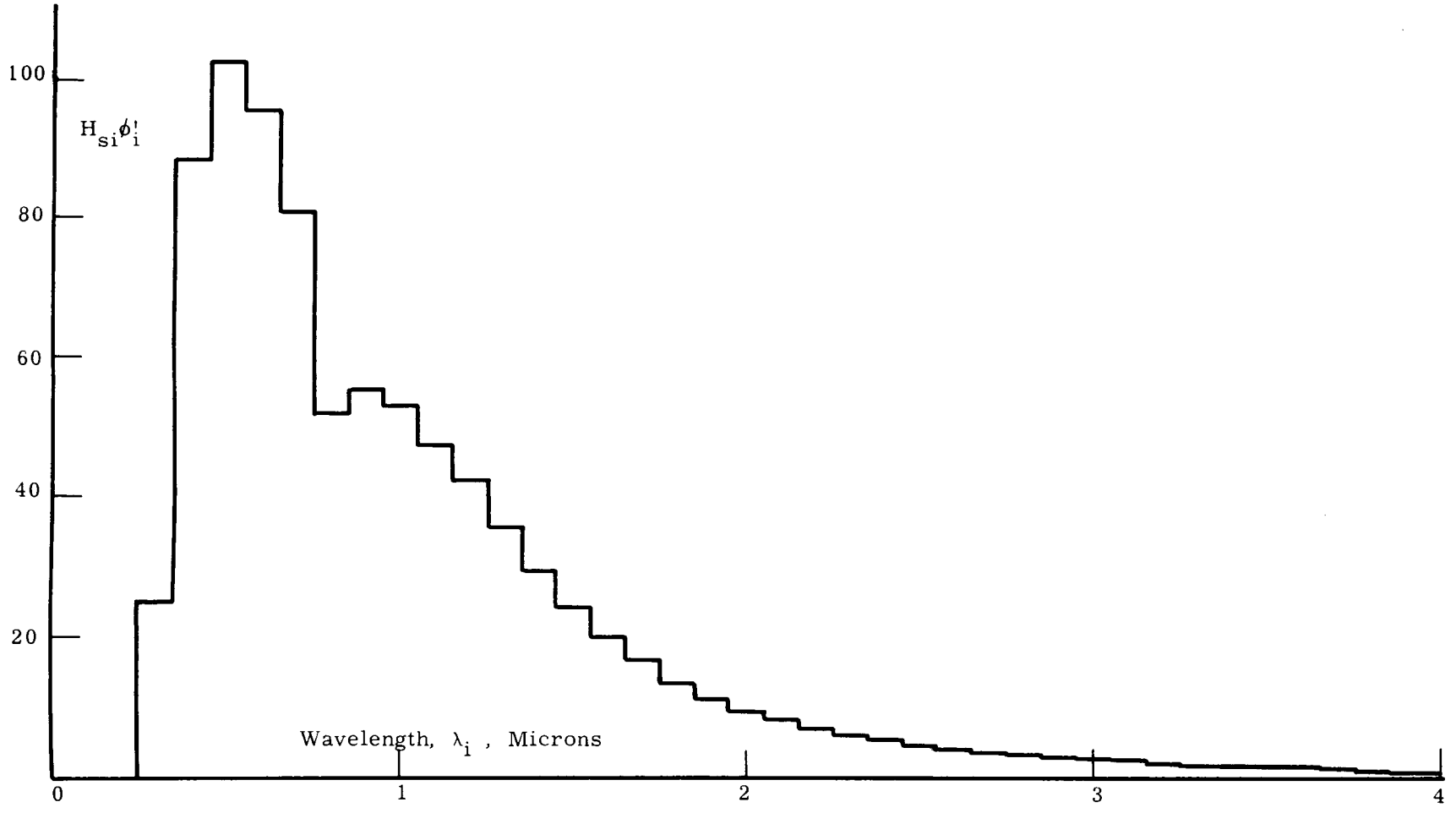

Figure 38. Effective spectral irradiance of sun, $H_{si}\phi_i'$, for 0.2-4.0 micron channel of F-4 MIRI.

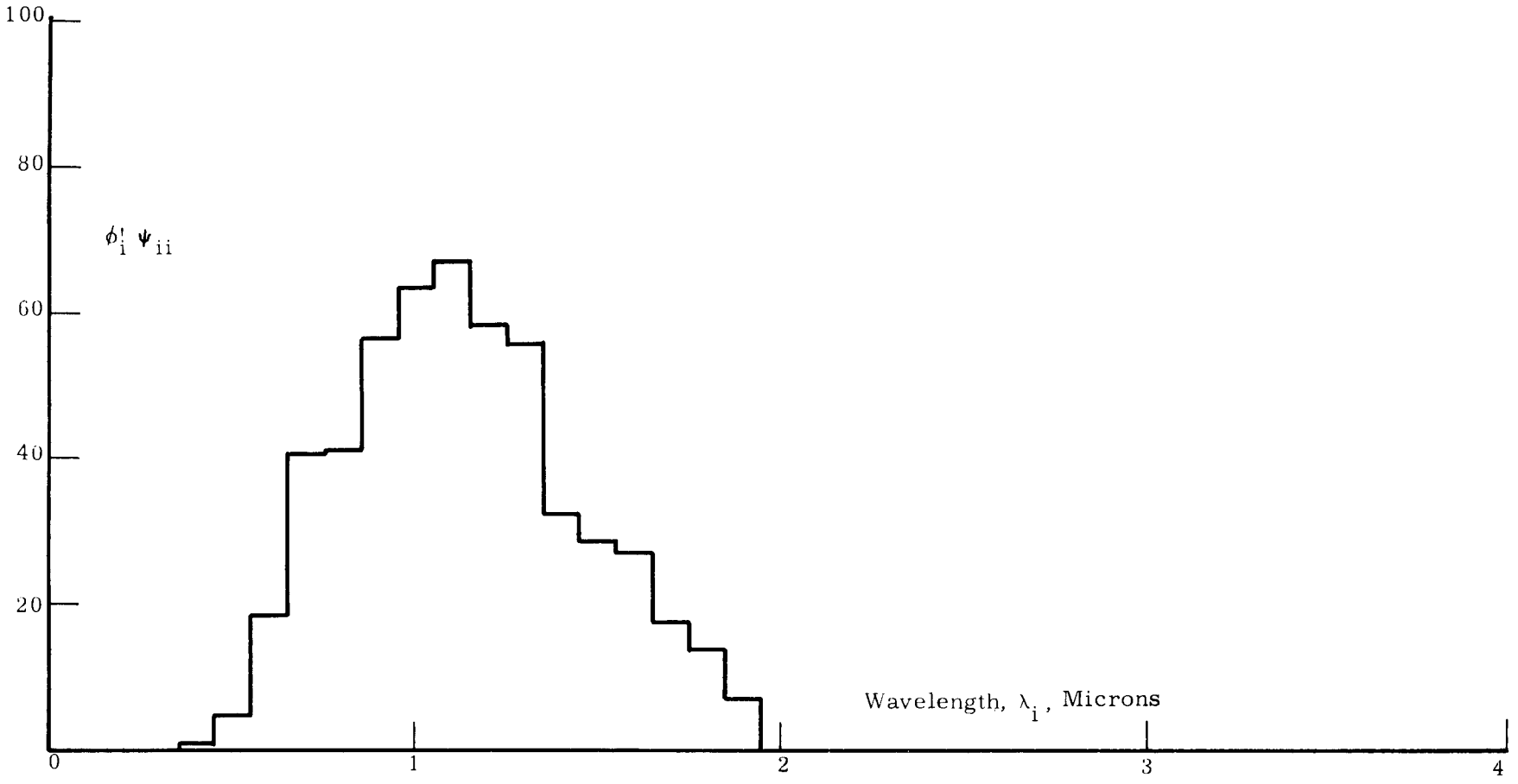

Figure 39. $\phi_i' \Psi_{ci}$ for hemisphere source and 0.2-4.0 micron channel of F-4 MRIR.

TABLE XI

CALCULATION OF EFFECTIVE SPECTRAL RADIANCE
OF SUN AND CALIBRATION SOURCES FOR 0.2-4.0 MICRON CHANNEL OF F-4 MRIR

λ, microns	ϕ_i'	H_{si} watts/m^2	$\phi' H_{si}$	ψ_{ci}	$\phi_i' \psi_{ci}$	λ, microns	ϕ_i'	H_{si} watts/m^2	$\phi' H_{si}$	ψ_{ci}	$\phi_i' \psi_{ci}$
0.3	0.90	62.79	25.12	---	---	2.7	0.983	3.66	3.60		
0.4	0.565	156.34	88.33	1.39	0.78	2.8	0.989	3.22	3.18		
0.5	0.504	203.54	102.58	8.99	4.53	2.9	0.995	2.84	2.83		
0.6	0.525	181.84	95.47	34.90	18.32	3.0	0.973	2.54	2.47		
0.7	0.538	149.80	80.59	75.00	40.35	3.1	0.962	2.24	2.15		
0.8	0.432	120.21	51.93	94.90	41.00	3.2	0.952	1.99	1.89		
0.9	0.580	95.08	55.15	97.30	56.43	3.3	0.927	1.81	1.68		
1.0	0.710	74.78	53.09	89.60	63.62	3.4	0.988	1.62	1.60		
1.1	0.815	58.09	47.34	82.30	67.07	3.5	0.937	1.46	1.37		
1.2	0.888	47.60	42.27	65.50	58.16	3.6	0.987	1.31	1.29		
1.3	0.928	38.18	35.43	60.00	55.68	3.7	0.850	1.18	1.00		
1.4	0.953	30.87	29.42	33.70	32.12	3.8	0.705	1.07	0.75		
1.5	0.963	25.17	24.36	29.60	28.65	3.9	0.661	0.97	0.64		
1.6	0.973	20.68	20.12	27.70	26.95	4.0	0.620	0.90	0.56		
1.7	0.991	17.13	16.98	17.60	17.44	4.1	0.520	0.84	0.44		
1.8	0.948	14.29	13.55	14.50	13.75	4.2	0.360	0.77	0.28		
1.9	0.961	12.00	11.53	7.40	7.11	4.3	0.180	0.71	0.13		
2.0	0.958	10.15	9.72	---	---	4.4	0.138	0.65	0.09		
2.1	0.975	8.63	8.40			4.5	0.180	0.58	0.10		
2.2	0.974	7.39	7.20			4.6	0.202	0.50	0.10		
2.3	0.978	6.36	6.22			4.7	0.100	0.44	0.04		
2.4	0.980	5.50	5.39			4.8	0.015	0.43	0.01		
2.5	0.952	4.78	4.55			4.9	---	0.42	--		
2.6	0.970	4.18	4.05			5.0	---	--	--		

$$\sum_i \psi_{ci} \Delta\lambda_i = 74.038$$

$$\frac{0.94}{\pi} \sum_i \phi_i' H_{si} = 258.8$$

$$0.94 \sum_i \phi_i' \psi_{ci} \Delta\lambda_i = 50.00$$

k_n is computed from:

$$k_n = \frac{N_c}{\sum_i \psi_{ci} \Delta\lambda_i}$$

The necessary numerical values are:

$$\sum_i \psi_{ci} \Delta\lambda_i = 74.038$$

$$\frac{0.94}{\pi} \sum_i \phi_i' H_{si} = 258.8$$

TABLE XII

UNIVERSITY OF MICHIGAN F-4 MRIR CALIBRATION DATA

Thermopile used: Epply No. 4609 with CaF_2 filter and special aperture
Thermopile sensitivity: 0.1325 $\mu V/watt/m^2$

Date	No. of Lamps	MRIR, Volts	Thermopile, μV	W_c, Watts/m^2	N_c, Watts/m^2 sr	$\bar{\rho}'$, % Reflectance
1/16/65	2	1.37-1.43	27.0	203.8	64.9	16.9
	4	2.75-2.95	56.2	424.2	135.0	35.2
	6	4.20-4.30	84.0	634.0	201.8	52.6
	8	5.45-5.63	111.0	837.7	266.6	69.6
	10	---	---	---	---	--
6/3-16/65	2	1.22-1.32	26.0	196.2	62.5	16.3
	4	2.63-2.81	54.0	407.5	129.7	33.8
	6	3.98-4.23	82.0	618.9	197.0	51.4
	8	5.36-5.61	108.0	815.1	259.4	67.7
	10	6.74-7.02	134.0	1011.3	321.9	84.0
1/14/66	2	1.22-1.28	25.0	188.7	60.1	15.7
	4	2.57-2.66	52.0	392.5	124.9	33.6
	6	3.92-4.04	80.0	603.8	192.2	50.1
	8	5.28-5.40	105.0	792.5	252.3	65.8
	10	6.56-6.61	131.0	988.7	314.7	82.1

$$0.94 \sum \Phi_i' \Psi_{ci} \Delta\lambda_i = 50.00$$

Thus,

$$\overline{\rho}' = \frac{50.00}{74.038} \cdot \frac{N_c}{258.8}$$

or

$$\overline{\rho}'(\%) = \frac{50.00}{74.038 \cdot 258.8} N_c = 0.2609 N_c$$

The calibration curves using the data of Table XII are plotted in Figure 40.

It is interesting to note that the output of The University of Michigan calibration source has decreased by about 6% in the year January, 1965, to January, 1966.

The (25,25) calibration curve of the F-4 MRIR has not changed significantly in this period according to The University of Michigan calibrations. It was indicated in Section 8.1 of this report that although at first glance it might indicate that there was a change in calibration of this channel between October, 1964, and December, 1965, this shift appeared to lie within the repeatability of the SBRC calibrations. Indeed an average of the 4 SBRC calibrations cannot be distinguished from the average of The University of Michigan calibrations.

8.3. DIRECT SUN SIGNAL CALIBRATIONS

Results of the direct sun signal calibrations are shown in Table XIII.

Note first that the sun signal received on the March 10, 1965 balloon flight was 3.0 volts with the balloon at 54 mb. pressure altitude. A correction factor of 1.05 for atmospheric absorption yields a predicted orbital direct sun signal of 3.15 volts.

The SBRC sun signal calibrations showed predicted orbital sun signal calibrations of 3.6 volts (November 19, 1966) and 3.16 volts (January 6, 1966), the latter value is in remarkably good agreement with the balloon flight result.

Surface calibrations at The University of Michigan gave a wider range of predicted orbital sun signal calibrations than the SBRC data did.

It is apparent that this method of calibration of the direct sun signal is not very reliable. The excellent agreement between the balloon flight data

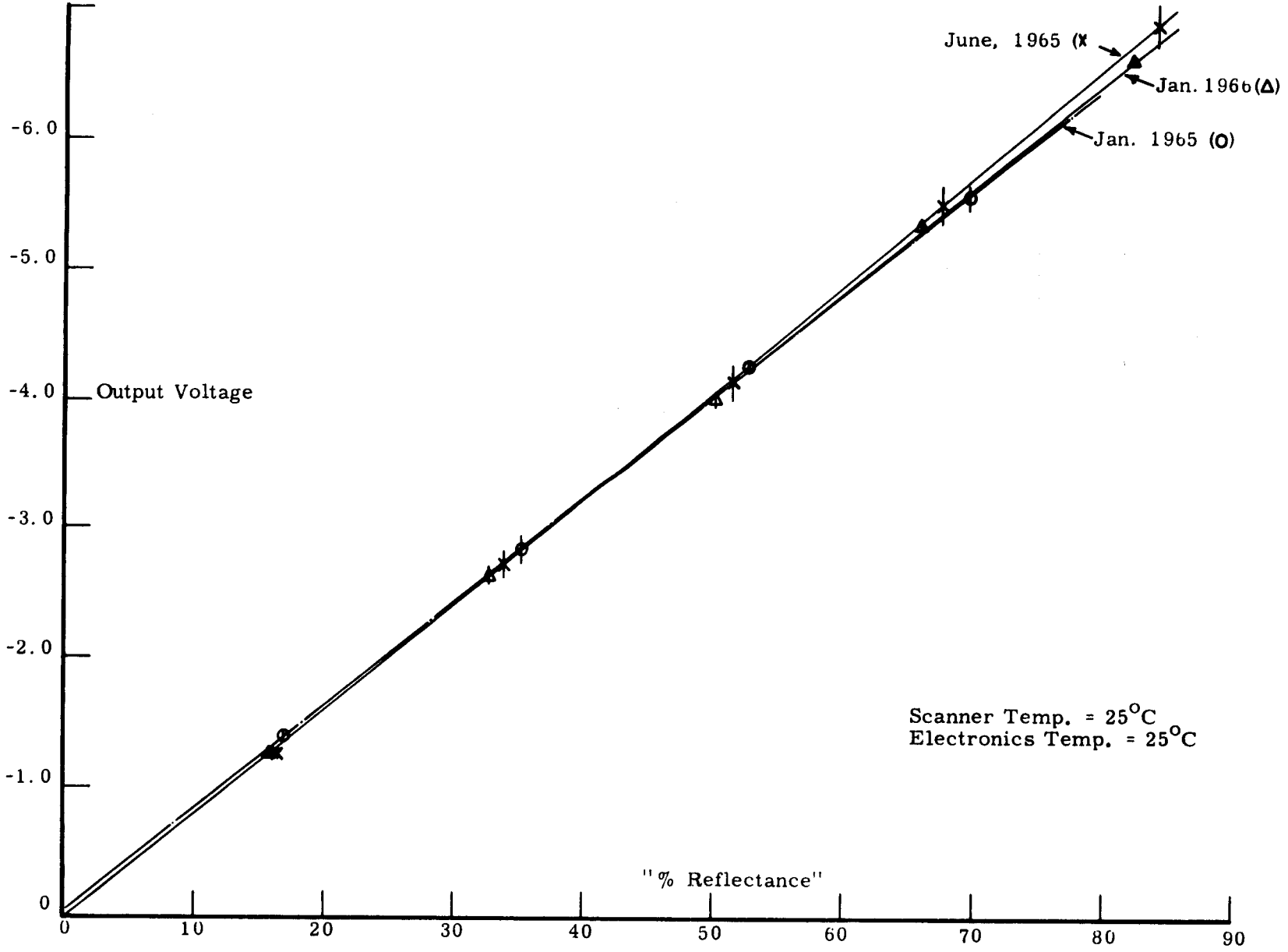

Figure 40. University of Michigan F-4 MRIR calibration data, 0.2-4.0 micron channel.

TABLE XIII

DIRECT SUN SIGNAL CALIBRATIONS OF F-4 MRIR

m = optical path length
V_s = MRIR sun signal
F = correction factor
$F \cdot V_s$ = predicted orbital direct sun signal

Date	Sun Elevation Angle	m	V_s	F	$F \cdot V_s$	Notes
11/19/64	38.7	1.6	2.4	1.5	3.6	At SBRC
3/10/65	13.4	0.232	3.0	1.05	3.15	Balloon Flight Data, 54 mb pressure altitude
5/19/65	66.4	1.09	1.84	1.31	2.41	At U. of Mich.
	65.6	1.095	1.77	1.31	2.32	
	53.7	1.24	1.77	1.37	2.42	
5/20/65	64.7	1.103	1.77	1.32	2.34	At U. of Mich.
	67.9	1.081	1.87	1.31	2.45	
	63.2	1.118	1.80	1.33	2.39	
	56.7	1.193	1.87	1.34	2.51	
	45.3	1.404	1.70	1.43	2.43	
	36.0	1.70	1.48	1.53	2.26	
	30.0	2.00	1.38	1.65	2.28	
5/21/65	37.5	1.64	1.62	1.51	2.45	At U. of Mich.
	45.4	1.40	1.38	1.42	1.96	
	54.3	1.227	1.87	1.37	2.56	
	60.8	1.142	1.89	1.33	2.51	
	67.1	1.089	1.88	1.31	2.46	
	64.4	1.101	1.70	1.32	2.24	
	60.2	1.148	1.55	1.33	2.06	
	53.9	1.23	1.46	1.37	2.00	
	47.2	1.36	1.46	1.42	2.07	
	37.5	1.64	1.29	1.51	1.95	
1/6/66	33.0	1.83	2.0	1.58	3.16	At SBRC
2/7/66	30.0	1.625	2.0	1.65	2.68	At U. of Mich. (hazy)
2/11/66	33.6	1.76	2.01	1.55	3.12	At U. of Mich. (blue sky between clouds)
2/12/66	33.8	1.79	2.32	1.56	3.62	At U. of Mich. (clear)

and the January 6, 1966, SBRC data and the February 11, 1966, University of Michigan data is apparently fortuitous. There are several possible sources of error in the technique used.

(a) First, the assumption that the Handbook of Geophysics data on Elterman's clear standard atmosphere can be used to correct for the attenuation of the direct solar beam may easily lead to error. It is apparent that Elterman's model does not fit the Michigan atmosphere in May under clear sky conditions. The data of May 21, 1965, especially indicate this in that the morning and afternoon data for the same solar elevation differ by as much as 20%. If calibrations are made which depend on corrections for atmospheric attenuation, much more accurate information on moisture and aerosol content must be available.

(b) Second, the calculation of the correction factor F uses the response function of the MRIR without consideration of the spectral response characteristic of the direct sun signal optics.

(c) Finally, the direct sun signal calibration is sensitive to angle variations within the field of view of its optics. This sensitivity can easily result in a reading smaller than the maximum value.

9. ERROR ANALYSIS

9.1. EXPERIMENTAL ERRORS IN CALIBRATION

The equations involved in the calibrations of the visible channels of the MRIR are

$$V_c = R' A_r \Omega \sum_i (k_r \phi_i') k_n \psi_{ci}) \Delta\lambda_i \tag{16}$$

$$\overline{\rho}' = \frac{\sum_i (k_r \phi_i')(k_n \psi_{ci}) \Delta\lambda_i}{\frac{1}{\pi} \sum_i (k_r \phi_i') H_{si}} \tag{17}$$

The radiometer voltage is proportional to the "actual" effective target radiance. In the calibration this voltage is plotted against $\overline{\rho}'$, the ratio of a calculated effective target radiance divided by a calculated effective radiance for 100% diffusely reflected solar radiance.

Errors in V_c are measurment errors, estimated to be less than 0.1 volt. Errors in $\overline{\rho}'$ arise from:

(a) Errors in measured values of ϕ_i'.

(b) Errors in measured values of $k_n \psi_{ci}$.

(c) Errors in values of H_{si} used.

If all work is done carefully and accurately maximum errors for $k_r \phi_i'$ should be less than 1%. The maximum error in measurement of $k_n \psi_{ci}$ should be less than 8% at 0.25 micron and less than 3% at 2.6 microns (the maximum uncertainty quoted by the National Bureau of Standards[8] for standards of spectral radiance). In addition values of $k_n \psi_i$ have a error in precision (repeatability) of about 1%.

Errors in values of H_{si} used should be less than 1%, if corrections are made for variations in values of earth-sun distance when interpretations of measured reflectances are made. If 5700°K to 6000°K black body radiation data are used instead of actual values of H_{si}, errors of up to 5% may result, especially in the 0.55-0.85 micron channel. This can be easily seen by reference to Figure 41, which compares the spectrum of solar irradiance with black body intensities for 6000°K and 5700°K.

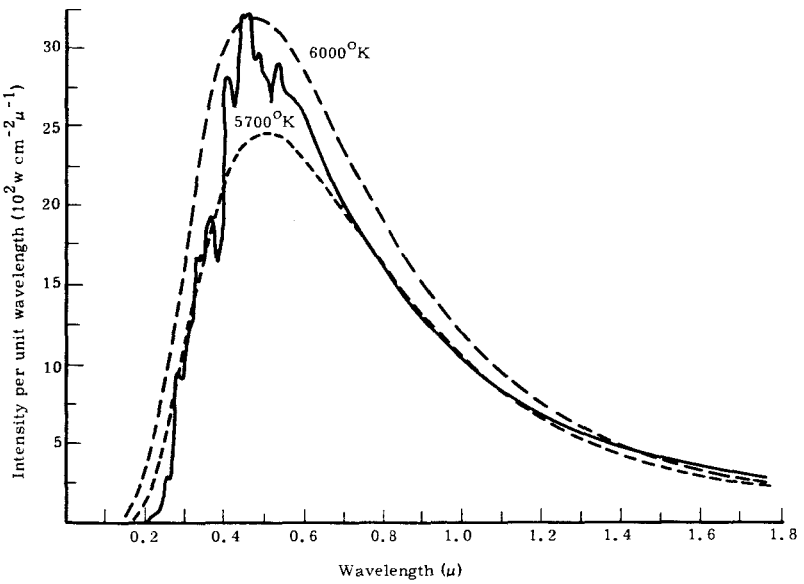

Figure 41. Observed solar spectrum and black body intensities for temperatures of 6000°K and 5700°K [after F. S. Johnson, J. Meteorol. 11, 431, 1954].

A summary of errors in the calibration and use of the visible channels of the MRIR is given in Table XIV. From this table it can be seen that the

TABLE XIV

SUMMARY OF ERRORS IN THE CALIBRATION AND USE OF THE MRIR

Quantity	Magnitude	Comments
V_c	1%	Precision (repeatability)
$k_r \Phi_i'$	1% less than 1%	Precision Systematic error
$k_n \Psi_{ci}$	less than 3-8%	Systematic error
H_{si}	less than 1%	Systematic error Correct for earth-sun distance! Do not use black body data!

Errors in interpretation:

Measured $\bar{\rho}'$ is a weighted average reflectance with weighting function $H_{s\lambda}\Phi_{\lambda}$.

whereas:

Desired $\bar{\rho}$ is weighted average reflectance with weighting function $H_{s\lambda}$.

Measured $\bar{\rho}'$ is bi-directional reflectance—not a total reflectance.

precision of the calibration should be better than 2%, the systematic error should be less than 3-8%. In addition, significant errors may be made in the interpretation of the data. This error of interpretation can easily be 10% or larger (see Section 9.3).

9.2. CORRECTED CALIBRATION CURVE FOR F-1 MRIR 0.2-4 MICRON CHANNEL

During the calibrations of the F-4 MRIR, it was noticed that an error could easily be introduced into readings of source radiance if too much time was taken in this process. The cause of the error was the increase of thermal radiation of the source with time. Since the thermopile with CaF_2 filter has a response out to and beyond 10 microns, it responds to thermal radiation as well as visible radiation. Comparison of readings of the same thermopile with CaF_2 and quartz filters indicated an error as great as 5.6% could occur.

A discussion of the experimental technique used on the F-1 MRIR calibration lead to the conclusion that this error probably did exist in the calibration of the F-1 MRIR. Indeed if a correction is applied to the (University of Michigan) data, excellent agreement is obtained between University of Michigan and SBRC calibrations. The modified University of Michigan calibration is shown and compared with the SBRC curves in Figure 42.

9.3. ERRORS IN INTERPRETATION, EXAMPLES

Two examples of the measurement of reflectance with the visible channels of the NIMBUS MRIR are considered, the reflectance of a "green leaf"[10] and of "middle layer clouds".[11]

The spectral reflectance curves considered are shown in Figure 43. For each curve the quantities $\bar{\rho}$ and $\bar{\rho}'$ have been calculated for each of the visible channels of the MRIR, i.e., the "true" average reflectances for solar radiation.

$$\bar{\rho}_{0.55\text{-}0.85} = \frac{\sum_{0.55}^{0.85} \rho_\lambda \, H_{s\lambda} \, \Delta\lambda}{\sum_{0.55}^{0.85} H_{s\lambda} \, \Delta\lambda} \qquad (18)$$

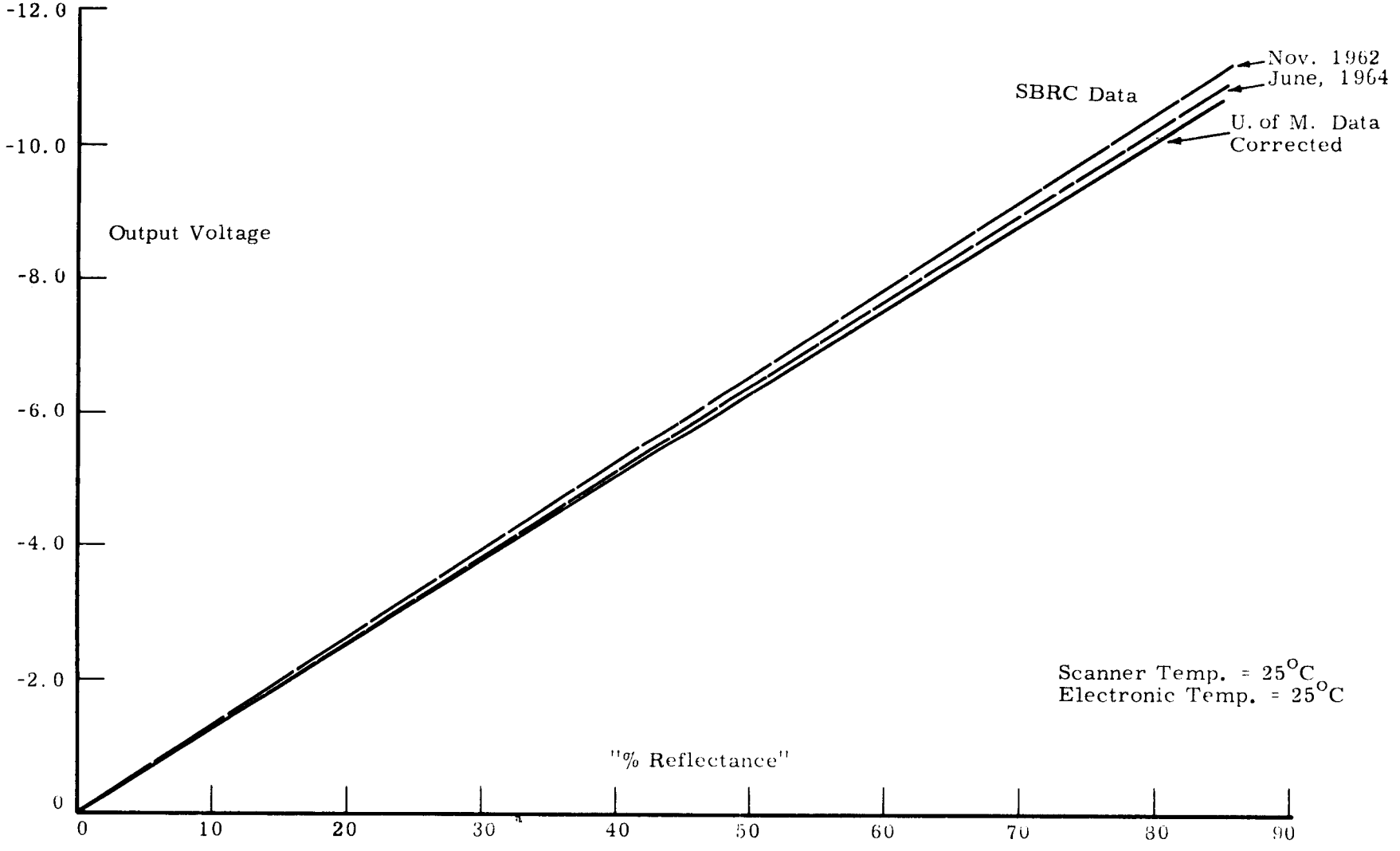

Figure 42. University of ... MRTR calibration data, 0.2-4.0 micron channel, corrected for error in thermopile reading.

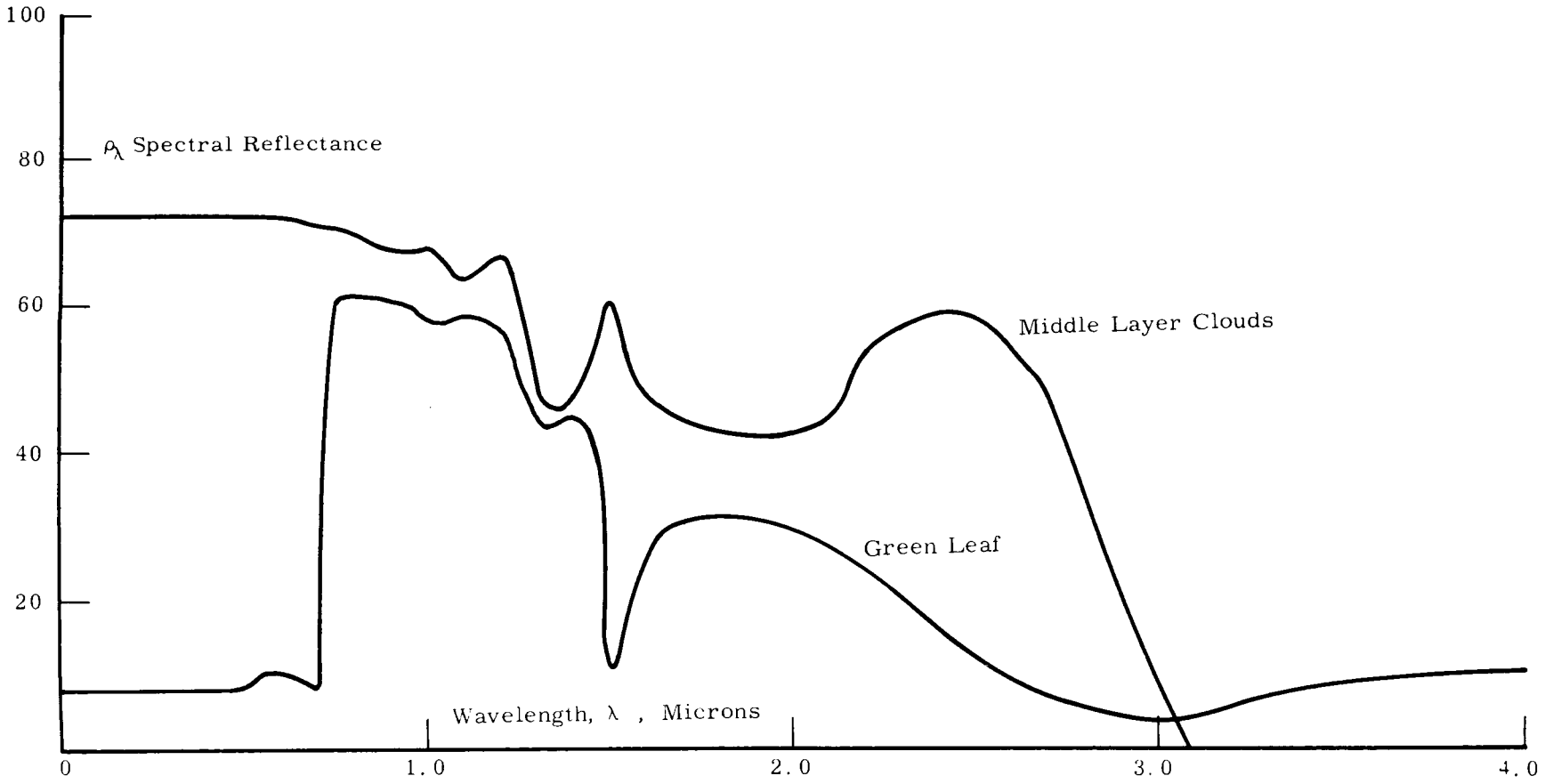

Figure 43. Spectral reflectance curves for "middle layer clouds" and a "green leaf."

$$\bar{\rho}_{0.2\text{-}4.0} = \frac{\sum_{0.2}^{4.0} \rho_\lambda \, H_{s\lambda} \, \Delta\lambda}{\sum_{0.2}^{4.0} H_{s\lambda} \, \Delta\lambda} \tag{19}$$

and the reflectances measured by the MRIR

$$\bar{\rho}'_{0.55\text{-}0.85} = \frac{\sum_{0.55}^{0.85} \rho_\lambda \, H_{s\lambda} \, \phi_\lambda \, \Delta\lambda}{\sum_{0.55}^{0.85} H_{s\lambda} \, \phi_\lambda \, \Delta\lambda} \tag{20}$$

$$\bar{\rho}'_{0.2\text{-}4.0} = \frac{\sum_{0.2}^{4.0} \rho_\lambda \, H_{s\lambda} \, \phi_\lambda \, \Delta\lambda}{\sum_{0.2}^{4.0} H_{s\lambda} \, \phi_\lambda \, \Delta\lambda} \tag{21}$$

where the values of ϕ_λ used are the appropriate values for the F-1 MRIR radiometer.

The results of these calculations are shown in Table XV. The true average reflectance of the "middle layer clouds" is almost the same for the 0.55-0.85 and 0.2-4.0 micron regions. Both channels of the MRIR would give excellent measurements of these average reflectances.

For the "green leaf" the situation is different and errors of interpretation could result. Although the spectral reflectance varies widely as a function of wavelength, the true average reflectances $\bar{\rho}_{0.55\text{-}0.85}$ and $\bar{\rho}_{0.2\text{-}4.0}$ are about the same, 0.26. The measured average reflectance $\bar{\rho}'_{0.2\text{-}4.0}$ gives an excellent result, 0.27, however the measured value $\bar{\rho}'_{0.55\text{-}0.85}$ is much too low, 0.16.

TABLE XV

REFLECTANCES MEASURED BY MRIR COMPARED WITH TRUE AVERAGE REFLECTANCES

Substance	$\bar{\rho}_{0.2\text{-}4.6}$	$\bar{\rho}_{0.55\text{-}0.85}$	$\bar{\rho}'_{0.2\text{-}4.6}$	$\bar{\rho}'_{0.55\text{-}0.85}$
Middle layer clouds	0.659	0.710	0.645	0.714
Green leaf	0.264	0.261	0.273	0.156

Use of $\bar{\rho}'_{0.55\text{-}0.85}$ for earth albedo would require a correction factor of 1.6 in the case of the "green leaf."

10. CONCLUSIONS AND RECOMMENDATIONS

The following conclusions are drawn from the calibration program described above.

(1) The program of calibrations of the 0.55-0.85 micron and 0.2-4.0 micron channels of the MRIR's has developed to the point at which reliable calibrations can be made.

(2). The hemisphere source which has been developed as a part of this program can be used with confidence in making this type of calibration. It provides a suitable range of intensities, 0-85% reflectance, of known spectral distribution; is stable and relatively efficient in its use of electrical power. As a calibration source it is far superior to the "carbon-arc—MgO reflector plate" or "tungsten lamp—MgO reflector plate" sources.

(3) The calibrations of the F-1 and F-4 MRIRs have been carried out satisfactorily, i.e.,

(a) Calibrations of the 0.2-4.0 micron channel of the F-4 MRIR are repeatable and agree with SBRC calibrations within the estimated precision and systematic error range of this type of measurement.

(b) Calibrations of the 0.2-4.0 micron channel of the F-1 MRIR carried out with the "carbon-arc—MgO reflector plate" and hemisphere sources are consistant and agree with SBRC calibrations, although a correction factor derived from F-4 calibration work was applied.

(c) Calibrations of the 0.55-0.85 micron channel of the F-1 MRIR show large variations as a function of time. This variation is explained by the deterioration of the filter used in this channel.

(4) The method of calibration and interpretation of the data in terms of percent reflectance can lead to large errors in interpretation for signals of some spectral distributions. An example is given in Section 9.3. Additional error results from the assumption that the bidirectional reflectance measured is a diffuse reflectance.

(5) The direct solar calibrate system is limited in its use by the method of calibration, in which the sun is viewed from the earth's surface and corrections are made for atmospheric transmission. The accuracy of this type of correction is poor and thus for NIMBUS satellite applications, the deterioration of the radiometer during the satellite launch phase may not be accurately measured.

Recommendations for future MRIR calibrations are:

(1) Reports on MRIR calibrations should include all calibration details, including

(a) Spectral distribution and intensities of calibrating source,

(b) Secondary standards to which radiation measurements are referred,

(c) Values of solar irradiance used for the calculation of percent reflectance, so that comparisons between the work of various calibrating groups may be better compared.

(2) The characteristics of the calibrating sources should be monitored and checked at regular intervals so that changes can be noted.

(3) The characteristics of the complete optical system used in the direct sun signal calibrations should be determined. A method of calibration which does not depend on estimated corrections for atmospheric transmission should be developed.

11. ACKNOWLEDGMENTS

This calibration work has been carried out as a part of a program of atmospheric radiation measurements under Contract NASr-54(03) with NASA Goddard Space Flight Center.

The many helpful discussions of the subject matter of this report with Dr. W. A. Nordberg, Mr. W. R. Bandeen, and Mr. A. McCullough of Goddard Space Flight Center, and Mr. F. R. Malinowski of Santa Barbara Research Center are gratefully acknowledged.

Members of the High Altitude Engineering Laboratory who have contributed to the calibration work are Messrs. M. T. Surh, Wan Y. Lee, L. W. Chaney, Gunar Liepins, L. W. Carls and M. G. Whybra.*

Thanks are also due to Professor E. S. Epstein and L. M. Jones for their helpful comments and suggestions on this report.

*Now with the Radio Astronomy Laboratory of The University of Michigan.

11. ACKNOWLEDGMENTS

This calibration work has been carried out as a part of a program of atmospheric radiation measurements under Contract NASr-54(03) with NASA Goddard Space Flight Center.

The many helpful discussions of the subject matter of this report with Dr. W. A. Nordberg, Mr. W. R. Bandeen, and Mr. A. McCullough of Goddard Space Flight Center, and Mr. F. R. Malinowski of Santa Barbara Research Center are gratefully acknowledged.

Members of the High Altitude Engineering Laboratory who have contributed to the calibration work are Messrs. M. T. Surh, Wan Y. Lee, L. W. Chaney, Gunar Liepins, L. W. Carls and M. G. Whybra.*

Thanks are also due to Professor E. S. Epstein and L. M. Jones for their helpful comments and suggestions on this report.

*Now with the Radio Astronomy Laboratory of The University of Michigan.

12. REFERENCES

1. Hummer, R. F. and F. R. Malinowski, "NIMBUS Five-Channel Scanning Radiometer," paper presented at Ninth National Infrared Symposium (IRIS), 6-8 May, 1963, Dallas, Texas.

2. "Data Book for NIMBUS Medium Resolution Infrared Radiometer (F-4)," Santa Barbara Research Center, Goleta, California, 30 November, 1964.

3. Holter, M. R., S. Nudelman, G. H. Suits, W. L. Wolff, G. J. Zissis, "Fundamentals of Infrared Technology," P. 54, The McMillan Co., 1962.

4. Sanders, C. L. and E.E.K. Middleton, "The Absolute Spectral Diffuse Reflectance of Magnesium Oxide in the Near Infrared," J. Opt. Soc. Amer., 43, 58, 1953.

5. Bandeen, W. R., M. Halev, I. Strange, "A Radiation Climatology in the Visible and Infrared from the TIROS Meteorological Satellites," Report No. X-651-64-218, Goddard Space Flight Center, Greenbelt, Maryland, August 1964.

6. Elterman, L., "Atmospheric Attenuation Model, 1964, in the Ultraviolet, Visible and Infrared Regions for Altitudes to 50 km.," Environmental Research Paper No. 46, AFCRL, Office of Aerospace Research, USAF., L. G. Hanscom Field, Massachusetts, September, 1964.

7. Malinowski, F. R., "Investigation of F-1 MRIR—Final Report," Report on Contract NAS 5-757, Santa Barbara Research Center, Goleta California, 2 November, 1964.

8. Stair, R., R. G. Johnston and E. W. Halbach, "Standard of Spectral Radiance for the Region of 0.25 to 2.6 Microns," Journ. Res. N.B.S., 64A, 291-296, July-August, 1960.

9. Johnson, F. S., "The Solar Constant," J. Meteorol., Vol. 11, p. 431-439, 1954.

10. Gates, D. M., H. J. Keegan, J. C. Schleter, and V. R. Weidner, "Spectral Properties of Plants," Applied Optics, 4, No. 1, January 1965.

11. Novosel'tsev, Ye. P., "Spectral Reflectivity of Clouds," NASA TT-F-328, National Aeronautics and Space Administration, Washington D.C., April 1965. (Translation of article from Trudy Glavnoy Geofizicheskoy Observatorii imemi A. I. Voycykova, No. 152, 1964.)